

POLITECNICO DI TORINO

Collegio di Ingegneria Chimica e dei Materiali

**Master of Science Course
in Materials Engineering**

Master of Science Thesis

Low cost process for carbon-based electronic boards production



Tutors

prof. Claudio Francesco Badini

prof. Alberto Tagliaferro

Co-tutors

dr. Antonino Veca

dr. Andrea Caradonna

Candidate

Enrico Alfonzo

October 2017

Table of Contents

Sommario

Preface

1. Introduction	1
1.1 Biochar	1
1.1.1 Production and modification methods of Biochar	2
1.1.2 Structure, properties and applications of Biochar	7
1.2 Polymer composites with Biochar	8
1.2.1 Preparation methods of polymer composites with Biochar	9
1.2.2 Mechanical properties of polymer composites with Biochar	10
1.2.3 Percolation theory and electrical conductivity of polymer composites with Biochar	12
1.3 Laser technology and ablation phenomenon	18
1.3.1 Technology, features and types of laser beams	18
1.3.2 Laser-material interaction: polymeric ablation	21
2. Materials	25
2.1 Polypropylene (PP)	25
2.2 Biochar	26
2.3 PP/Biochar composites	27
3. Equipment and methods	29
3.1 Mixing, granulation and injection moulding	29
3.2 Percolation threshold evaluation	33
3.3 CO ₂ laser scribing	34
3.4 Electrical characterisation	37
3.5 Mechanical characterisation	38
3.6 Thermal characterisation	38
3.6.1 Thermogravimetric analysis (TGA)	39
3.6.2 Differential scanning calorimetry (DSC)	39
3.7 Morphological and spectroscopic characterisation	39
3.7.1 Biochar Powders	39
3.7.2 PP/Biochar composites	40
4. Experimental results and discussion	41
4.1 Biochar characterisation	41
4.1.1 X-ray Powder Diffraction (XRD)	41
4.1.2 Raman spectroscopy	41
4.1.3 Field Emission Scanning Electron Microscopy (FESEM)	42
4.1.4 Energy-dispersive X-ray spectroscopy (EDS)	44

4.1.5 Thermogravimetric analysis (TGA)	45
4.2 Preparation of polymer composites with Biochar	46
4.3 Percolation threshold evaluation	46
4.4 Evaluation of the influence of the variation of the laser parameters on conductivity	47
4.4.1 Power	47
4.4.2 Scan rate	50
4.4.3 Repetition number	52
4.4.4 Frequency	53
4.4.5 Defocus	54
4.4.6 Optimisation of the laser parameters	55
4.5 Mechanical characterisation of PP/Biochar composites	60
4.6 Thermal characterisation of PP/Biochar composites	62
4.6.1 Thermogravimetric analysis (TGA)	62
4.6.2 Differential scanning calorimetry (DSC)	63
4.7 Morphological characterisation of PP/Biochar composites	64
4.7.1 Optical microscopy	64
4.7.2 Field Emission Scanning Electron Microscopy (FESEM) on laser tracks	65
5. Conclusions	71
 List of acronyms	75
 List of symbols	77
 Bibliography	79
 Acknowledgments	83

Sommario

1. Obiettivi

La finalità del presente lavoro è la realizzazione di circuiti elettrici, integrati per mezzo di ablazione laser all'interno di un materiale polimerico caricato con cariche (*fillers*) elettricamente conduttrici, al fine di utilizzarli su interni di autovetture quali moduli plancia e pannelli porta. Particolare attenzione si è prestata alla scelta di un materiale che fosse economico e che potesse dunque competere con il prezzo elevato del rame, tradizionalmente utilizzato nei cablaggi. Il progetto nasce da una collaborazione tra il Politecnico di Torino e lo *Smart Materials Lab* del *Polymer and Glass Department* del Centro Ricerche Fiat (CRF) di Orbassano. Il CRF è uno dei principali pilastri dell'innovazione tecnologica del panorama italiano, un polo eccellente nella ricerca e nello sviluppo del settore automobilistico.

L'industria automobilistica Fiat Chrysler Automobiles (FCA) investe gran parte delle sue risorse nella ricerca tecnologica al fine di ridurre il numero di materiali utilizzati nella costruzione del veicolo, diminuendo così il peso, il costo, il consumo di energia e l'impatto ambientale. L'azienda, come altre del settore, si sta orientando sempre più verso il concetto di "mono-materiale", ossia un unico materiale che riassume in sé diverse funzioni. Tale tipologia di materiale rientra nella categoria degli "*smart materials*", cioè materiali che presentano una o più proprietà (funzionalità) che possono cambiare significativamente attraverso stimoli esterni (stress, temperatura, pH, umidità, campi elettrici o magnetici).

Il protagonista di questo lavoro è un mono-materiale avente il compito di agire da conduttore elettrico per l'attivazione di dispositivi interni al veicolo. Inoltre, esso potrebbe essere sfruttato per le sue proprietà di antistaticità anche quando utilizzato per parti in contatto con membri del sistema di alimentazione carburante. In particolare, dovrà essere lo stesso componente dell'autovettura a mostrare in sé sia le funzioni strutturali che quelle elettriche. Ma al tempo stesso, dovrebbe essere leggero e poter essere fabbricato in forme complesse: entrambe proprietà appartenenti alla classe dei materiali polimerici. La scelta della matrice polimerica idonea a questo scopo è ricaduta sul polipropilene (PP), uno dei materiali più utilizzati per la realizzazione di componenti sia esterni che interni dell'automobile.

Per quanto riguarda i fillers da additivare al polimero, in precedenti lavori presso il CRF si è testato l'utilizzo dei nanotubi di carbonio (CNTs) raggiungendo ottimi risultati di conducibilità elettrica. Infatti, negli ultimi dieci anni, i CNTs sono stati impiegati come fillers ad alte prestazioni per la produzione di composti polimerici con elevate proprietà meccaniche, stabilità termica e proprietà elettriche. Ma il problema di questi composti è il costo elevato del processo di produzione dei CNTs stessi, stimato essere maggiore di quello dei fili di rame tradizionali, senza considerare la difficoltà della loro dispersione in una matrice polimerica. Alla luce della

sudetta esperienza, nel presente lavoro si è cercato di funzionalizzare la matrice polimerica con cariche carboniose più economiche. In particolare, si è fatto appello al bio-carbonio, comunemente noto come Biochar, un residuo solido ottenuto dalla carbonizzazione delle biomasse. La grande sfida di questo lavoro di tesi è stata quella di rendere polimeri conduttori utilizzando un riempitivo che praticamente non trova riscontro in letteratura. Infatti, tradizionalmente, il Biochar viene utilizzato come combustibile solido in cui la conducibilità elettrica è irrilevante per tale applicazione. La ricerca sull'impiego di Biochar come rinforzante di materiali polimerici per migliorarne varie proprietà è perciò insufficiente, ma questa ragione ha dato la forza per svolgere questo lavoro di tesi con motivazione.

Sebbene il comportamento da isolante elettrico del PP e dei materiali polimerici in generale sia ben noto, lo scopo di questo lavoro consiste nel renderli conduttori solo in quei punti in cui un fascio laser investe il materiale. L'interazione del fascio laser con questi materiali provoca una riduzione localizzata della resistenza elettrica, portando così alla realizzazione di circuiti elettrici. I parametri laser (potenza, velocità di scansione, defocalizzazione, frequenza e numero di ripetizioni) da impostare per eseguire la lavorazione devono essere modulati ad hoc, al fine di produrre tracce dedito al trasferimento di segnali elettrici. Il metodo utilizzato e descritto nel lavoro di ricerca è rapido e flessibile e non comporta alcun costo aggiuntivo. Infatti, le fonti laser proposte per la funzionalizzazione del composito sono già ampiamente utilizzate in impianti di produzione dell'industria automobilistica. Da queste iniziali e semplici considerazioni, è chiaro come questa prospettiva sia una miscela equilibrata d'innovazione tecnologica e metodologie moderne già in uso.

A seguito di brevi introduzioni di tipo scientifico, affinché il lettore acquisisca le conoscenze di base per comprendere gli argomenti discussi, saranno presentati i materiali e i metodi seguiti in questo lavoro di tesi. Verranno inoltre mostrati i risultati sperimentali, cercando di guidare il lettore almeno virtualmente lungo i punti salienti del sentiero seguito dallo sperimentatore, in particolare descrivendo approfonditamente le criticità emerse e le ragioni che hanno mosso le singole scelte. Infine, verranno esposte le conclusioni a cui si è giunti al termine del lavoro.

2. Introduzione

2.1 Biochar

La maggior parte dei materiali commerciali a base di carbonio proviene da fonti di origine fossile, come il petrolio e il carbone, che li rende costosi, non facilmente reperibili e irrispettosi dell'ambiente. Dunque, queste motivazioni hanno portato ad una crescente focalizzazione su precursori rinnovabili derivanti da biomassa per la produzione di carbonio "green", come il Biochar, che appare come un carbone a grana fine ricco in carbonio. La biomassa è costituita da materiali organici rinnovabili derivanti da piante ed animali. Le fonti primarie delle biomasse sono rifiuti (di industrie agricole o municipali) e colture energetiche appositamente coltivate.

Quindi, il vantaggio significativo dell'utilizzo del Biochar, derivante da biomassa, è il suo basso costo.

In particolare, il Biochar è un sottoprodotto solido dei processi di decomposizione pirolitica della biomassa. La pirolisi è un processo in cui la biomassa viene riscaldata in condizioni anossiche nell'intervallo di temperatura 300-900 °C. Oltre al residuo carbonioso solido (il *char*), la decomposizione della biomassa può anche produrre liquidi (una fase organica acquosa chiamata bio-olio) e gas (una miscela gassosa, chiamata syngas, contenente CO, CO₂, H₂ ed idrocarburi) considerati come combustibili alternativi a quelli fossili utilizzati per generare calore e potenza. I risultati della decomposizione dipendono dalle caratteristiche delle materie prime e dalle condizioni del processo di pirolisi della biomassa, come la temperatura, la velocità di riscaldamento ed il tempo di permanenza.

Sebbene una notevole disponibilità di fonti sia presente in letteratura per la pirolisi della biomassa, tuttavia sembra essere ignorata e trascurata la caratterizzazione del Biochar. Il Biochar è principalmente composto da strutture in carbonio amorfico e da piani grafitici (strutture turbostratiche). I piani grafitici costituiscono la fase elettricamente conduttiva del materiale. Oltre al carbonio, il Biochar comprende anche idrogeno, ossigeno, ceneri contenenti vari minerali e quantità di azoto e zolfo. Naturalmente, la composizione elementare del Biochar varia a seconda della biomassa grezza di partenza.

L'aromatizzazione del *char* è tipicamente dovuta alla liberazione di idrogeno (deidrogenazione) e idrocarburi leggeri dalla biomassa portata ad alta temperatura (600-700 °C), che riduce i rapporti atomici H/C e O/C. Il Biochar prodotto a temperature maggiori mostra perciò una più forte occorrenza di legami C-C rispetto ai legami C-H e C-O. Questa rimozione dell'idrogeno e dell'ossigeno a temperature più elevate porta ad un arricchimento in carbonio del Biochar.

Un'ampia superficie specifica, una struttura porosa, vari gruppi funzionali superficiali e ad elevati contenuti minerali, consentono di utilizzare il Biochar come adsorbente per acqua ed inquinanti atmosferici, come catalizzatore per rimuovere catrame e NO_x o per produrre biodiesel, ed infine come concimante del terreno per migliorarne la fertilità, la disponibilità di nutrienti e la capacità di ritenzione idrica.

2.2 Compositi PP/Biochar e teoria della percolazione

Recentemente, la ricerca sui materiali sta avanzando nello sviluppo di compositi contenenti diversi rifiuti, riciclati come riempitivi rinforzanti, in particolare le biomasse. Infatti, l'uso di fillers naturali nei compositi non solo riduce i costi, ma è anche ecologico a causa della caratteristica biodegradabilità, consentendo a questi compositi di risolvere i crescenti problemi di inquinamento. Nel nostro caso, i riempitivi utilizzati come rinforzo sono fini particelle di Biochar, quindi un materiale derivato dalla biomassa. I fillers a base di carbonio sono, in generale, da tempo utilizzati come fillers per la modifica delle proprietà dei polimeri, ma il protagonista di questo lavoro è una novità assoluta.

I polimeri sono generalmente considerati elettricamente isolanti, ma le loro proprietà cambiano se vengono dispersi al loro interno fillers conduttori. Con questo procedimento, nacquero negli anni '50 compositi polimerici elettricamente conduttori, con una resistività compresa tra quella dei conduttori metallici ($10^{-7} \Omega\text{m}$) e dei materiali isolanti ($10^{-15} \Omega\text{m}$). Sono materiali relativamente poco costosi ed utilizzati per molte applicazioni ingegneristiche, quali adesivi elettricamente conduttori, pellicole o rivestimenti antistatici, materiali per schermatura elettromagnetica in dispositivi elettronici e, più recentemente, per componenti sensoristici.

La teoria della percolazione può essere applicata per spiegare il comportamento elettricamente conduttivo dei compositi costituiti da filler conduttivo e matrice isolante. Secondo questa teoria, il ruolo del filler è quello di creare una rete percolativa tridimensionale, attraverso la quale è consentito il passaggio del flusso elettronico. In pratica, con un aumento del contenuto di carica, il composito passa da un comportamento isolante ad uno conduttivo poiché le particelle vengono a contatto tramite processi di aggregazione e coagulazione, creando una rete continua all'interno della matrice. Ciò avviene quando la quantità di filler nella matrice polimerica è al di sopra di una determinata concentrazione, chiamata soglia di percolazione. La soglia di percolazione è definita su base statistica in quanto, continuando ad aggiungere carica, le singole particelle verranno staticamente ad incontrarsi, formando almeno un reticolo conduttivo per tutto il volume del composito.

Le proprietà della matrice polimerica influenzano la soglia di percolazione così come il tipo di filler conduttivo. In primo luogo, la tendenza con cui i riempitivi possono formare una rete tridimensionale è dovuta principalmente al loro fattore di forma: più il rapporto superficie/volume è elevato, maggiore è la conduttività elettrica che possono fornire.

I fillers convenzionalmente utilizzati spaziano da cariche carboniose (ad esempio nerofumo e fibre di carbonio), a polveri o fibre metalliche. Per raggiungere la soglia di percolazione con questi riempitivi, bisogna utilizzarne un contenuto fino al 10-50% in peso, dando luogo ad un composito con proprietà meccaniche non sempre desiderate e ad alta densità. In conclusione, il contenuto di carica deve essere il minore possibile, consentendo comunque al composito di soddisfare i requisiti elettrici; altrimenti, la lavorazione della miscela diventa complicata, le proprietà meccaniche del composito peggiorano e il costo finale aumenta.

Rispetto ai fillers conduttori tradizionali, i nanofillers come i nanotubi di carbonio consentono la produzione di composti conduttori con percentuali molto inferiori (spesso fino allo 0,5% in peso). Ciò è dovuto alla bassa soglia di percolazione derivante dall'elevato rapporto di forma e dall'eccellente conducibilità elettrica dei CNTs. Sebbene sia stato dimostrato come la loro introduzione in materiali polimerici possa aumentarne la conducibilità di diversi ordini di grandezza (anche superiori a dieci), i CNTs stessi sono troppo costosi ed i loro metodi di dispersione in matrici polimeriche troppo complicati; di conseguenza non possono soddisfare l'obiettivo di questo progetto. Pertanto, il presente lavoro mira a indagare l'uso di cariche carboniose meno costose, come il Biochar.

Quando si parla di Biochar, un riempitivo paragonabile a particelle con un fattore di forma inferiore ai CNTs, la soglia di percolazione aumenta. Le particelle di Biochar si assemblano per formare aggregati primari, la cui dimensione e forma ed il numero di particelle per aggregato determinano il comportamento elettrico. Analogamente a quanto visto in precedenza, quando la distanza di separazione tra gli aggregati è inferiore a quella critica, gli elettroni possono scorrere attraverso la barriera polimerica per effetto tunnel.

Una dispersione perfetta si raggiunge quando le particelle vengono separate in aggregati primari discreti. Tuttavia, nel caso di applicazioni in cui il carattere conduttivo del materiale diviene importante, una perfetta dispersione non è desiderabile. Infatti, se all'inizio della miscelazione aumenta rapidamente la conducibilità grazie alla formazione di percorsi tra gli aggregati, poi, questi cominciano ad essere distrutti aumentando il divario tra di essi. Di conseguenza, la conducibilità diminuisce gradualmente durante una miscelazione spinta.

Per tali motivi, è indispensabile prestare particolare attenzione alla progettazione delle metodologie di dispersione per l'ottenimento di composti elettricamente conduttori per evitare un'insufficiente o un'eccessiva dispersione del filler conduttivo. Anche in questo lavoro, un passo fondamentale è stato la scelta del metodo di dispersione delle particelle di Biochar nella matrice polimerica.

2.3 Fenomeno dell'ablazione laser

Esiste un'ampia varietà di tipi di laser, ognuna con le proprie caratteristiche di lunghezza d'onda della radiazione (visibile, IR, UV...), modalità di utilizzo (impulso continuo o ripetuto), efficienza e potenza. Tutti questi parametri rendono un laser in grado di soddisfare specifiche lavorative, risultanti in un'opportuna interazione con il materiale.

La scelta del tipo di laser è molto importante per il raggiungimento del livello desiderato di modifica della superficie senza alcun danneggiamento della massa del campione.

Con l'espressione "ablazione laser" s'intende la rimozione localizzata e controllata di materia da un solido dovuta alla sua interazione con una radiazione ad alta intensità. L'interazione del laser con la materia è un argomento piuttosto delicato e complesso. Questa determina la profondità raggiunta dal fascio laser e quindi la quantità di materiale rimosso da un singolo impulso e dipende dalle specifiche della radiazione elettromagnetica emessa e dalla potenza d'irraggiamento del fascio, nonché, naturalmente, dalle proprietà termiche e ottiche del materiale da trattare. Proprio a causa dei molti fattori che influenzano il processo di ablazione laser, il fenomeno che ne sta alla base non è dovuto ad un singolo meccanismo chimico-fisico. I meccanismi di ablazione polimerica possono essere essenzialmente suddivisi in due tipi (anche se nella maggior parte dei casi il processo determina una miscela dei due): meccanismo fotochimico e meccanismo fototermico. Nel primo caso, a seguito dell'eccitazione elettronica, l'energia fotonica è sufficiente a rompere direttamente i legami chimici intramolecolari. Nel secondo, l'energia immagazzinata viene rilasciata sotto forma di calore che causa il degrado termico del polimero e quindi le rotture dei legami. Un esempio di questi due meccanismi può essere trovato

rispettivamente confrontando un laser emittente nell'ultravioletto (UV) con uno che emette invece nell'infrarosso, avente lunghezza d'onda più elevata.

Nel presente lavoro di tesi è stato utilizzato un laser CO₂, emittente nel medio infrarosso. Con questa tipologia di laser, l'energia associata ai fotoni incidenti non è sufficiente a rompere i legami molecolari all'interno del materiale polimerico, ma lo è a dissociare le macromolecole con processi termici. Quando il raggio laser raggiunge il campione, la frazione di energia assorbita tende a trasmettersi per conduzione, tuttavia, essendo il materiale polimerico un isolante termico, questa energia termica rimane concentrata sulla superficie causando un locale aumento della temperatura con conseguente ablazione localizzata. Il polimero subisce una degradazione termica (se in atmosfera inerte) o termo-ossidativa (se in presenza di ossigeno) e viene rimosso dalla superficie rilasciando frammenti macromolecolari e composti volatili. Le particelle di Biochar presenti nella zona interessata dall'ablazione devono pertanto accumularsi lungo la pista, non essendo degradate alle temperature raggiunte dall'azione del laser. La rimozione localizzata della materia, dunque, espone in superficie il reticolo percolativo delle particelle di Biochar, responsabili della conduzione elettrica. Allo stesso tempo, reazioni di deidrogenazione ossidativa possono portare alla creazione di doppi legami nella matrice polimerica. Quando il numero di questi legami è sufficientemente elevato da condurre ad una loro coniugazione, la formazione di orbitali π è in grado di contribuire al trasporto elettronico agendo come connessione conduttrice tra le particelle di Biochar per raggiungere e superare la soglia di percolazione solo localmente, lungo la pista laser.

3. Materiali

3.1 Polipropilene (PP)

Come detto, la scelta della matrice polimerica per la produzione di compositi a base Biochar è ricaduta sul polipropilene (PP); questa decisione è legata a questioni industriali, infatti, nel campo automobilistico, questo materiale viene comunemente utilizzato in componenti esterne, come paraurti, e interne come cruscotti, pannelli delle portiere e condotti dell'aria.

Il polipropilene in questione è prodotto da LyondellBasell sotto forma di pellets, con il nome commerciale HOSTACOM CR 1171 G1. È un copolimero (il comonomero è l'etilene) ad alto impatto, avente un medio melt flow index, contenente il 10% di carica minerale, progettato per stampaggio ad iniezione e avente una resistenza ai raggi UV a lungo termine.

3.2 Biochar

Le particelle di Biochar, presenti nei materiali compositi trattati in questo lavoro, fanno parte della serie OSR700 fornita dal UK Biochar Research Center. In particolare, la materia prima acquistata, sotto forma di pellets, deriva da paglia di semi di colza trasformata in Biochar utilizzando un'unità di pirolisi a forno rotante in scala pilota con una temperatura nominale di

picco di 700 °C. Questo particolare Biochar è stato scelto in quanto offre la maggiore conducibilità elettrica tra quelli presenti nel catalogo del fornitore.

4. Equipaggiamento e metodi

4.1 Caratterizzazione delle polveri di Biochar

Inizialmente, i pellets di Biochar sono stati meccanicamente macinati tramite un miscelatore, per 2 minuti, fino all'ottenimento di una polvere fine. La polvere, che dovrà essere dispersa nella matrice polimerica, è stata sottoposta a caratterizzazione spettroscopica, morfologica e termica.

Misure di diffrazione a raggi X (XRD) sono state eseguite sulla polvere di Biochar utilizzando un diffrattometro Siemens D5000.

La polvere è stata analizzata al Raman, modello Renishaw inVia Reflex, per studiarne il grado di grafitizzazione.

La morfologia della polvere di Biochar è stata studiata utilizzando un microscopio elettronico a scansione ad emissione di campo (FESEM), modello Zeiss MERLIN. L'analisi microscopica FESEM è stata fondamentale per studiare la forma e le dimensioni delle particelle di Biochar.

Un'ulteriore caratterizzazione è stata poi effettuata tramite spettroscopia a dispersione di energia (EDS), impiegata per scoprire i vari elementi chimici presenti nelle polveri. Il livello di carbonio contenuto nel Biochar è il valore più significativo da indagare, in quanto è misura del suo grado di carbonizzazione. Il contenuto di carbonio dovrebbe essere molto superiore al 50% in peso, corrispondente al valore tipico del legno secco. Infatti, la pirolisi estrae l'idrogeno oltre che l'ossigeno e provoca un aumento del contenuto di carbonio nel Biochar.

Infine, si è condotta una caratterizzazione termica tramite analisi termogravimetrica (TGA), utilizzando lo strumento Mettler-Toledo TGA/SDTA 851. La TGA è stata condotta in argon con una rampa di temperatura da 25 a 1500 °C a velocità di riscaldamento di 10 °C/min, seguita da un'isoterma di 1 ora a 1500 °C. Il gas argon è stato utilizzato per avere un'atmosfera inerte e prevenire la combustione dei campioni.

4.2 Produzione dei compositi PP/Biochar

I compositi in questione sono stati ottenuti miscelando le polveri di Biochar con la matrice di polipropilene. Per avere una migliore comprensione del fenomeno conduttivo e determinare il contenuto di filler ottimale, sulla base delle proprietà elettriche riscontrate, è stato ritenuto opportuno preparare mescole con differenti contenuti in peso di Biochar: 5, 15, 30, 40%. Per ogni mescola PP/Biochar, l'abbreviazione PPnBiochar sarà adottata durante la tesi, dove n è uguale alla percentuale in peso di Biochar.

La polvere di Biochar è stata dispersa nella matrice di PP per mezzo di un miscelatore interno PlastiCorder Brabender, modello W50E o impiegando un estrusore bivite Leistritz ZSE 18 HP-

PH. Queste due diverse tecnologie sono state scelte per valutare come un diverso grado di dispersione del filler possa influire sulle proprietà elettriche del composito finale.

Le polveri di Biochar e i granuli di PP sono stati inseriti nel miscelatore interno che ha lavorato nelle seguenti condizioni: 30 giri/min durante il carico dei materiali, 60 giri/min per 3 minuti durante la miscelazione a $T = 190^{\circ}\text{C}$. Queste condizioni sono state utilizzate per tutti i tipi di mescole:

- PP tal quale
- PP +5% Biochar
- PP +15% Biochar
- PP +30% Biochar

Il materiale dal miscelatore è stato poi trasferito in una macchina pellettizzatrice, modello Piovan RSP 15/15. La pelletizzazione è necessaria per avere un materiale in ingresso adatto al successivo processo di stampaggio.

Attraverso l'estrusore bivite sono state invece processate le seguenti mescole:

- PP tal quale
- PP + 30% Biochar
- PP + 40% Biochar

I parametri di estrusione sono stati modulati di volta in volta a seconda della mescola lavorata. Aumentando la percentuale di Biochar, infatti, aumenta la viscosità del fuso, che obbliga una sempre diversa impostazione delle temperature lungo le viti per facilitare la lavorazione evitando la degradazione termica. In serie all'estrusore bivite sono stati aggiunti un bagno di raffreddamento per il passaggio del filo estruso ed un pelletizzatore per ridurlo in granuli.

Dopo aver ottenuto i granuli con uno dei metodi di cui sopra, questi sono stati stampati utilizzando una pressa per stampaggio ad iniezione Babyplast, modello 6/10P, prodotta da Cronoplast SL. Per lo stampaggio sono stati ottenuti provini ad osso di cane con dimensioni standard secondo la norma UNI ISO 527-5A: un tratto utile di lunghezza di 20 mm, larghezza di 4 mm e spessore di 2 mm.

Lungo il testo, i campioni stampati da granuli precedentemente estrusi saranno seguiti dall'etichetta "Extr", per distinguerli da quelli ottenuti tramite il miscelatore interno, chiamati "Mix".

4.3 Valutazione della soglia di percolazione

Dopo l'ottenimento dei provini di materiale composito, a questo punto è risultato necessario ricercare la soglia di percolazione per conoscere il massimo contenuto di filler al di là del quale il materiale composito conduce elettricità anche prima di qualsiasi trattamento laser. Una volta trovata la percentuale adatta alla formazione del reticolo percolativo, si sarebbe dovuta scegliere una concentrazione leggermente minore di essa per evitare conduzione elettrica anche al di fuori dalla traccia laser (l'unica area in cui la soglia di percolazione deve venire localmente superata). Per questo scopo, sono state effettuate misure di resistenza elettrica superficiale lineare su provini

ad osso di cane non ancora laserati a diverso contenuto di Biochar, utilizzando il metodo a due fili con un multimetro Keithley 2700E, avente fondo scala pari a $120\text{ M}\Omega$.

Questa caratterizzazione elettrica preliminare è stata effettuata posizionando i due puntali del multimetro direttamente su due elettrodi depositati sopra il campione ad osso di cane. Applicando gli elettrodi è possibile rendere uniforme il valore di resistenza elettrica dell'area ricoperta da essi, consentendo di conseguenza una misura di valori di resistenza molto più stabili e precisi. Per la realizzazione degli elettrodi, è stato deciso di utilizzare una vernice conduttriva a base argento, a causa della facilità di applicazione (tramite un semplice pennellino), del contenimento dei costi e della disponibilità delle apparecchiature. Dopo l'applicazione, la vernice è stata lasciata asciugare per un tempo compreso tra le 2 e le 4 ore. La deposizione degli elettrodi è stata effettuata prestando particolare attenzione al rispetto della loro geometria, per garantire la riproducibilità della misura, dipendente dalla distanza tra di essi (3 cm) e dalla loro forma (1x1 cm).

4.4 Trattamento laser

La funzionalizzazione dei materiali compositi precedentemente ottenuti per la realizzazione delle piste elettricamente conduttrive è stata effettuata utilizzando un laser CO₂, modello Towermark XL, prodotto da LASIT S.p.a.. Il laser emette radiazioni nel medio infrarosso, ad una lunghezza d'onda di 10600 nm. L'emissione elettromagnetica è pulsata con una potenza massima di 100 W.

Per evitare la combustione del materiale e portare solo ad una pirolisi indotta dall'azione fototermica del laser, tutti i trattamenti sono stati condotti in un'atmosfera inerte di azoto. Prima di ogni lavorazione, la lente focale è stata accuratamente pulita con un panno imbevuto di acetone in modo che qualsiasi residuo derivante da precedenti lavorazioni non potesse pregiudicare l'efficienza del fascio laser. Il campione è stato posto su un supporto metallico, circondato da quattro bracci che, durante la lavorazione, insufflavano azoto ed un collettore più grande che fungeva da cappa aspirante per i fumi e residui prodotti durante l'ablazione.

La comunicazione tra l'operatore e la macchina avviene tramite il software Flycad, all'interno del quale è possibile disegnare il percorso che il raggio laser ha il compito di tracciare. Il modo in cui il laser interagisce con il campione può essere regolato variando i parametri d'ingresso, che possono essere modificati dal controllo macchina. In particolare, possono essere modificati i seguenti parametri di processo: potenza (P), velocità di scansione (v), frequenza (f), numero di ripetizioni (N) e defocalizzazione (D). I valori di potenza impostati sulla macchina sono espressi come percentuale della massima potenza erogabile dal laser. La velocità di scansione rappresenta la velocità con cui il laser investe il materiale, espressa in mm/s. Il numero di ripetizioni N, invece, indica il numero di volte in cui il laser ripete lo stesso trattamento. La frequenza, in kHz, indica il numero d'impulsi al secondo. Infine, la defocalizzazione, in mm, è intesa come distanza in altezza dal punto di messa a fuoco del campione.

Il primo passo nella realizzazione di circuiti elettrici integrati nel polimero è quello di studiare il fenomeno di ablazione attraverso il quale il raggio laser e il materiale interagiscono. Il primo approccio a quest'analisi è stato effettuato utilizzando un design sperimentale che ha reso

possibile la comprensione degli effetti dei principali parametri sulla risposta relativa alla resistenza elettrica: è stato scelto un valore standard per ogni parametro laser e mantenuto costante insieme alla variazione dei restanti quattro parametri. A seguito di una prima campagna sperimentale, comprendente 32 trials, comune a tutti i composti precedentemente preparati, si sono potuti ricavare dei grafici in cui viene riportata la resistenza elettrica superficiale lineare per unità di lunghezza in funzione di uno dei cinque parametri laser da valutare. I valori standard sono stati scelti sulla base di studi precedenti, presso il CRF, su nano-compositi contenenti nanotubi di carbonio, in modo da ottenere valori superficiali di resistenza elettrica al di sotto del fondo scala del multmetro anche con trattamenti poco invasivi.

Durante gli esperimenti, è stato definito un layout sperimentale costante per ridurre la variabilità dei loro risultati. In particolare, su ciascun campione sono state tracciate sei piste parallele di lunghezza pari a 1,5 cm. Ogni trial, ovvero ogni combinazione dei parametri di processo, è stato effettuato su gruppi di tre piste (su ciascun campione sono stati eseguiti complessivamente due trials). Dai valori di resistenza misurati per ciascuna delle tre tracce ne è stato calcolato quello medio.

4.5 Caratterizzazione elettrica dei composti PP/Biochar

Dopo aver eseguito tutti gli esperimenti descritti nel precedente paragrafo, sono stati realizzati gli elettrodi alle estremità delle piste. Questa volta la vernice è stata depositata in modo da rendere gli elettrodi circolari, tutti uguali in forme e dimensioni, al fine di mantenere la loro distanza costante lungo le tracce conduttrive.

L'obiettivo è quello di ottenere il minimo valore di resistenza elettrica superficiale lineare (R) attraverso un trattamento laser che sia riproducibile e che non deformi meccanicamente il campione a livello macroscopico. Sono state effettuate misure di resistenza elettrica superficiale lungo le tracce disegnate dal laser e tra le tracce adiacenti per rilevare la risposta elettrica del composito in base al trattamento laser eseguito. Infatti, l'interazione del laser con la superficie del materiale cambia al variare dei parametri impostati, con conseguenti tracce più o meno conduttrive. Questa caratterizzazione elettrica è stata eseguita dopo ogni lavorazione, posizionando i due puntali del multmetro direttamente sugli elettrodi circolari. La presenza di condutività tra diverse piste conduttrive adiacenti e non in contatto è indesiderabile poiché un simile segnale potrebbe portare al corto circuito del componente durante la messa in opera.

A seguito del fenomeno di ablazione, vi è la formazione di un residuo carbonioso debolmente adeso al fondo della pista, di composizione non precisamente nota, che avrebbe potuto portare a risposte falsate. Perciò, prima di effettuare le misure elettriche, la superficie di ciascun campione laserato è stata sottoposta ad un processo di pulizia, comprendente l'utilizzo di un getto d'aria compressa ed il passaggio di un panno. Pur eliminando il residuo, non si esclude che una parte di questo possa essere rimasta adesa alla superficie della pista laser, contribuendo alla sua conducibilità elettrica.

4.6 Caratterizzazione meccanica dei compositi PP/Biochar

Relativamente alle proprietà meccaniche dei compositi PP/Biochar, era importante dimostrare se l'aggiunta di Biochar alla matrice polimerica avesse agito da rinforzo meccanico o meno. Di conseguenza, sono stati eseguiti test di trazione a temperatura ambiente su cinque diversi provini ad osso di cane non laserati (a fini statistici) per ogni tipo di materiale composito derivante dal miscelatore interno (PP tal quale, PP5BiocharMix, PP15BiocharMix, PP30BiocharMix). Le prove di trazione sono state eseguite con una velocità di deformazione pari a 5 mm/min, per mezzo del dinamometro MTS Criterion 43.504 avente una cella di carico pari a 5kN.

4.7 Caratterizzazione termica dei compositi PP/Biochar

La caratterizzazione termica dei campioni è risultata necessaria per valutare l'influenza del Biochar sul comportamento termico del PP. I campioni non laserati derivanti dal miscelatore interno sono stati quindi analizzati mediante Analisi Termogravimetrica (TGA) e Calorimetria Differenziale a scansione (DSC).

La TGA è stata condotta su tutti i compositi derivanti dal miscelatore interno (PP tal quale, PP5BiocharMix, PP15BiocharMix, PP30BiocharMix). Per ogni campione composito, una rampa di temperatura è stata impostata da 25 a 700 °C a velocità di riscaldamento di 10° C/min. Le misurazioni sono state condotte sia in atmosfera inerte di argon sia in aria (ambiente ossidante). I dati sono stati elaborati per creare curve TGA, utilizzate per valutare la perdita di massa e la sua dipendenza dalla temperatura.

La DSC è stata condotta in ambiente inerte di azoto sulla stessa tipologia di campioni analizzati in TGA, utilizzando il macchinario TA Instruments Q100 DSC. Ogni campione è stato sottoposto a tre cicli termici, ognuno composto da una rampa di riscaldamento e di raffreddamento a 10 °C/min: da -50 °C a 200 °C in salita e consecutiva discesa. Il primo ciclo è stato eseguito per eliminare la "storia termica" del materiale, mentre il secondo ha fornito le varie temperature di transizione, dati confermati dal terzo ciclo. Di conseguenza, le informazioni sono state estratte dal secondo ciclo.

4.8 Caratterizzazione morfologica dei compositi PP/Biochar

Il grado di dispersione delle particelle di Biochar nella matrice polimerica è stato valutato utilizzando il microscopio ottico Leica DMI 5000 M, in seguito alla lucidatura della superficie dei campioni ad osso di cane non laserati derivanti dal miscelatore interno (PP tal quale, PP5BiocharMix, PP15BiocharMix, PP30BiocharMix).

I campioni, uno per ogni percentuale di Biochar (PP5BiocharMix, PP15BiocharMix, PP30BiocharMix, PP40BiocharExtr), che dopo il trattamento laser hanno dato le risposte più promettenti in termini di resistenza elettrica superficiale lineare per unità di lunghezza, sono stati sottoposti ad ulteriore caratterizzazione morfologica al FESEM precedentemente visto nella caratterizzazione del Biochar. Le tracce laser sono state esaminate al FESEM per determinarne meglio la morfologia al variare del contenuto di Biochar.

5. Risultati sperimentali e discussione

5.1 Caratterizzazione delle polveri di Biochar

Lo spettro di diffrazione delle polveri ha testimoniato la presenza di un certo grado di grafitizzazione che potrebbe spiegare un concreto livello di conducibilità elettrica. Infatti, lo spettro conferma la tipica struttura dei materiali carboniosi a base di grafite, con picchi appartenenti alla grafite 2H ed a quella esagonale. Tuttavia, la minore quantità di grafite esagonale spiegherebbe la conducibilità elettrica inferiore del Biochar rispetto a un materiale completamente grafitico. Esistono inoltre dei picchi che possono essere ricondotti a materiali di natura inorganica, probabilmente derivanti dalla biomassa di partenza.

Il Raman ha confermato la presenza di un ragionevole grado di grafitizzazione e un certo livello di disordine (amorfismo), data la natura del materiale stesso.

Come risultato dal FESEM, si è visto che le particelle sono molto irregolari sia in forma che dimensione. Infatti, esse si presentano con forme arrotondate, ma talvolta anche allungate o sottoforma di placchette. La loro dimensione varia da poche centinaia di nanometri a poche decine di micron.

Lo spettro EDS ha fortunatamente confermato un'elevata percentuale di carbonio (circa 83% in peso), con tracce di altri elementi derivanti dalla biomassa di partenza.

La conducibilità elettrica delle polveri di Biochar è influenzata dal contenuto di volatili. I volatili sono presenti nei pori del Biochar ed ostacolano la conduzione elettrica. La TGA ha fornito la prova che il campione contiene quasi il 10% in peso di contenuto volatile che evacua durante il riscaldamento fino a 700 °C. Successivamente, un residuo del 73% viene ottenuto con il riscaldamento fino a 1500 °C e dopo un'ora questo scende al 69%.

5.2 Produzione dei compositi PP/Biochar

Nonostante l'elevato contenuto di fillers, sorprendentemente, il filo in uscita dell'estrusore non ha mostrato la fragilità attesa. Anche tutti i provini sono stati stampati con facilità. Ciò ha dimostrato la possibilità di caricare il polipropilene anche in percentuali del 40% di Biochar.

5.3 Valutazione della soglia di percolazione

Sfortunatamente, nessun provino non laserato ha mostrato una resistenza superficiale lineare inferiore al fondo scala del multmetro. Per questo motivo, non è stato possibile trovare la soglia di percolazione, né scegliere di conseguenza la concentrazione ottimale di Biochar da utilizzare nei campioni da laserare. I risultati suggeriscono una distribuzione non omogenea di Biochar all'interno del campione. Infatti, la concentrazione di filler è maggiore nella massa dei campioni e minore nelle loro parti esterne. Queste tendenze possono essere spiegate considerando la presenza di pelle polimerica formata a seguito del raffreddamento preventivo della mescola sulla parete dello stampo.

5.4 Valutazione dell'influenza della variazione dei parametri laser sulla conduttività elettrica

Inizialmente, è stata testata l'influenza della variazione del parametro potenza (P). È stato subito osservato che i risultati ottenuti sono molto diversi a seconda dei valori di potenza impostati per il fascio laser. Le resistenze ottenute variano ad esempio da $50,84 \text{ M}\Omega/\text{cm}$ ($P = 5\%$) a $11,63 \text{ M}\Omega/\text{cm}$ ($P = 35\%$) per lo stesso composito PP30BiocharMix. Questa tendenza mette in evidenza l'importanza dell'identificazione del trattamento laser più appropriato per rivelare il carattere conduttivo del materiale e come non ci si possa semplicemente accontentare di una mera ablazione della pelle polimerica. Piuttosto, è necessario ottimizzare l'interazione in modo che tutti i parametri contribuiscano sinergicamente e comportino una resistenza elettrica superficiale lineare minima. Inoltre, da questi primi esperimenti, sembra che i composti PP/Biochar rispondano bene al trattamento laser e siano adatti ad un'ottimizzazione dei parametri. È infine necessario segnalare come tutti i campioni siano conduttori solo lungo le tracce e non tra di esse. La prime misure di resistenza elettrica superficiale lineare per unità di lunghezza (ottenute dividendo R per gli 1,5 cm di lunghezza della traccia) indicano che i valori misurabili (dell'ordine dei $\text{M}\Omega/\text{cm}$) possono essere ottenuti aumentando la P per tutti i composti. Ciò significa che quando il valore di potenza impostato aumenta, il valore medio di resistenza elettrica diminuisce e questo è in linea con quello che ci si aspetterebbe. Infatti, per l'ablazione laser, maggiore potenza indica una quantità più significativa di materiale polimerico isolante rimosso aumentando la concentrazione locale del filler conduttivo. Aumentando i valori di potenza, tuttavia, le tracce sono molto profonde, in quanto il laser interagisce maggiormente con il composito e questo potrebbe essere un limite applicativo per dispositivi a basso spessore.

A parità di trattamento laser, si registra una diminuzione della resistenza elettrica all'aumentare della percentuale di filler contenuta nella matrice polimerica. Infatti, con le stesse condizioni operative, si ottengono minori valori di R sui composti contenenti percentuali più elevate di Biochar. Questo è largamente in accordo con le previsioni sperimentali. Infatti, un incremento del contenuto di particelle di Biochar rende più facile la possibilità che esse vadano in contatto e formino una o più reti percolative responsabili della conduzione elettrica. È evidente come riducendo il contenuto di Biochar nel composito, sia più difficile raggiungere valori di R sufficientemente piccoli da ottenere materiali competitivi con i moderni dispositivi metallici. In particolare, per determinare l'insieme dei parametri che conducano a valori di R prossimi a $1 \text{ M}\Omega/\text{cm}$ anche con basse percentuali di Biochar, è necessario imporre condizioni operative di P, v, N, f e D che producono tracce molto ampie e profonde. Ciò può causare in molti casi anche la deformazione del campione, ovviamente indesiderabile per un'ipotetica industrializzazione del prodotto.

Mentre da un lato i composti PP30BiocharMix presentano un decadimento regolare di R con un aumento di P, dall'altro, i composti PP5BiocharMix e PP15BiocharMix hanno una tendenza più irregolare e valori di R significativamente più elevati. I composti PP5BiocharMix e PP15BiocharMix mostrano, per molti trattamenti laser, segnali elettrici al di sopra del fondo scala dello strumento ($80 \text{ M}\Omega/\text{cm}$). Inoltre, i loro valori di resistenza elettrica sono molto variabili a seconda della pressione esercitata con il panno durante la fase di pulizia delle piste successiva al trattamento. Ciò potrebbe significare una scarsa adesione tra le particelle di Biochar e la matrice

polimerica. A seguito delle considerazioni appena descritte, riguardanti i compositi con percentuali minori, si è concluso che questi materiali non fossero idonei per questo lavoro di tesi. Le piste su PP30BiocharExtr seguono lo stesso trend di R del PP30BiocharMix al variare dei parametri laser. PP30BiocharMix, tuttavia, si è rivelato più conduttivo di PP30BiocharExtr. Infatti, durante la miscelazione nell'estrusore bivite, gli aggregati iniziano a rompersi aumentando il divario tra le particelle. Comunque, i campioni PP30BiocharExtr appaiono meno fragili dei PP30BiocharMix a causa di una migliore dispersione del filler raggiungibile tramite il processo di estrusione.

La R delle tracce in PP40BiocharExtr diminuisce molto più velocemente rispetto a tutti gli altri compositi anche dopo trattamenti laser poco invasivi. Sebbene questo possa sembrare un buon risultato, sono sorti due problemi principali. Innanzitutto, la resistenza elettrica raggiunge un plateau, proprio come avviene con i campioni PP30BiocharMix e PP30BiocharExtr. Ciò è presumibilmente indicativo del fatto che il Biochar ha un limite fisico di resistenza elettrica e quindi è difficile diminuire ulteriormente la R di questi compositi semplicemente aumentando il contenuto di filler. Il secondo problema riguarda la presenza di conducibilità tra piste adiacenti. Infatti, purtroppo, tutti gli esemplari hanno mostrato valori di R inferiori al fondo scala del multimetro. È importante sottolineare che se non è possibile ottenere un segnale elettrico tra tracce non continue superiore al fondo scala, è inutile cercare un'ottimizzazione dei parametri laser per i compositi PP40BiocharExtr. Infatti, anche se il valore di resistenza trovato potrebbe essere migliorato, la presenza di un trasporto di corrente elettrica tra tracce adiacenti non renderebbe il materiale idoneo per l'impiego in circuiti elettrici. Per questi motivi, i compositi PP40BiocharExtr sono stati automaticamente esclusi da ulteriore sperimentazione.

I risultati finora esposti saranno simili anche per gli esperimenti successivi, in cui sono stati fatti variare v, N, f e D: i compositi caricati al 5 e 15% di Biochar portano a valori di R imprevedibili e poco ripetibili, i campioni PP30BiocharMix mostrano i minori valori di resistenza elettrica in assoluto, senza considerare il PP40BiocharExtr che mostra conducibilità interpista.

La velocità di scansione (v) del laser è un altro parametro che influenza la conducibilità e la morfologia delle tracce laser. Dagli esperimenti, è subito emerso come al diminuire della v la resistenza elettrica diminuisca. Questo trend è stato prevedibile in quanto a basse v il fascio laser interagisce più a lungo con la superficie del campione, con conseguente ablazione più duratura ed impattante. Al contrario, aumentando la v, la R aumenta come conseguenza di una minor quantità di polimero rimossa, anche se morfologicamente le tracce sono meno profonde e irregolari di quelle ottenute a velocità meno elevate.

Tramite il trial 11 si è conseguito il più basso valore di R tra tutti i test eseguiti in questo lavoro, precisamente un valore di $1,11 \text{ M}\Omega/\text{cm}$ per i campioni PP30BiocharMix. Questo trial è associato a velocità di scansione molto basse (20 mm/s) ed infima potenza (10%). Da questi valori, si comprende come v abbia un peso maggiore rispetto alla P, infatti, sono stati raggiunti valori di R di un ordine di grandezza inferiore rispetto a quelli in cui veniva fatta variare la potenza. Sebbene la potenza fosse impostata quasi al suo valore minimo, dare un tempo adeguato al raggio laser per

poter interagire con il materiale è sufficiente ad ottenere valori di resistenza di poche unità di $M\Omega/cm$.

È possibile ripetere più volte il trattamento ripassando il fascio laser sulla stessa traccia. Il numero di ripetizioni (N) è risultato essere uno dei parametri che influenzano maggiormente i valori di conducibilità raggiunti sui compositi PP/Biochar.

Vi è una marcata riduzione della resistenza al crescere di N. Modificando il numero di ripetizioni, sono stati raggiunti valori di R pari a $2,5 M\Omega/cm$ (20 ripetizioni) per i PP30BiocharMix. Ciò conferma come N sia il secondo parametro più influente sulla conducibilità delle tracce. In generale, l'incidenza di questa variabile è maggiore nelle prime ripetizioni; per esempio, la R diminuisce poco dalla settima ripetizione in poi. Ovviamente, all'aumentare di N, le tracce diventano più profonde, come conseguenza di successivi passaggi del laser sulla superficie del materiale.

La frequenza (f), che rappresenta il numero di impulsi laser al secondo, è stata la variabile meno influente riguardo sia i valori di resistenza elettrica che la qualità morfologica della pista. Alla frequenza di 0,1 Hz, la pista non è stata scavata omogeneamente ma presentava scanalature lungo tutta la sua lunghezza a causa della bassa frequenza con cui il laser aveva investito la superficie del composito durante la sua corsa. A frequenze superiori ai 5 kHz, la traccia è risultata più omogenea e la R è rimasta quasi costante. Il valore di resistenza minimo ottenuto è stato pari a $22,7 M\Omega/cm$ ($f = 50kHz$) sui PP30BiocharMix.

Il punto focale rappresenta l'area in cui esiste una maggiore interazione tra il laser e la superficie del campione. La defocalizzazione (D) del fascio sulla superficie del campione, indicante la distanza in altezza, in mm, dal punto di messa a fuoco sul campione, ha portato verso risultati imprevedibili. Infatti, mantenendo gli altri parametri costanti, il trend di R in funzione della D del fascio appare irregolare, con punti di minimo e massimo inaspettati. Da un punto di vista qualitativo, le tracce laser ottenute con valori di D maggiori sembrano essere molto diverse da quelle ottenute con D nulla. Infatti, sono molto più ampie e meno profonde, grazie alla proiezione più estesa del fascio sulla superficie dei campioni ed alla minore interazione tra radiazioni e materia. Da un lato, una pista più ampia ha meno resistenza, ma dall'altro, la sua profondità inferiore compensa questo effetto; ciò spiegherebbe la casualità nei valori di R riscontrati. Il minor valore di R è stato pari a $7,78 M\Omega/cm$ ($D = 60 mm$) sui campioni PP30BiocharMix.

A seguito di una corretta comprensione del modo in cui i singoli parametri sono stati responsabili dei valori di R trovati, si è deciso di continuare il lavoro sperimentale puntando direttamente allo scopo di questa ricerca: ottenere il minimo valore di R possibile. L'ottimizzazione dei parametri laser è stata eseguita solo sui campioni PP30BiocharMix, che si sono rivelati essere i materiali più adatti per l'obiettivo sopra menzionato. I valori dei parametri che avevano portato ad un valore di R oltre il quale la tendenza della curva corrispondente si stabilizzava (sembrava arrivare ad un asintoto) sono stati scelti come "nuovi parametri standard". Per ottimizzare i risultati sul materiale PP30BiocharMix, i nuovi parametri standard sono stati

mantenuti costanti, facendo variare i rimanenti quattro (analogamente a quello fatto per i trials da 1 a 32).

Se non ci si focalizza eccessivamente sui trend delle curve di R in funzione del parametro laser da valutare, ma piuttosto sui valori trovati in questa campagna sperimentale, si può notare che essi si aggirano attorno a poche unità di $M\Omega/cm$, ma non scendono mai al di sotto di 1,11 $M\Omega/cm$ ottenuto con il trial 11. Sembra, pertanto, che il composito PP30BiocharMix abbia raggiunto una soglia di resistenza elettrica sotto la quale sia proibito andare. Questo potrebbe essere dovuto ad un limite di conducibilità elettrica intrinseca del Biochar e non ad una scarsa modulazione dei parametri laser. Infatti, gli ultimi trattamenti, a seguito di un'ispezione visiva dei campioni, si sono dimostrati molto invasivi e tante volte hanno portato alla perforazione del campione. Dunque, non ci sono stati ulteriori incentivi nella scelta dei parametri laser al fine del raggiungimento di risultati migliori.

Al termine di questa parte del lavoro sperimentale, è stato chiaro come le ipotesi iniziali circa la sostituzione del cablaggio metallico con un mono-materiale economico in grado di trasportare segnale elettrico siano difficili da mettere in pratica. Il valore di resistenza ottenuto è comunque sufficiente a consentire il passaggio di corrente in tutte quelle applicazioni in cui sono richieste proprietà antistatiche. Inoltre, il valore di resistenza fra tracce adiacenti oltre il fondo scala del multimetro rende questa tecnologia facilmente gestibile da un'elettronica semplice e poco costosa.

5.5 Caratterizzazione meccanica dei composti PP/Biochar

I risultati delle prove meccaniche suggeriscono una diminuzione della duttilità dopo l'aggiunta del filler: la deformazione a rottura crolla anche con una piccola aggiunta del 5% di Biochar. C'è anche una tendenza decrescente per la resistenza a trazione all'aumentare del contenuto di Biochar, seppur meno drastica. L'aggiunta di Biochar aumenta, al contrario, il modulo elastico, a causa della rigidità intrinseca delle particelle.

Tali risultati sono probabilmente anche dipendenti dal basso grado di dispersione del Biochar all'interno della matrice polimerica. Infatti, al fine di ottenere un rinforzo meccanico, è necessario prestare particolare attenzione al grado di dispersione del filler all'interno della matrice per fornire un'interfaccia polimero/Biochar che possa trasferire il carico applicato dalla matrice al rinforzante. Tuttavia, il rafforzamento meccanico non è lo scopo di questo lavoro, che invece mira ad aumentare una prestazione funzionale per la quale spesso un'eccessiva dispersione e distribuzione del filler non è richiesta. Infatti, ciò porterebbe a fenomeni di conduzione elettrica anche tra piste adiacenti, con conseguente compromissione della possibilità di realizzare circuiti integrati.

5.6 Caratterizzazione termica dei composti PP/Biochar

Per quanto riguarda i risultati della TGA condotta in ambiente inerte, per tutti i materiali la degradazione termica avviene in un unico step a partire da circa 400 °C. Ciò significa che non c'è stato un miglioramento della stabilità termica con l'aumento della quantità di Biochar aggiunta. Al PP tal quale è associato un residuo di circa il 14% in peso dovuto al filler inorganico già

presente in esso. Tutti i compositi mostrano un residuo più elevato derivante dall'esistenza del Biochar che non degrada alle temperature di prova, sebbene ci sia una piccola percentuale volatile di esso che viene persa. La percentuale di residuo è, per tutti i compositi analizzati, in accordo con la teoria in quanto aumenta al crescere della percentuale di Biochar, che non brucia in atmosfera inerte.

I grafici della TGA condotta in aria seguono la stessa tendenza di quelli in atmosfera inerte. Infatti, il meccanismo di degradazione di tutti i materiali inizia a circa 350 °C e si verifica sempre in un unico step. L'unica differenza è che tutti i residui organici (il Biochar tra tutti) sono consumati a circa 700 °C per combustione con l'ossigeno contenuto nell'aria e successiva formazione di prodotti volatili. In tutti i compositi vi è un residuo finale del 14% in peso costituito dal filler inorganico che è immune al processo di combustione.

Dall'analisi delle curve DSC, si deduce come i compositi siano tutti semicristallini: i due picchi in cima alla curva corrispondono alla cristallizzazione, mentre quelli inferiori alla fusione. I picchi di minore intensità appartengono al PE, mentre quelli di maggiore al PP, in quanto il materiale in questione è un copolimero. All'aumentare del contenuto di Biochar, non si osserva alcuna modifica nelle due temperature di transizione del polimero, né tantomeno nella sua percentuale di cristallinità, suggerendo che non vi è stato un miglioramento delle prestazioni termiche, ma, molto più importante, nessun crollo della proprietà.

5.7 Caratterizzazione morfologica dei compositi PP/Biochar

Dalle microografie dei campioni analizzati al microscopio ottico è possibile vedere che, anche se le particelle sono ben distribuite all'interno della matrice, queste non sono disperse omogeneamente all'interno della stessa. Infatti, molti agglomerati non sono stati frantumati durante il processo di miscelazione con la matrice polimerica nel Brabender. La presenza di aggregati potrebbe spiegare i bassi valori di deformazione a rottura e resistenza a trazione di questi compositi.

Dalle analisi al FESEM, si nota come ai bordi delle piste laser vi è la prova di un accumulo di materiale probabilmente dovuto alla fusione localizzata e all'innesto di un flusso viscoso della matrice polimerica. È anche possibile notare che la zona più profonda delle piste si trova al centro, punto di maggiore interazione tra il laser e il materiale.

Ingrandimenti del campione PP5BiocharMix mostrano la quasi totale assenza di particelle di Biochar, dimostrando come un reticolato percolativo non possa mai essere raggiunto con queste piccole percentuali di filler. Infatti, la microografia è molto simile a quella di un polimero non rinforzato.

La pista sul campione PP15BiocharMix sembra essere più ruvida, dimostrando la presenza di una maggior quantità di filler nel materiale carbonizzato, che contiene, oltre al Biochar, quelle strutture coniugate responsabili della conducibilità della traccia.

Nella microografia della traccia incisa sul campione PP30BiocharMix è facile notare l'alta opacità della pista a causa dell'enorme quantità di riempitivo ora disponibile. Ad elevati ingrandimenti

compaiono anche gli aggregati di Biochar. Focalizzandosi sulle pareti laterali della pista, è possibile notare le particelle di Biochar emergenti dalle pareti stesse.

Ingrandimenti di una pista tracciata su PP40BiocharExtr dimostrano ancora la presenza degli agglomerati delle particelle di Biochar, ma in una maggiore concentrazione rispetto al precedente composito.

6. Conclusioni

Il lavoro svolto in questa ricerca sperimentale ha portato alla realizzazione di circuiti elettrici, integrati in un materiale polimerico inizialmente isolante, da incorporare nella plancia di autovetture o in altri componenti interni. Questo obiettivo è stato raggiunto tramite l'aggiunta di Biochar (dal 5% al 40% in peso) all'interno di una matrice in polipropilene, e tracciando piste conduttrive attraverso l'interazione diretta tra un fascio laser CO₂ e la superficie del materiale.

Le mescole di varie composizioni sono state ottenute usando un miscelatore interno o un estrusore bivite. Si è ricorso a queste due diverse tecnologie per valutare come un diverso grado di dispersione del filler possa influire sulle proprietà elettriche del composito finale. I pellets ottenuti sono stati quindi sottoposti a stampaggio ad iniezione per produrre provini ad osso di cane da sottoporre a trattamento laser. Il lavoro sperimentale è proceduto per raggiungere una maggiore comprensione del fenomeno di interazione tra il fascio laser ed il materiale, al fine di identificare i parametri che influenzano maggiormente le prestazioni del materiale. Gli effetti dei vari parametri sono stati valutati in base al valore di resistenza elettrica superficiale lineare (R) delle piste laser osservato. Il lavoro si è concluso con una caratterizzazione termica, meccanica e morfologica dei materiali ottenuti.

Lo sviluppo industriale di questa tecnologia offrirebbe la possibilità di realizzare circuiti elettrici integrati in polimeri permettendo di sostituire una parte dei cablaggi metallici utilizzati al giorno d'oggi, con un conseguente vantaggio in termini di leggerezza, resistenza alla corrosione e certamente anche riduzione dei costi. L'utilizzo di un materiale composito a matrice polimerica assicura anche un processo di produzione semplice e la possibilità di riciclo al termine del ciclo vita.

Parte del lavoro sperimentale ha contribuito in parte alla conferma delle conclusioni già tratte dai precedenti studi effettuati dal CRF, deducendo così l'unicità dell'interazione tra il fascio laser ed il materiale. I valori di resistenza elettrica misurati e la morfologia delle piste si sono dimostrati essere fortemente dipendenti dai parametri laser impostati. Si è concluso che la variabile più influente è la velocità di scansione del laser. Infatti, poiché l'effetto che si vuole ottenere non è solo quello di eliminare il primo strato superficiale di polimero, è necessario garantire un tempo sufficiente (basse velocità di scrittura) a far penetrare il fascio laser nel polimero e farlo interagire con esso. Entrando più nei dettagli, l'azione del laser CO₂ sulla superficie del composito produce un aumento localizzato della temperatura. Il riscaldamento causa l'attivazione di un flusso viscoso che comporta l'accumulo di materiali ai bordi della

traccia, contribuendo anche al degrado della matrice polimerica mediante la rimozione di frammenti macromolecolari e la formazione di prodotti volatili. La formazione di nuove strutture carboniose indotte dall'ablazione fototermica del laser si aggiunge alla rete conduttriva delle particelle Biochar.

I trattamenti che causano una maggiore interazione del fascio laser con la superficie del materiale danno vita a tracce con maggiore conducibilità. Ma la conducibilità elettrica è strettamente correlata al contenuto di Biochar oltre che alle condizioni di lavoro, infatti, con lo stesso set di parametri, sono stati ottenuti inferiori valori di R per i compositi contenenti un maggior quantitativo di Biochar. Con quantità troppo piccole di filler (5% e 15% in peso), è difficile ottenere tracce con una sufficiente conducibilità da immaginare un loro impiego in dispositivi commerciali attraenti. Tra questi materiali, solo i compositi caricati con il 30% hanno dimostrato di raggiungere, mediante trattamenti laser che non portano alla deformazione del campione, valori di R di circa $1 \text{ M}\Omega/\text{cm}$ (necessari per il trasporto del segnale elettrico) e valori di R tra tracce adiacenti al di sopra del fondo scala del multimetro utilizzato per le misurazioni. I materiali caricati con il 40% di Biochar non solo hanno portato agli stessi valori di resistenza di quelli al 30%, ma hanno mostrato una conduttività tra tracce adiacenti: un effetto indesiderato che porterebbe al cortocircuito del sistema. Pertanto, la ricerca è proseguita sui materiali caricati al 30%.

I campioni stampati da granuli derivanti dal miscelatore interno Brabender sono stati leggermente più conduttrivi di quelli derivanti dall'estrusore bivite. Infatti, durante la miscelazione nell'estrusore, gli aggregati iniziano a rompersi aumentando il divario tra le particelle. Quindi, se con l'estrusore si riesce ad ottenere una migliore distribuzione delle particelle all'interno della matrice polimerica, è anche vero che questo processo porta ad una dispersione eccessiva (rottura degli aggregati) non desiderata. Mentre queste maggiori dispersioni e migliori distribuzioni regalano una minor fragilità al composito, per contro, ostacolano la formazione di un reticolo percolativo peggiorando, di conseguenza, la conducibilità elettrica.

Tuttavia, dopo l'ottimizzazione dei parametri laser sui provini al 30% derivanti dal miscelatore, la conducibilità elettrica dei compositi non è scesa al di sotto di $1 \text{ M}\Omega/\text{cm}$. Questo potrebbe anche essere dovuto al basso fattore di forma delle particelle di Biochar, come si è potuto evincere dalla caratterizzazione microscopica delle polveri, che spiegherebbe la difficoltà nel formare un reticolo percolativo all'interno della matrice polimerica. Questi valori di R sono ancora troppo elevati per la realizzazione di circuiti integrati, ma possono essere adatti per tutte quelle applicazioni che richiedono proprietà antistatiche (sistemi per trasporto di combustibile e alimentazione carburante). Basti pensare a quelle materie plastiche che se accumulassero cariche e arrivassero a contatto con la benzina, condurrebbero ad un innesco della stessa.

In conclusione, i risultati ottenuti sono innegabilmente confortevoli: è stato possibile rendere un materiale isolante elettricamente conduttivo solo localmente impiegando un filler "green" estremamente economico. È stato certamente fondamentale aver dimostrato che la strada per la produzione di "cablaggi polimerici", anche se ancora lunga, si estende sotto i migliori auspici.

Prima di renderne possibile un'industrializzazione, sarebbe opportunamente utile intraprendere uno studio approfondito dell'influenza delle condizioni di lavoro e dei processi produttivi sulla conducibilità del campione. Un punto debole per l'applicazione di questa tecnologia potrebbe essere l'irripetibilità della sperimentazione, poiché si sa poco circa il meccanismo di interazione laser-materia e su come il processo produttivo influenzi questa interazione. Gli sviluppi futuri potrebbero quindi concentrarsi su uno studio approfondito dell'interazione, seguito da una caratterizzazione del residuo carbonioso e delle specie responsabili del comportamento conduttivo. O ancora, si potrebbe studiare il processo su un materiale diverso, che abbia più affinità con le particelle di Biochar, facilitando perciò la loro distribuzione all'interno della matrice. Ma l'operazione più convincente sarebbe quella di diluire il Biochar con altri riempitivi funzionali, come i nanotubi di carbonio, anche se ciò aumenterebbe i costi di produzione. Questa scelta è dovuta all'impossibilità di scendere a valori inferiori a $1 \text{ M}\Omega/\text{cm}$ di resistenza elettrica anche dopo l'ottimizzazione dei parametri laser, proprio come se si fosse raggiunto un limite di conducibilità intrinseca delle particelle di Biochar. Senza il coinvolgimento di altri riempitivi oltre al Biochar, una grande soluzione futura per il CRF sarebbe quella di utilizzarne una tipologia maggiormente conduttiva, ottenuta mediante trattamenti termici o acquistata da altri fornitori.

Infine, è possibile valutare l'utilizzo di questi materiali compositi anche come sensori di pressione valutando le loro proprietà piezoresistive. Infatti, questa ricerca è stata portata avanti presso il CRF con ottimi risultati su materiali compositi contenenti CNTs. La combinazione del comportamento conduttivo con quello piezoresistivo renderebbe possibile la produzione di un circuito completo e privo di metallo direttamente su un materiale isolante, integrando anche il rispettivo pulsante.

La conducibilità elettrica di piste "metal-free" tracciate mediante ablazione laser su un composito a matrice polimerica caricato con particelle di Biochar è un campo finora inesplorato. La speranza è che questo lavoro sia solo il primogenito di una lunga lista di sviluppi futuri atti ad ottimizzarne il processo produttivo, e che possa contribuire ad una migliore comprensione del fenomeno per arrivare, un giorno, ad una produzione industriale di questa classe di materiali compositi.

Preface

The aim of the present work is the realisation of electrical circuits, integrated by functionalization with laser ablation into a polymeric material loaded with conductive fillers, to use them on car interiors such as dashboard modules and door panels. Of course, particular attention must be paid to the use of cheap materials, so that they can compete with the price of copper traditionally used in wiring. The project is born in collaboration between the Politecnico di Torino and the *Smart Materials Lab* of the *Polymer and Glass Department* at Centro Ricerche Fiat (CRF) in Orbassano. CRF is one of the major technological innovation pillars of the Italian landscape, a pole that excels in research and development in the automotive field.

The automotive industry Fiat Chrysler Automobiles (FCA) invests most of its resources in technological research to reduce the number of materials used in the vehicle construction, thus reducing the weight, the cost, the energy consumption, and the environmental impact. For this to be possible, they are focusing towards the concept of "mono-material," that is a material containing in itself several functions. Therefore, these materials fall into the category of "*smart materials*," which are materials that have one or more properties (functionalities) that can significantly change by external stimuli (stress, temperature, pH, moisture, electric or magnetic fields).

Like previously stated, the protagonist of this work is a mono-material which has to act as an electrical conductor. More precisely, it will be the same plastic, constituting the automobile interiors, to exhibit both structural and electrical functions. This kind of materials has to show electrical conductivity to be able to perform signal transfer allowing the ignition of an electric load for the activation of in-vehicle devices or to have antistatic properties when used for parts in contact with fuel system components. But at the same time, they should be light and also manufactured in complex shapes: both features belonged to polymeric materials. The choice of polymer matrix for this purpose is affected by polypropylene (PP) since it is the material most used for the realisation of both external and internal components of the car.

As far as the fillers are concerned, in earlier works at CRF, they have tried to use carbon nanotubes (CNTs), with acceptable results regarding electrical conductivity. In fact, over the last decade, carbon nanotubes have been exploited as high performance fillers for the production of polymer composites with high tensile properties, thermal stability, and electrical properties. This last feature can enable the use this new class of nanocomposite as sensors, capacitors, batteries, and many other electrical applications.¹ But the real problem of these composites is the high cost of the manufacturing process of CNTs themselves, estimated to be greater than that of the traditional copper wires, without considering the difficulty of their dispersion in a polymer matrix. So in this work, we have tried to functionalize the polymer matrix with more economic carbonaceous fillers, with the hope that they could replace the CNTs for this type of applications.

In particular, it appeals to the use of bio-carbon, commonly known as Biochar, which is the remaining solid product obtained from the carbonisation of biomass. The great challenge of this work of thesis is to make polymers conductive with a filler that finds virtually no acknowledgement in the literature. In fact, traditionally, Biochar is used as a solid fuel for combustion where electrical conductivity is largely irrelevant and ignored: the research on using Biochar as reinforcement of polymeric materials to enhance various properties is insufficient. But this reason has given the strength to carry out this research work with motivation.

Although the electrical insulating behaviour of PP and polymeric materials, in general, is well known, the challenge of this research is to make them conductive only at those points where a laser beam strikes the material. The interaction of the laser beam with these materials causes a localised electrical resistance lowering, thus leading to the realisation of electrical circuits. The laser parameters (power, scan rate, defocus, frequency and repetition number) to be set to perform the machining must be varied for the production of the tracks intended for electrical signal transfer. This technique, specifically designed for integration in dashboard modules, is extremely versatile and potentially applicable to other parts of the car in the future, especially for the possibility of bringing the electrical signal into difficult areas of interior components. The method described in this research work is quick and flexible and would not result in any additional economic value since the laser sources, proposed for the functionalisation of the composite, are already widely used in production facilities in the automotive industry. From these straightforward and initial considerations, it is clear that this future vision is a balanced blend of technology innovation and modern methodologies already in use.

After a brief scientific introduction, for the reader to acquire the basic knowledge for understanding the topics discussed, the materials, the techniques and the methods underlying this thesis work will be presented. Subsequently, the experimental results will be submitted, trying to guide the reader to at least virtually rethink the salient points of the path followed by the author of this work, specifically trying to convey the critical issues found and the reasons behind individual choices. Finally, the appropriate conclusions will be proposed.

1. Introduction

1.1 Biochar

Nowadays, energy is a cardinal element in the quality of our livelihood, and it is a protagonist in all sectors of the modern economy. Moreover, the worldwide energy demand by 2050 is expected to double compared to today's consumption level.² Unfortunately, is well-known how the combustion of fossil fuels like gasoline, coal and natural gas traditionally employed as an energy resource has led to both environmental and geopolitical issues. In fact, the CO₂ generated by their combustion is believed to be responsible for global warming and climate change, together with the formation of air pollutants, such as SO_x and NO_x. In addition to these global environmental problems, fossil fuels exhaustion and the increasing oil price are pushing towards the development of renewable and sustainable energy sources.³ In order to solve these growing problems, an absolute attention is now turning to the use of biomass, consisting of renewable organic materials derived from plants and animals. Hence, these natural sources of energy range from living organisms up to the excrement of animals or waste wood.³ The primary sources of biomass are wastes (such as agricultural industries wastes and municipal wastes) and purposely-grown energy crops.⁴ Biomass is made up of carbohydrate, and it is chemically composed of carbon, hydrogen, oxygen, nitrogen and traces of sulphur and chlorine. In particular, woody biomass contains lignocellulosic materials like hemicellulose, cellulose and lignin, contained in varying proportion according to the derivation from one plant species to another, and small amounts of pure sugar, protein, starches and lipids.⁴ Biomass is considered as a potential replacement of fossil fuel for two main reasons, without regard to the fact that it is renewable. The first one consists of the compensation between the CO₂ emitted from combustion of biomass and that assimilated during the photosynthesis of plants. The second one is due to a lower content of sulphur and nitrogen in biomass, resulting in fewer pollutants formation in the atmosphere.³

In recent years, an ever-expanding field is that on the research and development of green carbon materials, especially those having the potential for agro-industrial waste mitigation. Most of the commercial carbon materials come from a fossil fuel based precursor, such as petroleum and coal, which makes them be expensive, non-readily available and environmentally non-friendly.⁴ Therefore, those motivations have brought to an increasing focus on renewable biomass precursors for the production of green carbon material like Biochar, which has found many outstanding applications in various areas because of its versatile physicochemical properties.² Biochar is a solid byproduct of the thermochemical decomposition processes of biomass and appears as a fine-grained charcoal rich in carbon.⁵ Since it is composed of mostly stable aromatic forms of carbon, it cannot readily return to the atmosphere as carbon dioxide.² Another significant advantage of using Biochar is in its low cost, estimated being lower than US \$ 500/ton.² Apart from Biochar, decomposition of biomass may also produce liquids (an aqueous

organic phase called bio-oil) and gases (a gaseous mixture, called syngas, containing CO, CO₂, H₂, and hydrocarbons), regarded as alternative fuels to fossil fuels and thus used to generate heat and power.³ Biochar has caught the eye only freshly since newly technologies went towards the direction to maximising liquid products in an attempt to develop crudes which could be easily and economically refined.²

Various thermochemical decomposition processes of biomass for the production of Biochar with different properties as long as the modifications to improve it are reviewed in section 1.1.1. Since Biochar is cheap, environmentally friendly, and usable for various purposes, several studies have been conducted to develop new applications, which are reported in section 1.1.2. In particular, this research work aims to contribute regarding the use of Biochar as electrically conductive filler in polymer matrices since none research has been conducted on it.

1.1.1 Production and modification methods of Biochar

There is a multitude of diverse carbonisation processes involving the application of high temperatures to produce Biochar from biomass: pyrolysis, gasification, hydrothermal carbonisation (HTC) and other thermochemical technologies. The typical operating conditions of these different processes will be briefly described below, while a comparison between the various products obtained is reported in Table 1.

Pyrolysis is a process where the biomass is heated in anoxic conditions in the temperature range 300-900 °C. Since this process is conducted under oxygen-free atmosphere, combustion of the biomass is prevented, and only chemical bonds scissions (depolymerisation or fragmentation) or formation (crosslinking) occur. That is the case of the thermally weak constituents making up the biomass like cellulose, hemicellulose, and lignin, which during thermal decomposition produce char, bio-oil and syngas.³ The decomposition results depend on the raw materials features as well as the biomass pyrolysis process conditions chosen such as temperature, heating rate and residence time.³

Normally, an increase in pyrolysis temperature has the effect of diminishing the yield of Biochar, its volatile content, the quantity of ion-exchangeable cations, and acidic functional and polar groups (e.g. oxygen functional group), but heighten the yield of syngas, the ash content, the carbon content, the aromatic structures, the specific surface area, and porosity (Figure 1.1).³ The figure also shows how Biochar particles became finer with increasing carbonisation temperatures since more severe operating conditions bestows a more destructive effect on the material.⁶

Increasing the pyrolysis temperatures, the gaseous product yield increases while the Biochar yield decreases because of the higher rate of Biochar primary decomposition (devolatilization of biomass components in the range 200-400 °C) or more secondary decomposition (lesser volatile matter released since Biochar residues undergo noteworthy chemical and physical transformations above 400 °C).²

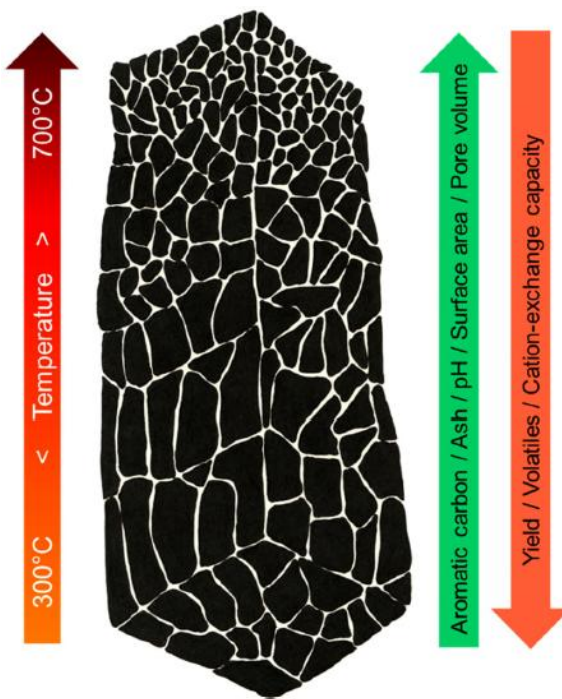


Figure 1.1 - Evolution of Biochar properties with pyrolysis temperature.²

In a slow pyrolysis, in which the rate of the increase in temperature is 0.1-1 °C/s, the char yield (approximately 30% of the raw biomass material mass) is greater than of a fast pyrolysis (15-20 wt%) with a 10-200 °C/s heating rate.² In fact, in a slow pyrolysis, the pyrolysed vapours reside for more time (10-100 min) in the reactor at low temperatures, to allow the ongoing vapour-phase reactions to increase the char yield, in contrast to fast pyrolysis having a vapour residence time of 30-1500 ms.³

As far as the liquid product is concerned, while the bio-oil yield increases up to 500 °C, temperatures greater than that has been shown to reduce bio-oil content since a cracking process (decomposition of large molecules) takes place resulting in the formation of small molecules which raise the gas product yield.⁶

As one might imagine, the ash content increases with pyrolysis temperature because of the removal of organic species from the feed. Ash contains several inorganic components of the original biomass as well as impurities (typical elements available in the ash are K, P, Ca, Mg, Na, Si, Al and Fe), and their concentrations increase with pyrolysis temperature as a result of the removal of most nonmetallic compounds from the precursor.⁶

The volatile content of the Biochar decreases with an increase in pyrolysis temperature since up to 500 °C the decomposition of hemicellulose, cellulose and lignin occur. While increasing the temperature, even more, the released volatiles derive from an aromatisation process.⁶ The aromatisation of char is typically due to generation of hydrogen (dehydrogenation) and light hydrocarbons (de-methanation, decarboxylation and decarbonylation of oligosaccharides) from biomass at high temperatures (600-700 °C), which reduces the atomic H/C ratios. In fact, Biochar

produced at higher temperatures shows a stronger occurrence of C-C bonds compared to C-H and C-O bonds.² This removal of hydrogen and oxygen at higher temperatures results in enrichment of the carbon content in Biochar.⁶ To confirm this thesis, Figure 1.2 reports a van Krevelen diagram to compare atomic H/C and O/C ratios of Biochars produced from raw biomass at temperatures ranging from 100 to 1000 °C.² Thus, the van Krevelen diagram can be seen as a qualitative estimation of the degree of aromaticity contained in Biochar. For example, large values for H/C means low aromaticity, due to incomplete destruction of the biomass structure. The shift in the H/C value from 0.7 to 0.2 denotes a mutation in the structure from non-condensed to highly condensed aromatic.⁶

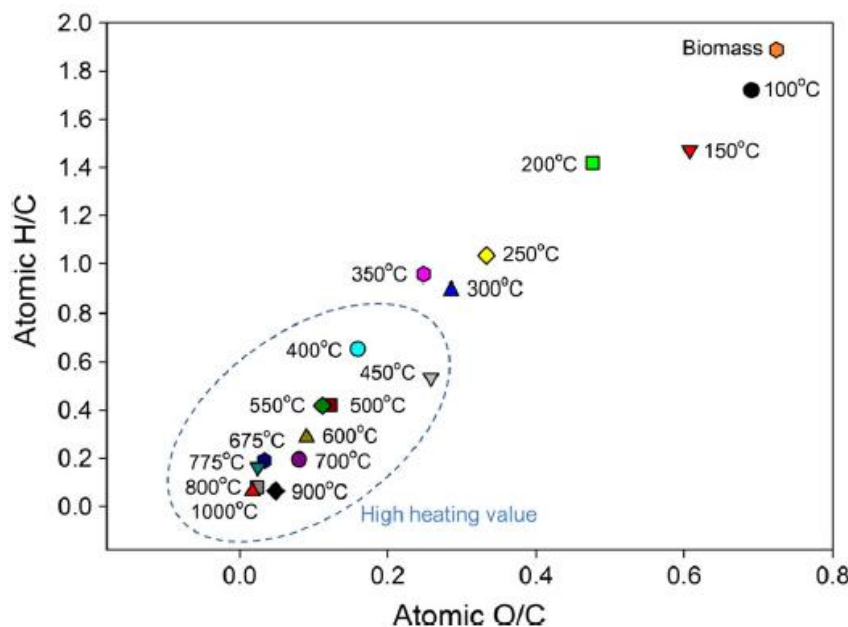


Figure 1.2 - The van Krevelen plot for Biochar at different pyrolysis temperatures with reference to raw biomass.²

Like previously mentioned, the original composition of biomass has to be considered influencing Biochar yields. For example, it has been demonstrated how pyrolysis of high lignin-containing biomass, such as woody biomass, has a firm inclination for high Biochar yields. Moreover, it leads to higher aromaticity degree in the resulting Biochar.² That can be explained by the fact that lignin has higher carbon content and lower oxygen levels compared to that of cellulose and hemicellulose.² Also, high moisture containing biomasses (e.g. agricultural residues such as straw and husk) are reported to have a particular predilection in increasing Biochar yield.²

Gasification is a thermochemical process which exploits gasification agents (air, steam, oxygen, carbon dioxide or other gas mixture) to partially oxidise the biomass converting it to gaseous, liquid, and solid products.³ The gasification process occurs in different temperature rising step. Firstly, the moisture content of biomass is evaporated. Then, pyrolysis occurs over the temperature range 150-400 °C, decomposing biomass and producing char, other than gases and

liquids (oil and tar). In the oxidation step, the gasification agent pumped into the gasifier reacts with the combusting species and the char previously obtained, to develop energy required for the next gasification reactions, in which the char is finally converted to CO, CH₄, and H₂.³ Since the chief purpose of gasification is to produce gaseous products, the char yield achieved is only approximately 5-10%, which is even lower than that of fast pyrolysis.

Hydrothermal carbonisation (HTC) takes place in a closed reactor containing biomass mixed with water. This process was born to counter the problem of a significant amount of moisture present in the biomass, which necessarily requires a separate drying step to reduce the energy loss in dry processes such as pyrolysis and gasification.³ During the hydrothermal process, the temperature is raised along with the pressure to allow water to maintain a liquid state above 100 °C. Depending on the temperature, the main products are Biochar (often called hydro char) below 250 °C, bio-oil at 250-400 °C and gaseous products above 400 °C. Therefore, the hydrothermal carbonisation only covers that part of the hydrothermal process in the temperature range below 250 °C. Compared to dry processes, this production method leads to a char with a higher carbon content.³

Other thermochemical technologies are flash carbonisation and torrefaction, both rarely found in the literature. In the first one, high temperatures (300-600 °C) are attained thanks to a flash fire ignited on a packed bed of biomass at a high pressure (1-2 MPa). In this way, about 40% of biomass is converted into solid-phase product, while the remainder goes away in the gas phase.³ Torrefaction is a process in which solid products are achieved removing moisture, carbon dioxide, and oxygen and depolymerising long polysaccharide chains contained in biomass under an inert condition at 200-300 °C. The slow heating rate makes this process similar to a “mild” pyrolysis.³

Table 1 - Effects of the usual operating conditions on the properties of various products in different processes for Biochar production.³

Process	Process temperature (°C)	Residence time	Solid product yield on a dry wood feedstock (mass%)	Carbon content of the solid product (mass%)	Carbon yield (mass _{carbon.product} /mass _{carbon.feedstock})
Slow pyrolysis	~400	Minutes to days	~30	95	~0.58
Fast pyrolysis	~500	~1s	12-26	74	0.2-0.26
Gasification	~800	~10-20s	~10	-	-
HTC	~180-250	1-12h	<66%	<70%	~0.88
Flash carbonisation	~300-600	<30min	37	~85	~0.65
Torrefaction	~290	10-60min	61-84	51-55	0.67-0.85

Before being used, the produced Biochar is usually subjected to an activation process to increase its pore fraction and thus the specific surface area or to form functional groups in it, depending on the application purpose.³ Most of the studies relating to the activation of Biochar have mainly focused on the fields of adsorption, contaminant remediation, and filtration related operations.⁷ Two activation methods can be distinguished: physical activation and chemical activation.³

Physical activation relies on the use of oxidising gases (steam, CO₂ and ozone), which have the task of activating the Biochar in two different steps at temperatures exceeding 700 °C.³ This activation is characterised by a pore formation closely related to the depletion of carbon by reactions and elimination of volatile matters. In the first step, there is a decomposition targeted to unstructured parts of the carbonised material, to open small pores (micropores) enclosed in the carbonaceous structure. While in the second step, crystalloid carbon is depleted by the activation reactions, forming larger pores (mesopores).³ Just to cite one example of activating reactions, the effects induced by the use of steam are shown in equations 1.1-1.3:



where parentheses represent the attachment of the chemicals to the solid carbon surface of Biochar. Summing up the above reactions, the water vapour attached to the carbon surface firstly decomposes to emit hydrogen gas, while the remaining oxygen reacts with carbon forming CO, which moves away leaving a pore. An increase in specific surface area and micropore volume has been demonstrated to be induced by higher activation temperatures.³

Chemical activation regards the doping of char with a chemical agent (basic chemicals such as KOH, NaOH as well as acids such as H₃PO₄, H₂SO₄), which will lead to the formation of micropores by dehydration and oxidation.³ Often, chemical activation is carried out simultaneously with carbonisation in the temperature range of 300-950 °C thus influencing the pyrolytic decomposition. Therefore, a better porous structure and increased carbon yield are obtained.⁴ If its activation efficiency is higher than that of physical activation, on the other side it carries all the disadvantages of using chemicals. An example of the reaction between the solid carbon surface of Biochar and KOH as a chemical agent above 700 °C is as follows (equation 1.4):⁴



with consequent decomposition of K₂CO₃ which enhances the pore formation in inert atmosphere (equations 1.5 and 1.6):





Also the metallic potassium in the carbon matrix contributes to the pore formation since it widens the space between carbon atomic layers.⁴

The specific surface area of Biochar has been demonstrated to increase with a growing dose of this activating agent.³ Like previously stated, Biochar can also be modified by forming functional groups in it. For instance, nitrogen functional groups are formed by the reaction of the carbon matrix with ammonia.

All these processes seen in this section will lead to the production of Biochar powder having uneven particle size. Hence, if the future application needs it, Biochar has to be pulverised (e.g. using a ball mill) for a particular time, until its average particle size decreases up to hundred or even tens of nanometers.⁵

1.1.2 Structure, properties and applications of Biochar

Although a substantial supply of literature is attainable for biomass pyrolysis, yet it appears to be ignored and neglected for Biochar characterisation. Biochar is mainly composed of amorphous carbon structures and turbostratically stacked graphene sheets, which constitute the electrically conductive phase of the material.¹ Whereas the non-graphitic structures hold abundant functional groups that promote the formation of chemical bonds with different polymer matrices in which the Biochar is dispersed.¹ Since the presence of oxygen and various kinds of aliphatic groups, the Biochar structure differs from that of structured carbon materials such as graphite.⁶

Other than carbon, Biochar also incorporates hydrogen, oxygen, ash containing various minerals (diverse species of silicates, carbonates, sulphates and phosphates²), and trace amounts of nitrogen and sulphur.³ Of course, Biochar elemental composition varies depending on the starting raw biomass and the characteristics of the carbonisation and modification processes.³ In fact, these heteroatoms are derived from the biomass and thus became part of the chemical structure due to incomplete carbonisation or introduced during the activation process.⁴ Modification of surface functional groups of carbon materials usually leads to changes in the double-layer properties such as wettability, capacitance and electrical conductivity.⁴ For example, activated Biochar often has a high porosity along with a great specific surface area and contains oxygen functional groups (mainly carboxylic, lactone, carbonyl and ether groups) and aromatic compounds on its surface.³

It is possible to assume that the electrical conductivity of the Biochar increases with the graphitic degree of the carbons (high presence of condensed aromatic structures), whose quantity depends on the processing temperature and activation methods.⁴ But given that increasing the pyrolysis temperature, on the one hand increases the aromatic fraction, which has as a consequence an increase in electrical conductivity, but on the contrary enhances the content of ash, which hinders the electrical conductivity, in the first instance we cannot directly correlate an increase in pyrolysis temperature with an increase in electrical conductivity.

Das O. et al.⁸ in their studies showed how an increase in aromaticity of the Biochar could bring to higher values of hardness and modulus. Results also revealed that Biochar derived from the same stock of raw material has an increased hardness and modulus corresponding to an increase in elemental carbon percentage. Therefore, both pyrolysis temperature and residence time have a significant effect on Biochar properties.⁸ That is a good point because higher surface area, carbon content, hardness, and stiffness of activated Biochar could potentially enhance the performance of the resulting composites.⁷

Modification of char is necessary for increasing its reaction activity, depending on the application purpose. In fact, the activation processes lead to large specific surface area, porous structure, surface functional groups, and high mineral content (such as quartz, calcite, feldspar and anhydrite⁶), which allow Biochar to be used as an adsorbent for water and air pollutants, a catalyst to remove tar and NO_x or produce biodiesel, and as a soil amendment to improve its fertility, nutrient availability and water retention capacity. Freshly, the applications of Biochar to fuel cells and supercapacitors have also been presented.³

It is important to underline how the capacity of Biochar for these applications are strongly dependent on the raw biomass material and the process used to produce it as well as the process parameters.

1.2 Polymer composites with Biochar

In recent years, more and more interest has been addressed to the class of composite materials because of their particular characteristics, first of all, their high strength-to-weight ratio (specific strength). It has proven them to be an excellent alternative to metallic materials, traditionally used in automobile and aerospace industries. Since the best combination of high specific strength and specific modulus are found in polymer composites, this class of material is undergoing enormous development.

In this study, it has focused on the development of particulate composites, which are composite material in which the dispersed phase has approximately the shape of spherical particles. These spherical fillers affect the mechanical properties of the composite firstly depending on their size, shape, volume fraction, distribution, and interfacial adhesion with the matrix.⁵ When the size of the filler is at the microscale or even more at the nanoscale, it is spoken about micro-composites and nano-composites respectively, which are a new class of material that offers significant enhancement in properties at very low filler loading. Thanks to an exceptionally high surface area per unit volume, they have a strong interaction with the matrix creating a substantial amount of interphase in the composite.

More recently, research is going on in developing composites with various recycled wastes as reinforcing fillers, especially biowastes. In fact, the use of natural substances as fillers in composites not only reduces costs but it is also environmentally friendly because of the characteristic biodegradability, enabling these composites to solve the growing pollution

problems.⁵ In our case, the fillers used as reinforcement are fine particles of Biochar, a carbonaceous material derived from biomass. Carbonaceous fillers have long been used as a filler material for modification of polymer properties, but the protagonist of this work is an absolute novelty.

In section 1.2.1 will be described the preparation methods of these composites, whereas in 1.2.2 a slight nod about their mechanical properties found in the literature. Finally, in section 1.2.3 a possible explanation about electrical conductivity of these composites is reviewed.

1.2.1 Preparation methods of polymer composites with Biochar

Dispersion is the most delicate and fundamental stage in the preparation of conductive polymer composites. During the following discussion, Biochar has been assimilated to the Carbon Black (CB) filler, of which it is easy to find much information in the literature about its dispersion methods. The usual compounding equipments are intensive dry mixers, intensive internal batch mixers, two-roll mills, and extruders.⁹

The most common technique to disperse CB particles into polymer matrices is extrusion mixing.⁹ The extrusion process starts by feeding plastic material (e.g. in pellets or granules) together with the filler from a hopper into the barrel of the extruder. The polymer is gradually melted by the mechanical energy generated by turning screws and by heaters arranged along the barrel, in order to facilitate the mixing process with the filler particles. The mixture is then forced into a die, which shapes it into a pipe that hardens during cooling.

For realistic laboratory simulation, a measurement mixer is sometimes used. It is a discontinuous mechanical mixer used to mix the materials in small quantities, an undersized version of the mixers used in the major industries for the production of polymer blends. The mixing chamber is formed by a cavity inside which two rotors rotate in the opposite direction (counter-rotating) to mix the filler with the polymer. The temperature is measured by a thermocouple and can be set through a control thermostat.

CB particles in the matrix are assembled to form primary CB aggregates, which in turn, because of the van der Waals forces, join in more loosely constructed agglomerates.⁹ The purpose of the compounding is to apply shearing forces which act on CB agglomerates and break them into primary aggregates. It has been proposed that during the early stage of mixing, the role of the polymer is to penetrate into the interstices between powder particles separating them, depending on the CB void volume: the penetration is easier as the void volume increases.⁹ An absolute dispersion is achieved when the surfaces of discrete primary aggregates are completely covered with polymeric material.

Richard et al.⁵ carried out a morphological study on Biochar particles dispersed in an unsaturated polyester matrix using SEM (Scanning Electron Microscopy) images in magnified form. In Figure 1.3 it is possible to see the differences between a good degree of dispersion and a bad one, in which particles agglomerates are present.

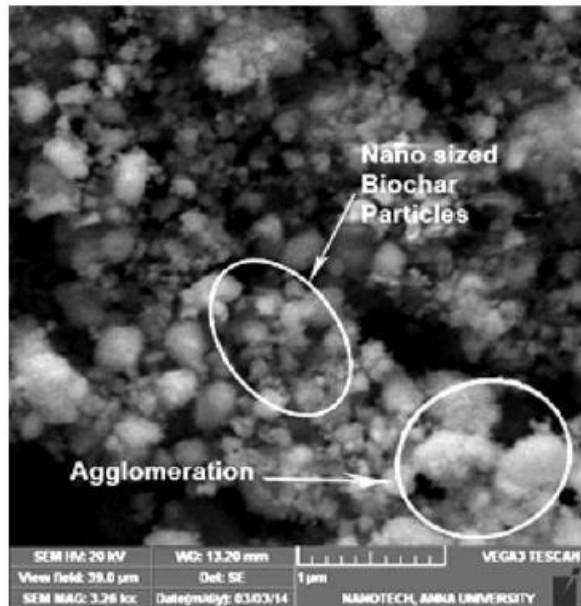


Figure 1.3 - SEM image of Biochar particles after milling.⁵

1.2.2 Mechanical properties of polymer composites with Biochar

It is vital for renewable materials to have commensurable features which can potentially take the place of materials derived synthetically or from inorganic sources. In studies on activated Biochar dispersed in wood/PP composites, Ikram S. et al.¹⁰ hypothesised that a molten polypropylene with high melt flow index (MFI) would be able to flow and penetrate into the pores of Biochar during processing with ease, creating a beneficial mechanical bonding that strengthens the composite. However, since Biochar does not potentially react with the polymer chemically, the presence of a coupling agent (e.g. maleic anhydride) was essential to assist interfacial bonding to achieve high tensile and flexural properties.

In another study, Richard et al.⁵ show that the tensile strength at yield and break of polyester resins decreases with the introduction of nano-sized Biochar particles derived from the pyrolysis of rice husk. However, the rate of reduction in tensile strength with the increase in particle loading is reduced with particles of lower size (Figure 1.4). This decrease of tensile strength at a higher weight fraction of Biochar can be derived from the impeded interactions and thus the poor interfacial adhesion between fillers and the polymer matrix, which is necessary to transfer the stress from the matrix to the fillers upon deformation. The poor interfacial bonding results from an increase in the void fraction with a higher Biochar particle loading. With the presence of the filler, the fracture behaviour of the composite under tensile loading passes from a ductile mode of failure (more plastic regions and debris are noticeable on the fractured surface) to a brittle one, since fillers restrict the mobility of the polymer thus nullifying its elastic character. At the same weight percentage of filler, the smaller the Biochar particles, the greater their surface area that

will interface to the matrix allowing a greater possibility to transfer the stress from the matrix to the reinforcing fillers.

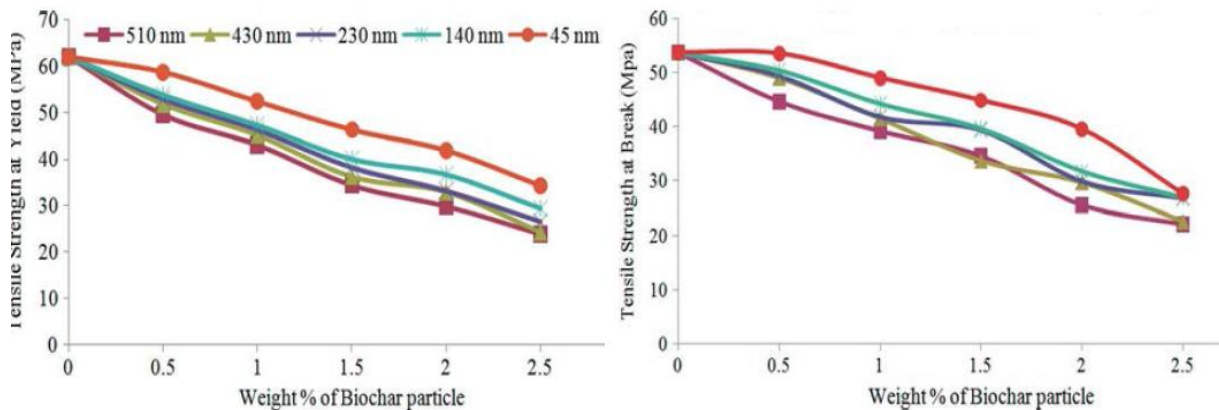


Figure 1.4 - Variation of tensile strength at yield (on the left) and break (on the right) with the weight percent of Biochar in polyester resins.⁵

From SEM morphology studies of Izod-tested specimens, Richard et al. showed that the impact strength of Biochar particle-reinforced polyester resins increases upon a decrease in particle size and an increase in particle loading (Figure 1.5).⁵ The fractured surfaces due to the impact testing witness the fracture mechanism: while the pure polyester resin fractured surfaces were very smooth and plain, Biochar particle-reinforced composites surfaces appeared rough and coarse. At the same filler content, the impact energy is uniformly absorbed at finer particle size, due to the presence of more obstacles which deflect the path of the cracks propagating in the composite.

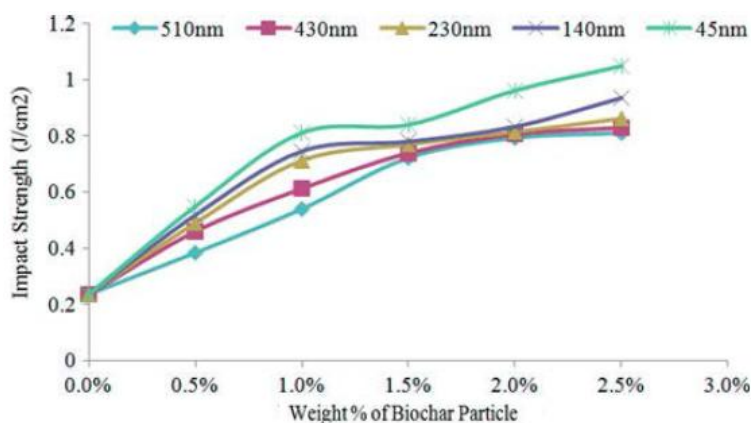


Figure 1.5 - Variation of impact strength with the weight percent of Biochar in polyester resins.⁵

Richard et al.,¹¹ in another study on tribological properties on the same composite, demonstrated using a pin-on-disk test apparatus how an increase in particles content can bring to a gradual decrease in the specific wear rate and the coefficient of friction when compared to that of cured pure resin (Figure 1.6). The most plausible explanation for this trend is the fact that

carbon present in Biochar particles has extremely high dry lubricating properties. Moreover, a reduction in particle size has the same effect on the trend. Since bigger particles have poorer bonding with the matrix because of lower contact area compared to smaller particles, they lead to a higher dry sliding friction and a major plastic deformation along the direction of wear. As the friction increases, more heat is generated, and the surface temperature increases more, together with the possibility of plastic deformation and debonding. As a result, there will be bigger wear debris and broken particles on the sample surface. Whereas lesser particle size-composites appear with a smooth surface (less plastic deformation, few voids, and very fine wear debris).

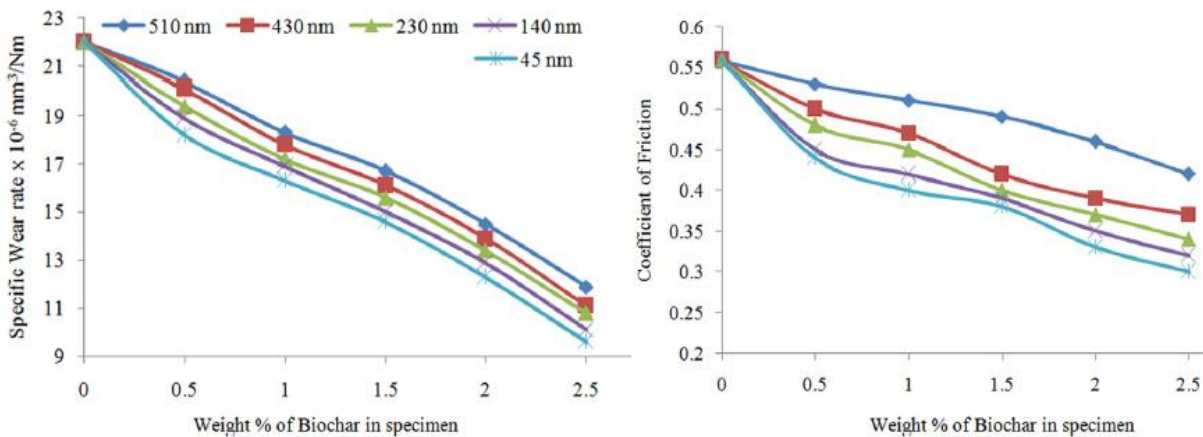


Figure 1.6 - Variation of specific wear rate (on the left) and coefficient of friction (on the right) with the weight percent of Biochar in polyester resins.¹¹

1.2.3 Percolation theory and electrical conductivity of polymer composites with Biochar

Polymers are typically considered to be electrically insulating materials, but their conduction properties change if conductive fillers are dispersed in them. In this way, electrically conductive polymer composites have come to exist since the 1950s, with a resistivity between that of metallic conductors ($10^{-7} \Omega\text{m}$) and insulating materials ($10^{-15} \Omega\text{m}$).¹² They are relatively inexpensive materials used for many engineering applications, such as electrically conductive adhesives, antistatic coatings or films, electromagnetic interference shielding materials for electronic devices and more recently for sensing components.¹³ The fillers used range from carbonaceous fillers (carbon black, exfoliated graphite, carbon fibres, and nano-fillers such as nanotubes and graphene), to metal powders or fibres.⁹

The percolation theory can be applied to explain the electrically conducting behaviour of composites consisting of conducting fillers and insulating matrix.¹³ According to this theory, the role of these fillers is to create a three-dimensional percolation network through which the electron flow passage is allowed. In practice, with an increase in the filler content, the composite passes from an insulator to a conductive behaviour since the particles come in contact with aggregation and coagulation processes, creating a continuous network within the matrix. That happens when the filler amount in the polymer matrix is above a certain concentration, called

percolation threshold: the lowest level of conducting filler particles at which continuous conducting chains or branching is formed.⁹ The percolation threshold is defined on a statistical basis since continuing to add fillers, the individual particles will statistically come to touch, forming at least one conductive continuous percolating network throughout the composite volume. This concept is schematically shown in Figure 1.7 in which it is possible to observe how increasing the filler content, carbon nanotubes (CNTs) in this case, a first continuous pattern of filler throughout the material is created.

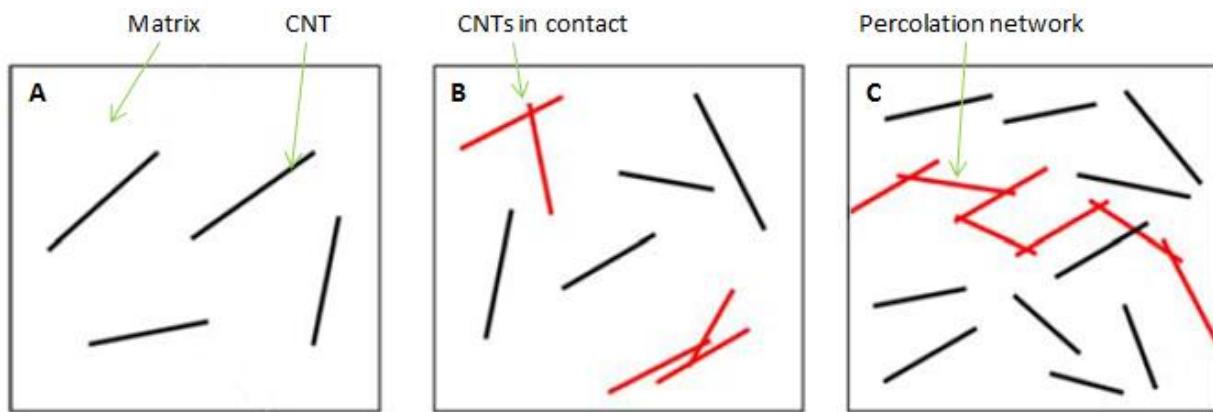


Figure 1.7 - Formation of a percolation network with increasing percentage of nanotubes. (A) Content of nanotubes below the percolation threshold: no nanotubes are in contact. (B) Content of nanotubes below the percolation threshold: some nanotubes are in contact. (C) Achievement of the percolation threshold with the formation of the first percolation network.

In Figure 1.8 is reported a typical percolation curve that shows how the jump between the absence and the presence of a conductive path, in reality, is more gradual (sigmoid) than what one might expect. In fact, it is possible to divide the percolation curve into three regions.

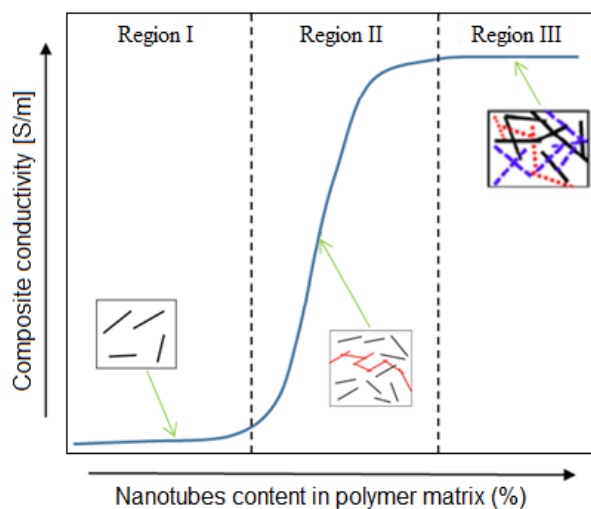


Figure 1.8 - Example of percolation curve showing the trend of electrical conductivity of the composite varying the amount of conductive fillers (CNTs in this case).

In the first region, in which the content of the filler is below the percolation threshold, the nanotubes are not touching, and the insulating behaviour of the matrix prevails. The distance that separates them is greater than a certain critical distance that indicates the minimum distance to achieve the conductivity for "tunnel effect". In fact, in the tunnelling effect theory, it is stated that the electric conduction happens not only because of the interparticle contact, according to the percolation theory. But the increase in conductivity also arises from a high propensity of electrons to tunnel between conductive domains (the filler) isolated from each other by the insulating matrix (seen as a potential barrier).¹² The tunnelling is a quantum mechanical process, which operates when the distance between the conductive components within the insulating matrix is close to a threshold value, usually a few nanometers. In the case of tunnelling, the resistivity is a function of temperature and voltage. Whereas a voltage can excite electrons promoting their motion (they can easily jump through the gap), tunnelling is hindered at high temperatures. Raising the temperature, the potential barrier increases and the resistivity increases accordingly. It is due to a greater expansion of the plastic material compared to the conductive filler, which will grow the gap between the conductive particles.⁹

In the second region the filler concentration is increasing, thus lowering the distances between the nanotubes: there is an initial increase in conductivity thanks to the tunnel effect between neighbouring nanotubes. When the percolation threshold is reached creating the first conductive path due to direct contact between the CNTs, there is a rapid increase in conductivity with minimal additions of fillers. This change in the electrical conductivity (σ) of the composite beyond the percolation threshold can be expressed as a universal law (equation 1.7):⁹

$$\sigma = \sigma_0(V - V_c)^p \quad (1.7)$$

where σ is the electrical conductivity of the composite, σ_0 is the electrical conductivity of the filler, V is the volume fraction of filler above the critical concentration, V_C is the volume fraction of filler at percolation (it can also be seen as the probability of formation of a conducting network) and p is the conductivity exponent that it has been shown to depend on the dimensions of the sample and on the polymer matrix. p usually has a theoretical value in the range $1.3 \leq p \leq 2.1$,¹² and these values are only valid for spherical particles (e.g. CB), whereas for fibrillar fillers they are much greater.

According to Janzen⁹ model, V_C can be related to the average number of contacts between filler particles as follows (equation 1.8):

$$V_C = \frac{1}{1 + 0.67z\rho\varepsilon} \quad (1.8)$$

where z is the filler coordination number, ρ is the density of the filler particles, and ε is the specific pore volume of the filler particles.

Finally, in the third region, beyond the percolation threshold, there is the formation of many conductive paths, but the addition of fillers does not involve any increase in conductivity since a kind of saturation is reached.

The properties of the polymer matrix affect the percolation threshold. These properties and their effects are listed and discussed below.

In previous studies, it was shown that the higher the polarity of a given polymer, as well as the greater its surface tension, the larger is the critical content of filler to reach the percolation.¹² If the interaction between the filler and polymer prevails over the filler-filler interactions, the filler can be dispersed separately without contact, delaying the formation of a conductive path until a significant concentration of filler is added.⁹

Also, the polymer molecular weight and accordingly the viscosity play a prominent role: the higher they are, the higher is the percolation threshold. Firstly, high molecular weight polymers are harder to spread on fillers, slowing the formation of conducting networks.⁹ But this delay in the formation of three-dimensional conductive networks is also due to the higher shearing force required during mixing, which induces a greater breakdown of the particles aggregates (e.g. CB) and a pronounced drop of the aspect ratio of fibres.¹² Now it is easy to understand how an addition of a plasticiser into plastic, which lowers the average molecular weight and melt viscosity, can reduce the percolation concentration.⁹

Not less important is the role of the crystallinity degree. In fact in semi-crystalline polymer matrices, the fillers would be ejected from the crystalline regions during crystallisation, and they would tend to accumulate in the amorphous phase thus reducing the percolation threshold compared to amorphous polymers.¹²

Lastly, it has been demonstrated that also a selective localisation of particles in multiphase polymeric materials (in one phase or at the interface of binary blends) can decrease the percolation threshold.¹² Since the particles tend to accumulate in specific areas of the material, the percolation threshold is locally exceeded. Double percolation indicates the filler percolation in the filler rich-phase and the phase continuity of this phase.¹⁴ Thanks to a selective distribution of particles into one phase depending on their affinity to the polymer components and the processing history, conducting properties can be achieved at lower filler content. In this way we improve mixture processability and mechanical properties, both worsen by high-filler content. As long as the viscosities of two polymers are comparable, the primary factor determining an uneven distribution of fillers in the two phases is the interfacial energy.¹⁴

As far as the type of conductive filler is concerned, its structure and properties have significant roles in determining the percolation threshold.

Firstly, the tendency with which the fillers can form a three-dimensional network is mainly due to their aspect ratio: the higher it is, the higher conductivity they can impart. That is why the fibrillar form of short carbon fibres ensures better electrical response than the CB filler. But attention must be paid during the dispersion of the fibres, where they usually experience shear forces which lead to a drop of aspect ratio.¹²

Like previously stated, conventional conductive fillers are usually metal powders or micrometre-scale carbonaceous materials. To achieve the percolation threshold with these fillers, we have to use a filler content as high as 10-50 wt%, resulting in a composite with not always wanted mechanical properties and a high density.¹³ Moreover, another problem of metal powders, in

addition to their greater weight, is their natural tendency to oxidation with the following formation of an insulating layer on their surface.⁹

In conclusion, the filler content must be as small as possible still allowing the composite to fulfil its electrical requirements; otherwise, the mixture processing gets complicated, the mechanical properties of the composite worsen and the final cost increases.¹² Therefore, it is important to try to reduce the percolation threshold of conductive fillers, and there are several ways to do it: the use of additives, the optimisation of processing conditions, and the control of their size and distribution.¹²

Compared with traditional conducting composites, conductive CNTs-based composites can be constructed at low loading of fillers (often as little as 0.5 wt%).¹⁵ That is due to low percolation threshold originated from the high aspect ratio and excellent electrical conductivity of CNTs. Although it has been shown that the introduction of CNTs into polymers can increase the conductivity of the nanocomposite to several orders of magnitude (even higher than ten orders),¹⁵ CNTs themselves are too expensive, and their dispersion methods in polymeric matrices are too complicated; consequently, they can't satisfy the aim of this project. Therefore, this work aims to investigate the use of less expensive carbonaceous fillers, like Biochar.

When we talk about Biochar, a filler comparable to particles with an aspect ratio lower than CNTs, the percolation threshold increases. In order to study the percolation theory in composites filled with Biochar, reference is made to previous studies of composites loaded with CB.

The size of CB particles is due to the type of production process. The most typical process, the furnace process, leads to the obtaining of particles having a diameter spacing from 10 to 100 nm and a surface area from 25 to 1500 m²/g. Only the smallest particles (greater surface area) are suitable as the filler to improve electric conductivity under a particular filling since they can quickly form aggregates.

As reported in section 1.2.1, CB particles assembly to form primary CB aggregates. The aggregate size and shape and the number of particles per aggregate determine the electrical behaviour. Similarly to that previously seen, when the separation distance between aggregates is lower than a critical distance, electrons can flow across the polymer barrier. Consequently, high-structure black (Figure 1.9), a CB characterised by primary aggregates composed of many particles forming marked branching and chaining, is essential in reaching good electrical conductivity. Since this structure is characterised by stronger attractive forces between the aggregates (higher melt viscosity), a dispersion process should provide more energy to separate them. Conversely, if relatively few particles make up the aggregate (in this case the CB is referred to as a low-structure black), smaller aggregates are in contact and separated by bigger distances, resulting in lower conductivity.⁹

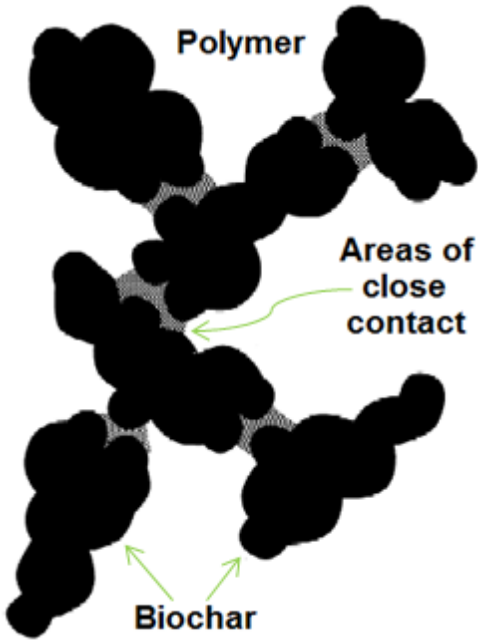


Figure 1.9 - Schematic representation of a high-structure CB, where CB is assimilated to Biochar. Here, the distances between the neighbouring aggregates are small enough to allow the tunnelling of electrons.

The areas of close contact represent the effective tunneling distances.¹⁶

Also, the particles structure and their surface chemistry are reported to be significant features to influence the percolation threshold.⁹ For example, a strong interaction between polymer chains and the CB surface contribute to the dispersion of CB in the matrix reducing the contact between CB particles and thus the electrical conductivity. Moreover, a low volatile content, like the oxygenated groups chemisorbed on the surface of CB, is necessary for achieving lower percolation threshold. In fact, these groups, aside from acting as electron traps, are negatively charged and can be attracted by cationic groups contained in the chains of the polymer matrix, enhancing the CB dispersion.⁹

Which are the effects of processing on conductivities of CB polymer composites? In section 1.2.1, it has been said that a perfect dispersion is achieved when the particles are separated into discrete primary aggregates. However, in the case of conductive applications, a perfect dispersion is not desirable.⁹ In fact, if at the beginning of mixing the conductivity speedily increases thanks to the formation of pathways between the aggregates, then, they start breaking down increasing the gap between the particles. Consequently, the conductivity decreased gradually during further mixing. It is easy to understand how the conductivity of the composites with high-structure CB is more sensitive to processing time than low-structure CB composites (more porous).

Bayer and co.¹⁷ showed how an anisotropic distribution of the CB particles could lead to higher conductivity and lower percolation concentration, compared to isotropic samples made with other techniques (e.g. compression moulding). Moreover, Kato and co.⁹ demonstrated that higher moulding temperatures and longer moulding time bring to a superior conductivity. That is

explained by the development of a CB network due to coagulation of CB promoted by thermal vibration and Van der Waals forces.

In conclusion, some attention must be paid to the design of the dispersion procedures to obtain conductive composites to avoid under or over dispersion of CB particles. Consequently, a fundamental step of this work will be the choice of the dispersion method of Biochar particles into the polymer matrix.

1.3 Laser technology and ablation phenomenon

1.3.1 Technology, features and types of laser beams

Acronym for Light Amplification by Stimulated Emission of Radiation, the LASER is a coherent photon amplifier, which is a device that, when an incident photon with a given frequency and phase appears at its input, has the ability to generate other photons that exit with the same frequency and phase of the input photon, actually amplifying the incoming light. That is made possible by the physical phenomenon of stimulated emission. Although Einstein had already theorised the possibility of realising a light amplifier in 1916, only in 1960 the first laser was made by Theodore Maiman (the ruby laser).¹⁸

The stimulated emission process, schematized in Figure 1.10, happens when a photon with frequency ν hits an electron in the excited state and causes the emission of several photons at the same frequency ν while the electron decays from the E_2 energy level to a lower energy level E_1 .

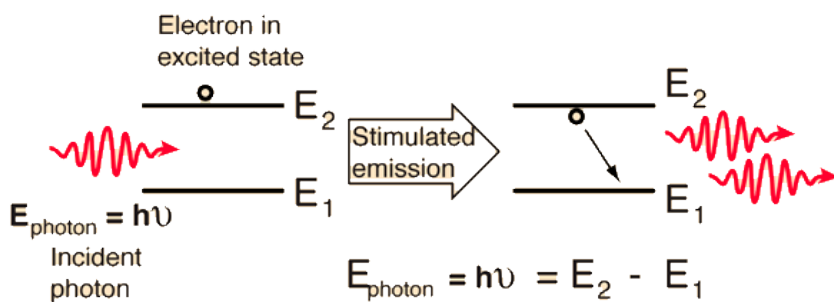


Figure 1.10 - Schematisation of the stimulated emission process: a photon with frequency ν hits an excited electron and causes the emission of several photons with frequency ν while the electron falls to a lower energy level.¹⁹

For it to occur continuously over time, it is necessary to force the electrons to the excited state, so that more free photons may be emitted. That allows to amplify the radiation and to achieve a continuous laser source. A fundamental concept in the laser field is, therefore, the inversion of the population. A population in the fundamental state is characterised by most electrons in the fundamental state. In a laser, it is necessary to have a population reversal, where most of the particles are excited (Figure 1.11). This result can be obtained by administering energy (an

electrical or luminous stimulus) to the active material so that the atoms are kept in the excited state. This action is called laser pumping.

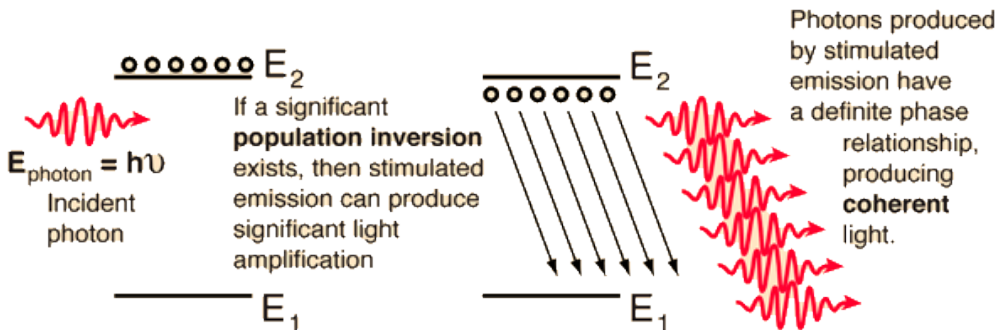


Figure 1.11 - Schematisation of the stimulated emission process from a laser in which population inversion is occurred: many electrons at the E_2 state of energy decay into E_1 state causing multiple photons with frequency ν .¹⁹

Laser instrumentation is suitable to achieve the amplification of the radiation to produce a beam with precise characteristics regarding temporal and spatial distribution, spectral amplitude, coherence, geometry and polarisation. The laser, therefore, is a device capable of generating a beam of electromagnetic radiation with high power and particular features:

- Monochromaticity: a laser beam concentrates its electromagnetic radiation on a single wavelength and frequency (depending on the active medium), as opposed to a conventional light source, whose electromagnetic radiation is distributed over a wider spectrum;
- Coherence: electromagnetic waves that make up the laser beam have the same phase both in space and time;
- Low divergence and high resolution.

In addition to these features, irradiance, brilliance and flux of the beam make the laser a unique radiation source of its kind.

Laser, now found among the most relevant technologies, is destined for continuous evolution due to its enormous versatility and applicability to any industry. The high power provided by the laser, coupled with high-performance speed and quality of the result, allows it to be used in various areas, such as optoelectronics, electronics, aerospace and automotive industries, where a high accuracy compensates the often expensive laser instruments.²⁰ Laser sources are widely used in telecommunications and optical fibres for data transmission and processing and for industrial laser measuring interferometers for metrology as well as in metalworking such as cutting, welding and thermal processing. In fact, the electromagnetic radiations that make up the laser beam transmit high energy to the workpiece by inducing a temperature increase to allow local fusion and vaporisation.²¹

Only recently it has found new applications in fields such as printing, selective ablation, also on non-metallic materials, such as ceramic, polymeric and natural materials (wood and leather). That

was possible thanks to the introduction of laser sources characterised by new constructive architectures and capable of generating different wavelength beams. In fact, the interaction between the laser beam and the material is strongly influenced by the absorption coefficient of the material, which will, in turn, depend on the wavelength of the incident radiation.

The main advantages of adopting a laser marking system are the following:

- Extremely fast process: speed is one of the highest achievements with energy-beam technologies;
- Narrow tracks: the marking path is very narrow and allows to reduce machining chips;
- High quality: quality is generally very good, in terms of depth and regularity of the track;
- Easily automated process;
- Silent marking: the noise of the process is remarkably low.

There is a wide variety of laser types, each with its characteristics in the wavelength of the radiation (UV, visible, IR ...), mode of use (continuous or repeated pulse), efficiency and energy (or power) output. All these parameters make a laser capable of satisfying specific job demands, resulting in an appropriate interaction with the material.

Different types of lasers are classified according to the state of aggregation of the active medium, which is the material that needs to be excited to generate the photons. In fact, there are solid-state lasers (crystals, glass or semiconductor), liquid lasers, and gas lasers (further divided into neutral atoms lasers, ion lasers, molecular lasers, excimer lasers and free electron lasers).

Due to the diversification of laser parameters based on the choice of the active medium, the technology associated with the laser is extremely versatile, making it interesting for a wide range of application areas. Choosing the type of laser is very important for achieving the desired level of surface modification without damaging the bulk of the material; it must be done first and foremost considering the optical and thermal properties of the treated material, as these affect the working conditions during and after laser treatment on the surface. In particular, it is necessary to know the thermal properties to minimize any damage caused by the laser beam, while the knowledge of optical properties determines whether the material is or is not sensitive to the specific wavelength of the instrument.²²

For the present experimental work, the selected laser was carbon dioxide (CO_2 laser) which was one of the first models of gas laser produced, by Kumar Patel in 1964, and is now one of the most widely used in the industrial field. This type of laser emits an infrared light beam whose the main wavelength is centred between 9.4 and 10.6 μm . This choice has been evaluated on appropriate considerations about the characteristics of the irradiating beam and the properties of the treated composite (which will be further clarified in the following paragraph). In addition, being a prevalent type of laser in the automotive field, the process described in this research thesis would not require additional costs for the automotive companies.

1.3.2 Laser-material interaction: polymeric ablation

By the term "laser ablation" is meant the localised and controlled removal of material from a solid due to its interaction with a high-intensity radiation. Laser interaction with matter is a rather delicate and complex topic. It depends on the specifications of the emitted electromagnetic radiation and the beam irradiation power, as well as, of course, the thermal and optical properties of the material to be treated. In this case, it is preferable to deepen the ablation phenomenon of polymeric materials, as it is the technology used for the production of electrically conductive tracks in PP/Biochar composite materials.

Electromagnetic radiations that make up the laser beam transmit high energy to the workpiece by inducing an increase in temperature to allow local fusion and vaporisation, or if streams are high, plasma conversion.²¹ The interaction between the laser beam and the material determines the depth reached by the laser beam, and consequently the amount of material removed from a single pulse. Also, due to the lack of contact between the energy source and the sample and the ability of the laser beam to deposit energy into the material in brief time and before the thermal diffusion can occur, the heat-affected zone, where fusion and solidification take place, is significantly reduced. That involves the possibility of micro-structuring the surface with a high ratio of shape and high spatial accuracy, with the least impact regarding mechanical and thermal deformation.²¹

The exhaustive description of the phenomena associated with laser ablation can be complicated by several factors such as: the different types of existing lasers (each operating at different wavelength and power values), the operating regime (pulsed or continuous), the working environment (inert or reactive atmosphere), the surface irradiation duration and, of course, the chemical nature of the material to be treated. Precisely, because of the many factors influencing the laser ablation process, the underlying phenomenon is not due to a single chemical-physical mechanism. In any case, the laser ablation mechanism can be schematized in three steps, shown in Figure 1.12:

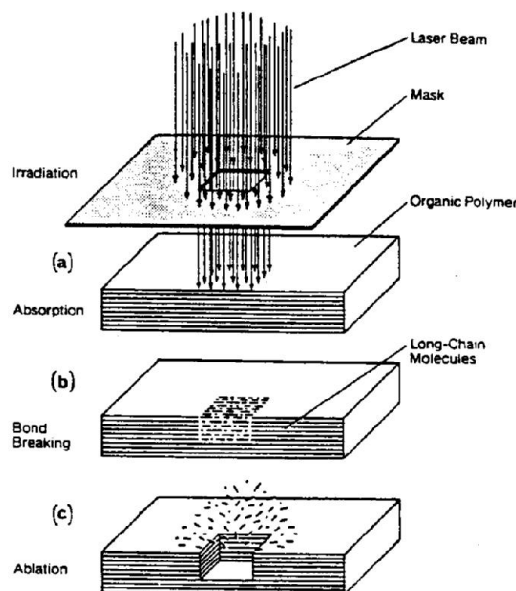


Figure 1.12 - Schematic representation of the laser ablation phenomenon on a polymeric surface.²³

- a) Light absorption by the polymer substrate resulting in electronic excitation.
- b) Part of the electronic excitation due to energy absorption is converted to heat inducing phase changes, indirect bonds-breakage, evaporation and desorption of low molecular weight polymeric chain fragments (thermal mechanism); the other part of the electronic excitation directly produces chemical bond breakage, evaporation and desorption (photochemical mechanism). The relative importance of the possible decomposition processes is highly debated, but it is certain that this depends on the different types of materials and wavelengths of the incident radiation.
- c) Ablation products (gases, vapours, solid or liquid clusters) move away from the surface of the polymer. The expansion of ablation products results in the formation of a pressure propagating inside the material.

Actual removal of material from the surface takes place only at the last stage of the process. In fact, the ablation begins only when the density of the surface broken bonds reaches some critical value.

As mentioned shortly, the polymeric ablation mechanisms can be essentially divided into two types (although in most cases the process determines a mixture of the two):

- Photochemical mechanism: following the electronic excitation, photonic energy is sufficient to break intramolecular chemical bonds directly;
- Photothermal mechanism: stored energy is released in the form of heat which causes thermal degradation of the polymer and so breakages of the bonds, in this case not due to the direct action of the incident light.²⁴

An example of these two mechanisms can be found by comparing a ultraviolet (UV) emitting laser with one that instead emits infrared, having higher wavelengths. In the first case, the interaction of the laser with the material causes an excitation of the electronic type, while in the second case the excitation is of a vibrational form.²⁴

Since the CO₂ laser used in this work is emitting in the medium infrared, the energy associated with incident photons is not sufficient to break the molecular bonds inside the polymeric material but dissociate the molecules by thermal processes.²⁰ When the laser beam reaches the sample, the fraction of absorbed energy tends to transmit to it by conduction, however, being the polymeric material a thermal insulator, this thermal energy remains concentrated on the surface causing a local temperature increase with consequent localised ablation.²⁵ It should be emphasised that this perturbation is restricted to the area treated by the laser, while the remaining part of the polymer remains unchanged, thus retaining its characteristics. Going more in detail, after the ablation due to the photothermal mechanism, the high temperature on the surface results in a reduction in viscosity which causes a sort of viscous flow to the edge of the laser track.

UV radiation, on the other hand, is absorbed by the vast majority of polymers, so it transfers the excitation energy to the molecules, and this results in the direct breaking of intramolecular bonds.²⁰

Therefore, if a CO₂ laser is used, photothermal ablation determines, for local heating of the material, a degradation process of the polymer, called pyrolysis. Pyrolysis is a thermal degradation in a non-oxidizing atmosphere, from which gaseous, liquid and solid products are

obtained. It is an endothermic phenomenon given by a set of reactions that leads to the cleavage of the polymer chain, thus to the breakages of the covalent bonds present in it.

Reaction mechanisms depend on the type of polymer and are divided into those relating to the side chains and substituent groups (elimination or cyclisation) and those involving the atoms present on the main chain (chain scission and crosslinking).²⁶ Chain scissions may be depolymerisation reactions leading to the starting monomer, or intermolecular and intramolecular hydrogen transfer reactions that generate unsaturated chain fragments of variable molecular weight. Polyolefins, for example, degrade almost exclusively through chain scission reactions for hydrogen transfer and only in a small percentage for depolymerisation. In particular, the degradation mechanism of polypropylene, which will be the polymer matrix used in this thesis work, is a radical process that includes an initiating, a propagation and a termination stage. In the initial stage, the formation of radicals due to the cleavage of the polymer chain is detected, and these propagate the degradation through radical mechanisms: the radicals thus obtained act as initiators for the degradation of a new polypropylene chain. In fact, the radical formed after the chain breakage captures a hydrogen from a carbon of the same chain or a neighbouring one, respectively in the case of intramolecular or intermolecular extraction. Finally, the termination phase involves the recombination of the radicals.²⁷ Concerning the products obtained, they are divided into alkanes, alkenes, and dienes. The large percentage of unsaturated hydrocarbons is a feature of polypropylene pyrolysis: unsaturations originate precisely from the β -scission process and hydrogen extraction.

It is now easy to understand how the reasons for the choice of the use of a CO₂ laser as a surface polymeric ablation system for the production of "metal free" conductive tracks are explained in the ablation mechanism of this laser, that is, thermal degradation. The formation of conjugated structures formed during degradation could contribute to the electronic transport to reach and exceed the percolation threshold only locally along the "laser" written track along with Biochar's particles accumulation. Summing up, laser action would result in polymeric ablation, Biochar's build up along the track, and formation of new conjugated structures by thermal degradation of the PP. These effects bring to a very conductive network in the laser track along which it is locally passed the percolation threshold of the composite.

The use of a CO₂ laser for the ablation of polymeric materials loaded with CNTs to produce electrically conductive tracks is available in the literature, albeit in a small number.²⁸⁻³⁰ The innovation of this paper lies in choosing the filler: nothing similar to the purpose of this thesis work was found in the literature for the composite PP/Biochar. It is therefore indispensable to start the experimental work to make this an applicable, predictable and consolidated technology.

2. Materials

2.1. Polypropylene (PP)

The use of polymeric materials in the car has shifted from the pure imitation of traditional materials to aesthetic and constructive solutions that derive from their specific characteristics. The choice of the polymer matrix for the production of Biochar's composites in this thesis work is recaptured on polypropylene (PP); this decision is related to industrial issues, in fact in the automotive field, it is commonly used in external components such as bumper, and interior such as dashboards, door panels, air ducts, and linings.

The starting monomer is propylene or propene, and the polymer is obtained by polymerisation reactions in which Ziegler Natta catalysts or metallocenes are used (Figure 2.1).

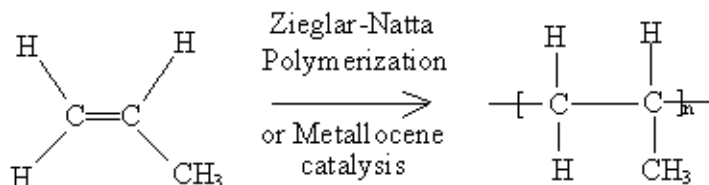


Figure 2.1 - Polymerisation of the monomer propylene into the polymer polypropylene.

The PP may have different stereochemical configurations (tacticities), which depends on the way in which the methyl group is positioned along the polymer chain (Figure 2.2). This aspect is crucial as it involves various physical and rheological properties of the final product.

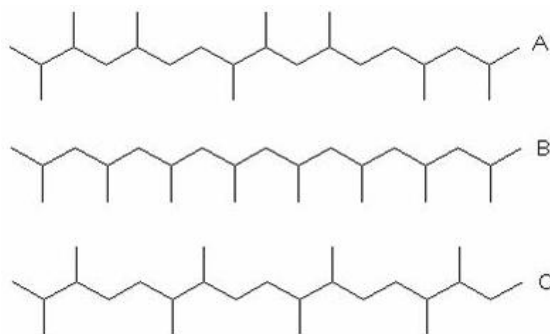


Figure 2.2 - Atactic (A), isotactic (B) and syndiotactic (C) polypropylene.

Ziegler Natta catalysts direct the polymerisation to the formation of isotactic PP, the one most used due to its peculiar mechanical properties; the regularity of the configuration allows for a

high crystallinity degree to which the best chemical, physical and mechanical characteristics of the polymer correspond.

Polypropylene is also commonly produced as a copolymer (block or random) where the comonomer is ethylene. This finding allows it to achieve higher levels of tenacity, flexibility and impact resistance, especially at high temperatures. Both as a homopolymer and as a copolymer, polypropylene is highly resistant to moisture, acids, alkalis and solvents, but is particularly susceptible to ultraviolet radiation and atmospheric agents, which is why protective additives are often used to increase its resistance to UV rays.

The polypropylene used in this work is manufactured by LyondellBasell in the form of pellets, with trade name HOSTACOM CR 1171 G1. It is a medium melt flow index, 10% mineral filled, high impact polypropylene copolymer designed for injection moulding. It features a long term UV resistance and other characteristics listed in Table 2.1. This grade is available in custom colour and pellet form.

Table 2.1 - Typical properties of the polypropylene-ethylene copolymer HOSTACOM CR 1171 G1.

Typical Properties	Method	Value	Unit
Physical			
Density (Method A)	ISO 1183	0.990	g/cm ³
Melt flow index (MFi) (230°C/2.16Kg)	ISO 1133	11	g/10 min
Mechanical			
Flexural modulus	ISO 178	1800	MPa
Impact			
Notched izod impact strength (23 °C, Type 1, Notch A) (-30 °C, Type 1, Notch A)	ISO 180	30.0 6	kJ/m ² kJ/m ²
Thermal			
Heat deflection temperature A (1.80 MPa) Unannealed	ISO 750A-1, -2	54	°C

2.2 Biochar

Biochar particles, present in the composite materials covered by this work, are part of the OSR700 series supplied by the UK Biochar Research Center. The Biochar was purchased in the form of pellets (Figure 2.3) and subsequently reduced to powder as will be discussed in chapter 3. In particular, the feedstock derived from oil seed rape straw, transformed to Biochar using a pilot-scale rotary kiln pyrolysis unit, with a nominal peak temperature of 700 °C. This particular Biochar was chosen in the first instance as showing the greater electrical conductivity among those in the catalog. In Table 2.2 you can observe its main features and production parameters.



Figure 2.3 - Biochar pellets derived from oil seed rape straw.

Table 2.2 - Basic features (on the left) and production parameters (on the right) of the Biochar utilised in the composite (OSR700 series).

Basic Features		Production parameters	
Moisture	3.63 wt%	Nominal HTT	700 °C
C	67.74 wt%	Reactor wall temp.	700 °C
H	1.09 wt%	Max. char HTT	677 °C
O	7.84 wt%	Heating rate	103 °C/min
H:C	0.19	Kiln residence time	12 min
O:C	0.09	Mean time at HTT	5.14 min
N	1.26 wt%	Biochar yield	22.62 wt%
Total ash	21.92 wt%		
pH	10.41		
Electric conductivity	3.11 dS/m		

2.3 PP/Biochar composites

The composites were obtained by integrating Biochar particles into the polypropylene matrix. In order to have a better understanding of the conducting phenomenon and determine the optimum filler content, based on the electrical properties found, it was considered appropriate to prepare compounds with different Biochar contents: 5, 15, 30, 40 wt%. For each PP/Biochar compound, the abbreviation PPnBiochar will be adopted during the thesis, where n is equal to the weight-percentage of Biochar. Such compositions were obtained using a measuring mixer or using a twin screw extruder. The obtained granule materials were then subjected to injection moulding to produce the specimens used during the experiment. Along the text, the samples moulded from previously extruded granules will be followed by the label "Extr" to distinguish them from those obtained through a measuring mixer, called "Mix".

3. Equipment and methods

3.1 Mixing, granulation and injection moulding

Biochar pellets were mechanically grinded in a mixer for two minutes until a fine powder was obtained (Figure 3.1).

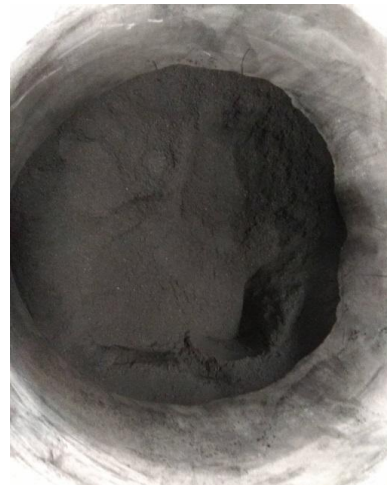


Figure 3.1 - Biochar powder obtained after mechanical grinding.

The resulting powder was dispersed in the PP matrix using a measuring mixer PlastiCorder Brabender, W50E model (Figure 3.2) or employing a twin screw extruder Leistritz ZSE 18 HP-PH (Figure 3.3). These two different technologies have been chosen to evaluate how a different degree of dispersion can affect the electrical properties of the final composite.

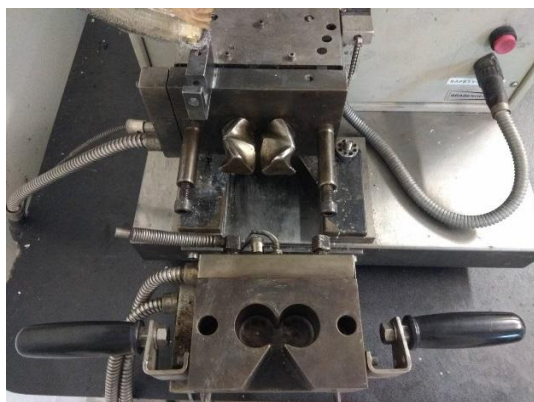


Figure 3.2 - Measuring mixer PlastiCorder Brabender, W50E model.



Figure 3.3 - Twin screw extruder Leistritz ZSE 18 HP-PH.

Biochar powders and PP granules were inserted into the measuring mixer working under the following conditions: 30 rpm during loading of the materials, 60 rpm for 3 minutes during mixing at T = 190 ° C. These conditions have been used for all types of compounds:

- PP unfilled (*PPUnfilledMix*)
- PP +5 % Biochar (*PP5BiocharMix*)
- PP +15 % Biochar (*PP15BiocharMix*)
- PP +30 % Biochar (*PP30BiocharMix*)

The material out of the mixer was then transferred to a pelletizing machine, Piovan RSP 15/15 model (Figure 3.4). Pelletization is necessary in order to have an input material suitable for the subsequent moulding process.



Figure 3.4 - Pelletizing machine Piovan, RSP 15/15 model.

Through the twin screw extruder the following compounds have been processed:

- PP unfilled (*PPUnfilledExtr*)
- PP + 30% Biochar (*PP30BiocharExtr*)
- PP + 40% Biochar (*PP40BiocharExtr*)

The extrusion parameters were modulated from time to time according to the specific mixture. Increasing the percentage of Biochar, in fact, increases the viscosity of the melt, which has led to the reset of temperatures along the screw to facilitate machining and avoid thermal degradation. Table 3.1 shows the temperatures along the screw profile for the different composites. Zones 1 to 8 indicate areas where progressively the feed goes from the feed hopper, near the extruder head (die), to the exit zone of the fuselage. Also the feed rate and rotation speed of the screw were modulated depending on the mixture to be extruded. A cooling tank for the still hot extruded material and a pelletizer to reduce it to granules were added at the end of the twin screw extruder.

After obtaining the granules with one of the above methods, these were moulded using a Babyplast injection moulding machine, 6/10P model, manufactured by Cronoplast S.L. (Figure 3.5). By moulding, "dog-bone" samples were attained according to the UNI ISO 527-5A standard: a gauge length 20 mm long, 4 mm wide, and 2 mm thick. In next chapters, the samples obtained will be subjected to laser treatment as well as mechanical and thermal tests.

Table 3.1 - Parameters used in the compounding process in the twin screw extruder.

Parameters	PP	PP + 30% Biochar	PP + 40% Biochar
T1 (°C)	190	190	190
T2 (°C)	190	190	190
T3 (°C)	190	190	190
T4 (°C)	180	180	180
T5 (°C)	180	180	180
T6 (°C)	175	175	175
T7 (°C)	175	175	175
T8 (°C)	175	175	175
Rotation speed (rpm)	350	350	350
Total flow (Kg/h)	1	1	1
Torque (%)	35	40	40



Figure 3.5 - Babyplast injection molding machine, 6/10P model, manufacturered by Cronoplast S.L.

Table 3.2 shows the parameters used for a correct moulding process.

Table 3.2 - Parameters used in the injection moulding process.

Parameters	PP (Mix)	PP + 5% Biochar (Mix)	PP + 15% Biochar (Mix)	PP + 30% Biochar (Mix)	PP (Extr)	PP + 30% Biochar (Extr)	PP + 40% Biochar (Extr)
Plastification temperature (°C)	200.0	200.0	200.0	200.0	200.0	210.0	210.0
Melting chamber temperature (°C)	195.0	195.0	195.0	195.0	195.0	205.0	205.0
Nozzle temperature (°C)	190.0	190.0	190.0	190.0	190.0	200.0	200.0
Mold temperature (°C)	80.0	80.0	80.0	80.0	80.0	80.0	80.0
Shot size (mm)	10	10.5	11.5	11.5	10.0	11.5	11.5
Cooling time (sec)	15.5	15.5	15.5	15.5	15.5	15.5	15.5
1st inj. pressure (bar)	30.0	30.0	30.0	30.0	30.0	40.0	40.0
1st inj. pressure time (sec)	2.5	2.5	2.5	2.5	2.5	2.5	2.5
2nd inj. pressure (bar)	20.0	20.0	20.0	20.0	20.0	20.0	20.0
2nd inj. pressure time (sec)	1.5	1.5	1.5	1.5	1.5	1.5	1.5
2nd pressure setting (mm)	0.1	0.1	0.1	0.0	0.1	0.0	0.0
Decompression (mm)	1.0	1.0	1.0	1.0	1.0	1.0	1.0
Injection speed (%)	30.0	30.0	30.0	30.0	30.0	30.0	30.0
2nd injection speed (%)	10.0	10.0	10.0	10.0	10.0	10.0	10.0
2nd speed point (mm)	0.1	0.1	0.1	0.0	0.1	0.0	0.0

3.2 Percolation threshold evaluation

It is necessary at this point to search for the percolation threshold to know the maximum filler content beyond which the composite material conducts electricity even before any laser treatment. Once the percentage of filler suitable for the formation of the percolating pattern would have been found, it would have been necessary to choose one concentration slightly below it to avoid conduction outside the laser track. To this end, linear surface electrical resistance measurements were performed on non-lasered specimens with different Biochar percentages, using the two-wire method with a Keithley 2700E multimeter, having an overflow limit of 120 MΩ (Figure 3.6).



Figure 3.6 - Keithley 2700E multimeter.

This preliminary electrical characterisation was performed by positioning the two multimeter tips directly on two electrodes deposited above the dog-bone sample (Figure 3.7).



Figure 3.7 - Linear surface resistance measurements per unit length on non-lasered specimens. The multimeter tips are placed directly on the two electrodes.

By applying the electrodes, the conductivity of the covered area is uniform, and it is possible to measure much more stable and accurate resistance values without a punctual measurement. Bibliographic studies have highlighted the possibility of using different techniques to deposit conductive layers, including deposition by thermal evaporation, by sputtering or by the use of conductive paints. For ease of application, cost containment and equipment availability, it has

been decided to use Ag-based conductive paints to make the electrodes. The deposition method of the conductive layer involves the use of silver-charged conductive paint (RS 186-3600) applicable with a brush. Then, the paint was left to dry for a time between 2 and 4 hours. The deposition of the electrodes must be carried out by paying particular attention to respecting the geometry to ensure the reproducibility of the measurement, as it depends on the distance between them and their shape. For the present thesis work, the electrodes were made of 1x1 cm and distanced 3 cm apart.

3.3 CO₂ laser scribing

The functionalisation of the previously obtained composite materials for electrically conductive tracks realisation was carried out using CO₂-type Towermark XL laser, produced by LASIT S.p.a. (Figure 3.8).

The laser emits radiation in the medium infrared, at a wavelength of 10600 nm. Electromagnetic emission is pulsed with a maximum power output of 100 W. To prevent the combustion of the material and only lead to a pyrolysis induced by the laser photothermal action, all laser treatments have been conducted in an inert nitrogen atmosphere. Before each machining, the focal lens has been thoroughly cleaned with a cloth soaked in acetone so that any residual material from previous work could not affect the efficiency of the laser beam. In Figure 3.9 it is possible observe the typical experimental set-up used in this thesis work. The sample is placed on a metal support, surrounded by four arms which, during processing, blow nitrogen, and a larger manifold that acts as a suction hood for fumes and residues produced during ablation.

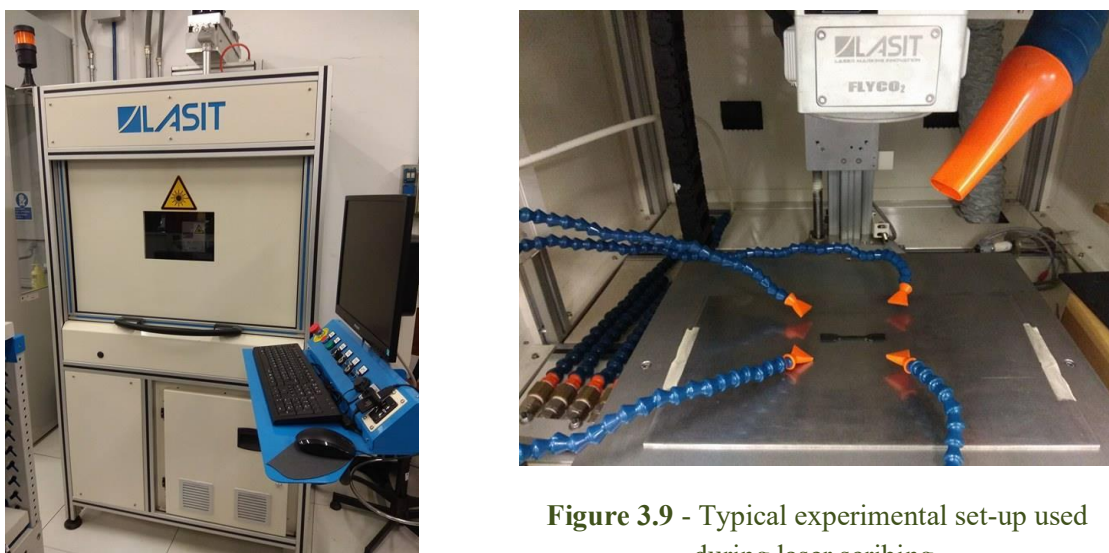


Figure 3.9 - Typical experimental set-up used during laser scribing.

Figure 3.8 - CO₂-type Towermark XL laser produced by LASIT S.p.a.

Communication between the operator and the machine is done via the Flycad software, within which you can draw the path that the laser beam will have to track. The way the laser interacts with the sample can be adjusted by varying the input parameters that can be changed by the machine control. In particular, the following process parameters can be modified: power (P), scan rate (v), frequency (f), number of repetitions (N), and defocus (D). The power values set on the machine are expressed as a percentage of the maximum laser power. Scan rate represents the speed with which the laser invests the material, expressed in mm/s. The number of repetitions N, on the other hand, indicates the number of times the laser repeats the same treatment. The frequency, in kHz, denotes the number of pulses per second. Finally, the defocus, in mm, is understood as the height distance from the sample focus point.

The first step in the realisation of electrical circuits integrated into the polymer by laser ablation is to study the ablation phenomenon through which the laser beam and the material interact. The first approach to this analysis was carried out using an experimental design that made possible to understand the effects of the main parameters on the response regarding electrical resistance: a standard value for each laser parameter was chosen and kept constant together with the variation of the remaining four parameters (Figure 3.10). In this way, it was possible to obtain curves in which the linear surface electrical resistance (R) was plotted as a function of one of the five laser parameters to be evaluated. Standard values (with a red background in Figure 3.10) were chosen based on previous studies at CRF on nano-composites containing carbon nanotubes, in order to obtain R values below the multimeter's overflow limit also with low-invasive laser treatments.

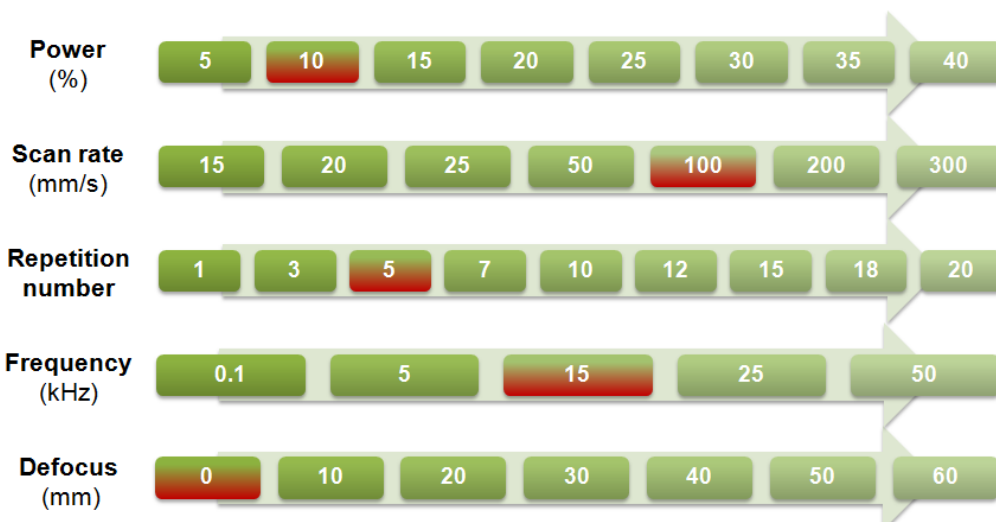


Figure 3.10 - Laser parameters range of variation. The values with a red background are the standard values chosen.

Thus, a first experimental campaign consisting of 32 trials was common to all composites previously prepared to be able to draw considerations on the study of the phenomenon in general, but also to evaluate any similarities or inconsistencies in the trends of the individual materials.

This step was decisive for assessing the direction to be taken to pursue the desired outcome. Table 3.3 shows the values of the five parameters used for each trial.

Table 3.3 - List of values of the parameters chosen for each trial.

Trial	Power (%)	Scan rate (mm/s)	Repetition number	Frequency (kHz)	Defocus (mm)
1 (std.)	10	100	5	15	0
2	5	100	5	15	0
3	15	100	5	15	0
4	20	100	5	15	0
5	25	100	5	15	0
6	30	100	5	15	0
7	35	100	5	15	0
8	40	100	5	15	0
9	10	50	5	15	0
10	10	25	5	15	0
11	10	20	5	15	0
12	10	15	5	15	0
13	10	200	5	15	0
14	10	300	5	15	0
15	10	100	1	15	0
16	10	100	3	15	0
17	10	100	7	15	0
18	10	100	10	15	0
19	10	100	12	15	0
20	10	100	15	15	0
21	10	100	18	15	0
22	10	100	20	15	0
23	10	100	5	5	0
24	10	100	5	25	0
25	10	100	5	50	0
26	10	100	5	0.1	0
27	10	100	5	15	10
28	10	100	5	15	20
29	10	100	5	15	30
30	10	100	5	15	40
31	10	100	5	15	50
32	10	100	5	15	60

A constant experimental layout was defined throughout the experiments to reduce the variability of their results. Specifically, six parallel tracks, 1.5 cm long, were written on each specimen. Each trial was performed on three-track groups (two trials were performed on each sample). The experimental layout for a generic sample is schematized in Figure 3.11. Resistance values measured for each of the three tracks were averaged.



Figure 3.11 - The experimental layout for a generic sample: three laser tracks per trial, two trials per sample.

3.4 Electrical characterisation

After carrying out all the experiments described in the previous paragraph, electrodes have been realised, and the linear surface electrical resistance was detected.

This time the paint was deposited to make circular electrodes all equal in shape and size, and keep their distance constant along conductive tracks. Figure 3.12 shows one of the prepared specimens, within which it is possible to observe the laser tracks with the silver electrodes at their ends.

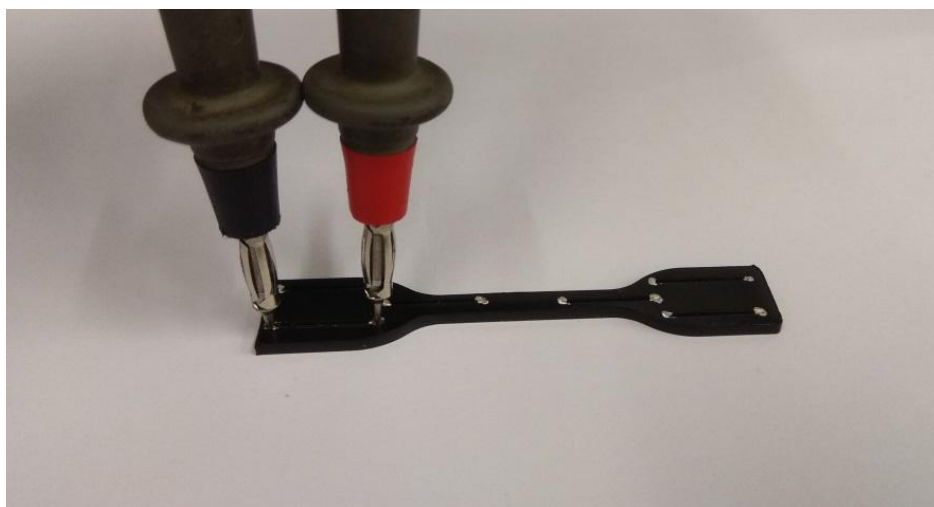


Figure 3.12 - Linear surface resistance measurements in lasered specimens. Example of circular electrodes, at the extremities of each laser track, prepared with conductive silver paint.

Linear surface electrical resistance measurements were made along the tracks drawn by the laser and between adjacent tracks to detect the electrical response of the composite based on the laser treatment performed. In fact, the interaction of the laser with the surface of the material changes with the variation of the set parameters, resulting in more or less conductive tracks. This electrical characterisation was performed in real time after each treatment positioning the two multimeter tips directly on the circular electrodes; in this way, it was possible to quickly evaluate and optimise the laser parameters to be set to achieve the desired electrical resistance values from time to time.

A critical analysis of these information has allowed gaining a basic knowledge of the influence of the different parameters on the electrical response. Thus, it has allowed the optimisation of the laser ablation phenomenon to obtain minimal electrical resistance along the track and a signal beyond the instrument's overflow limit between adjacent tracks not in contact: that has made possible the realisation of an electrical circuit for the transport of signals.

Before the electrical resistance measurements, the surface of each laser-treated specimen was subjected to a cleaning process, consisting of compressed air jet and passage of a cleaning cloth. This step has been necessary to eliminate any carbonaceous residue weakly attached to the bottom of the track previously exposed to the laser beam, which could have led to false responses. An increase in electrical resistance after cleaning is to be associated with the removal of the carbonaceous residue formed by the laser ablation, which was first spread throughout the lasered surface of the sample.

3.5 Mechanical characterisation

Firstly, it was important to demonstrate whether the addition of Biochar to the polymer matrix would act as a mechanical reinforcement for the composite material. Consequently, tensile tests were performed at room temperature on five different dog-bone samples (for statistical purposes) per each type of material obtained from the mixer. The tests were conducted with the dynamometer MTS Criterion 43.504, with a 5kN load cell, and managed by a software that allows the operator to modulate the different tests according to needs and to provide data acquisition. Tensile tests were carried out at a deformation rate of 5 mm/min.

3.6 Thermal characterisation

Thermal characterisation has become necessary to evaluate the influence of Biochar on the thermal behaviour of the PP. Non-lasered specimens derived from the measuring mixer were then analysed by Thermogravimetric Analysis (TGA) and Differential scanning calorimetry (DSC). The TGA was also performed on Biochar powders.

3.6.1 Thermogravimetric analysis (TGA)

Thermogravimetric analysis (TGA) measures the weight variations of a heat-treated material in a temperature ramp or in isothermal, in a controlled atmosphere. The TGA was conducted using the Mettler-Toledo TGA/SDTA 851 instrument. In TGA, it is always essential to indicate the exact heating speed since the same sample analysis carried out with different speed ramps will produce different thermograms.

The TGA was carried out both on Biochar powders and PP/Biochar composites. For the powders, the TGA was conducted in argon with a temperature ramp from 25 to 1500 °C at heating rate of 10 °C/min, followed by an isotherm of 1 hour at 1500 °C. For each composite sample, a temperature ramp was set from 25 to 700 °C at heating rate of 10 °C/min. The measurements were carried out both in an inert atmosphere of argon and in the air (oxidative environment). The data was processed to create TGA curves, which are used to evaluate the mass-loss and its dependence on temperature.

3.6.2 Differential scanning calorimetry (DSC)

Differential scanning calorimetry (DSC) is a thermal analysis that allows measuring the difference in heat flow between the sample and a reference when both are subjected to controlled heating or cooling ramps to assess the heat resistance of materials. In the case of polymers, some examples of measurable phenomena are the glass transition, fusion and crystallisation temperatures.

In the present work, DSC was conducted in inert nitrogen environments on PP samples as well as PP loaded with the different contents of Biochar, using the TA Instruments Q100 DSC machine. Each sample has undergone three thermal cycles, each consisting of a heating ramp and a cooling at 10 °C/min: from -50 °C up to 200 °C, and consecutive descent. The first cycle was carried out to eliminate the "thermal history" of the material, while the second provided material transition temperatures, data confirmed by the third cycle. As a result, material information has been extracted from the second cycle.

3.7 Morphological and spectroscopic characterisation

3.7.1 Biochar Powders

X-ray Powder Diffraction (XRD) measurements were performed on the filler powder, using a Siemens D5000 diffractometer. Scans (with Cu-K α radiation) were carried out over the 2 θ range of 10-80°, using a step size of 0.028° and scan speed of 2 s/step.

The powder was also analyzed at Raman, Renishaw inVia Reflex model, to study its graphitisation degree using a laser with a wavelength of 514 nm (green) in three different points. The morphology of Biochar powder was investigated with a Field Emission Electron Scanning Microscopy (FESEM) using a Zeiss MERLIN microscope.

A final characterisation was then carried out with Energy-dispersive X-ray spectroscopy (EDS), used to discover the various chemical elements present in the powders.

3.7.2 PP/Biochar composites

Dispersion degree of Biochar particles in the polymer matrix was evaluated using Leica DMI 5000 M optical microscope after polishing the surface of the non lasered dog-bone specimens obtained by the mixer.

Moreover, the samples that, following the laser treatment, gave the most promising responses regarding linear surface electrical resistance per unit length, were subjected to further morphological characterisation by the FESEM seen in the previous section. The observation was conducted along the track written by the laser. To avoid charging, a few nanometers layer was deposited by a chromium metallization process on the analysed surface, that is the one that interacts with the primary electron beam of the SEM.

4. Experimental results and discussion

4.1 Biochar characterisation

4.4.1 X-ray Powder Diffraction (XRD)

X-Ray Diffraction spectrum of Biochar powders in Figure 4.1 provides us with some insight into an increase in conductivity due to a potential graphitisation. The spectrum confirms the typical structure of graphite-based carbonaceous materials, with graphite 2H and hexagonal graphite peaks. The lower amount of hexagonal graphite would explain the lower electrical conductivity of the Biochar compared with a fully graphitic material. It is also possible to notice numerous peaks that can be traced back to inorganic materials, likely derived from the raw biomass.

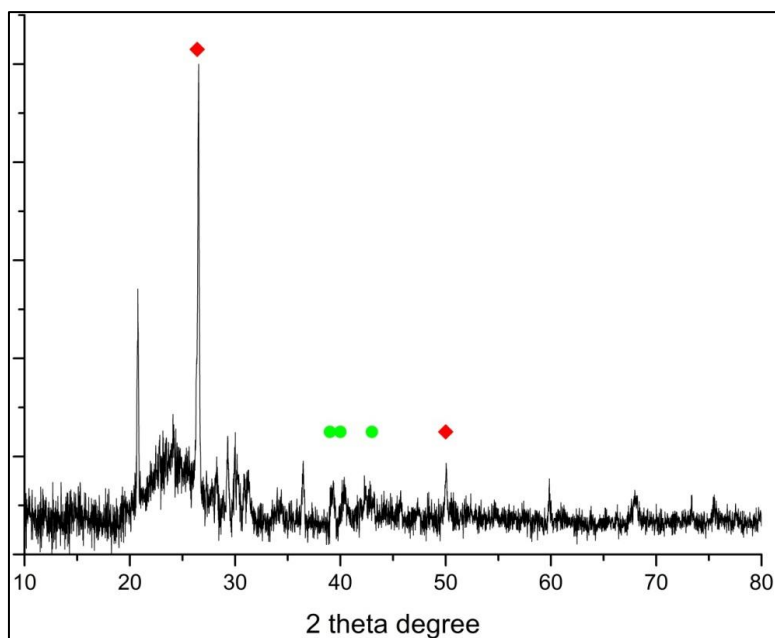


Figure 4.1 - Biochar powders diffraction spectrum. The green peaks represent hexagonal graphite, whereas the red ones the graphite 2H.

4.1.2 Raman spectroscopy

Figure 4.2 shows a mediated Raman spectrum. The D and G peaks were fitted each with two Gaussians, and the ratio of their intensity (I_D/I_G) was obtained as a ratio between the respective Gaussian's areas. Remember that the I_D/I_G ratio (1.15 in this case) indicates the relationship between disorder (I_D) and degree of graphitisation (I_G) of the material. Secondary peaks (2D, D + G, 2G) were not considered in this analysis.

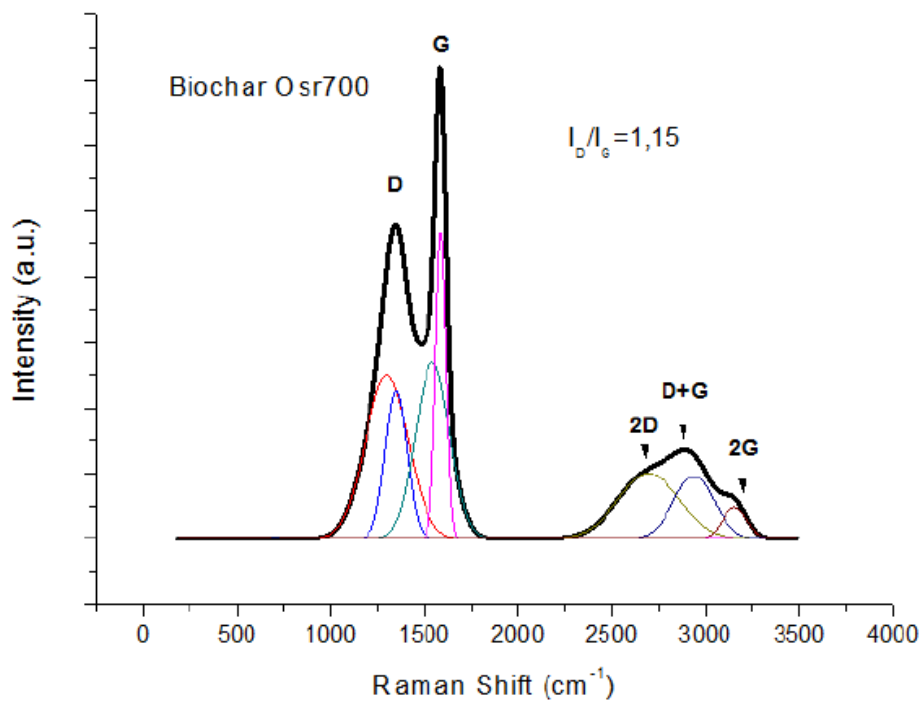


Figure 4.2 - Raman spectrum.

The material has a reasonable degree of graphitisation and an acceptable disorder given the nature of the material itself. The material has a medium level of amorphism that emerges from the height of the gap between the D and G peaks. The lower this difference (the D and G peaks are well separated), the better is the crystallinity degree of the material.

4.1.3 Field Emission Scanning Electron Microscopy (FESEM)

FESEM microscopic analysis was of utmost importance for studying the shape and size of the Biochar particles. In figure 4.3 it is possible to notice how Biochar particles are very irregular in shape and size. The particles come in rounded, elongated or in the form of platelet shapes. Their size ranges from a few hundred of nanometers to a few tens of microns. In general, sizes with low aspect ratio would explain the difficulty in forming a percolating pattern within the polymer matrix.

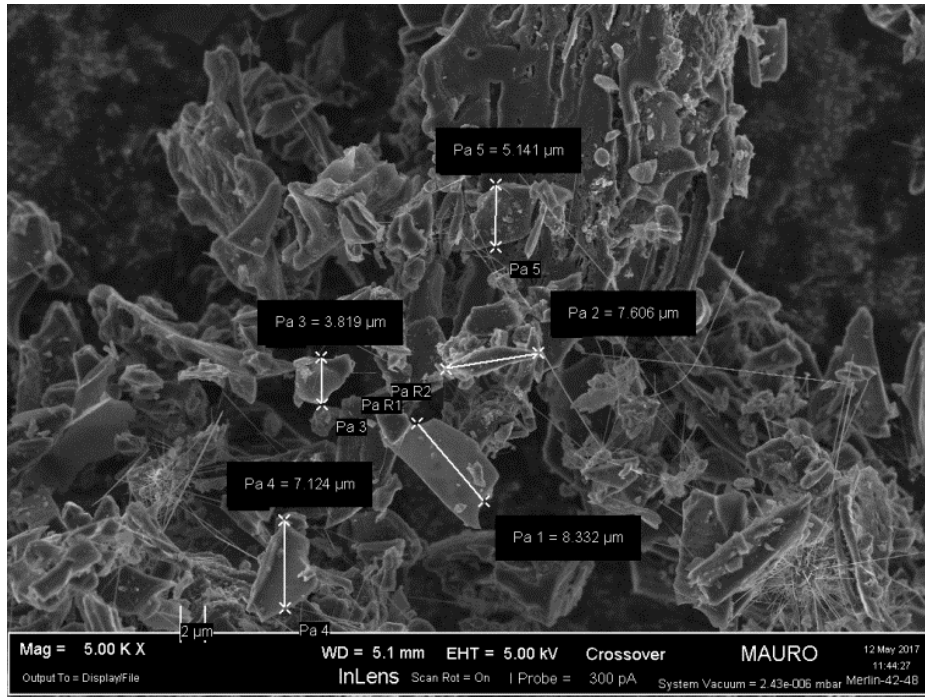


Figure 4.3 - FESEM micrograph of Biochar powders at 5Kx magnification.

Figure 4.4 shows a Biochar particle having the shape of a platelet and numerous smaller and more rounded satellites around it. Whereas in Figure 4.5 is possible to observe how the thickness of the platelet is small compared to the other two dimensions. That testifies its high aspect ratio.

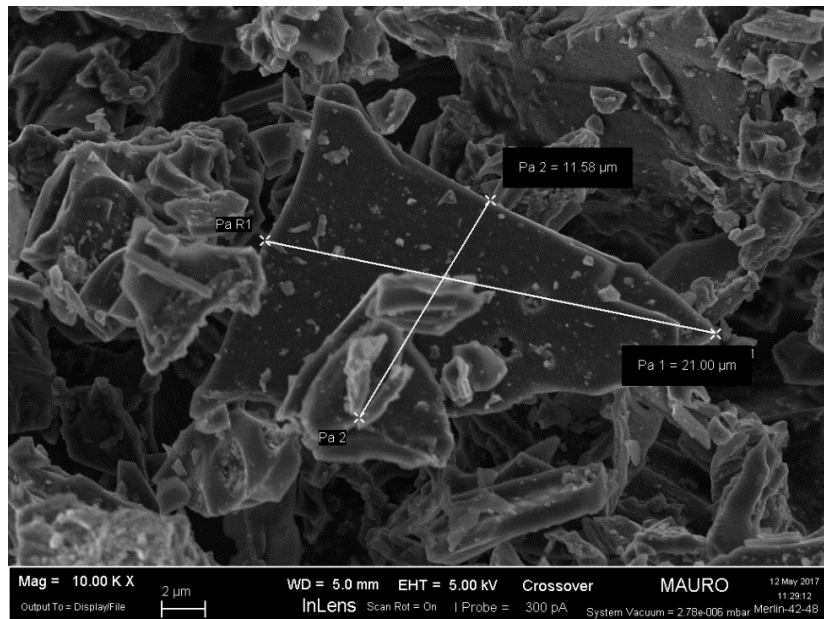


Figure 4.4 - FESEM micrograph of a Biochar particle in the form of a platelet at 10Kx magnification.

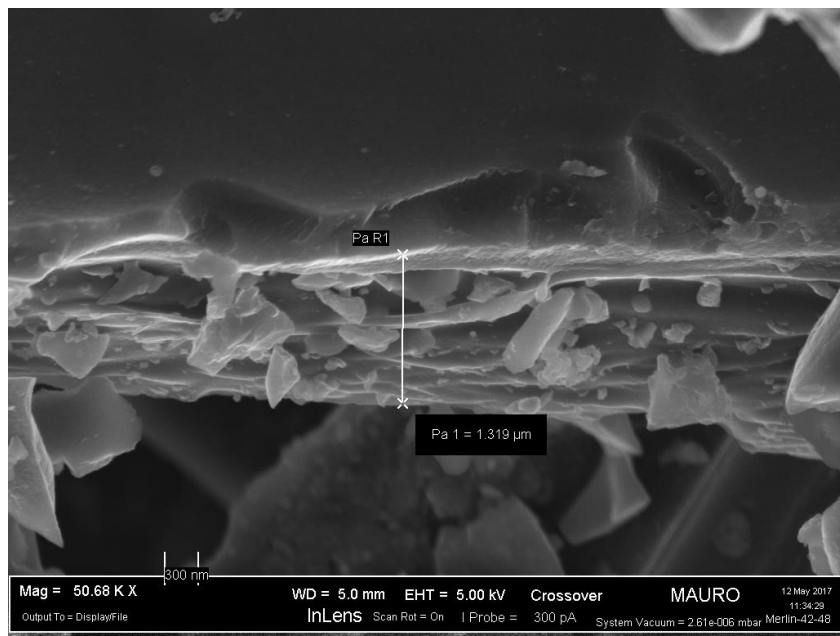


Figure 4.5 - FESEM micrograph along the thickness of a Biochar particle in the form of platelet at 50Kx magnification.

4.1.4 Energy-dispersive X-ray spectroscopy (EDS)

The carbon content of Biochar is the most significant value to investigate, as it is a measure its degree of carbonisation. The carbon content of Biochar is expected to be much greater than 50 wt%, which is the typical value of dry wood.³¹ In fact, carbonization or pyrolysis drives out hydrogen as well as oxygen and results in an increase in carbon content of the Biochar. As can be seen from the Figure 4.6, the EDS spectrum confirms that Biochar is composed of a high percentage of carbon (about 83 wt%) with traces of other elements derived from the pyrolysed biomass. Table 4.1 displays the results of elemental analysis of the commercial Biochar samples selected for this study.

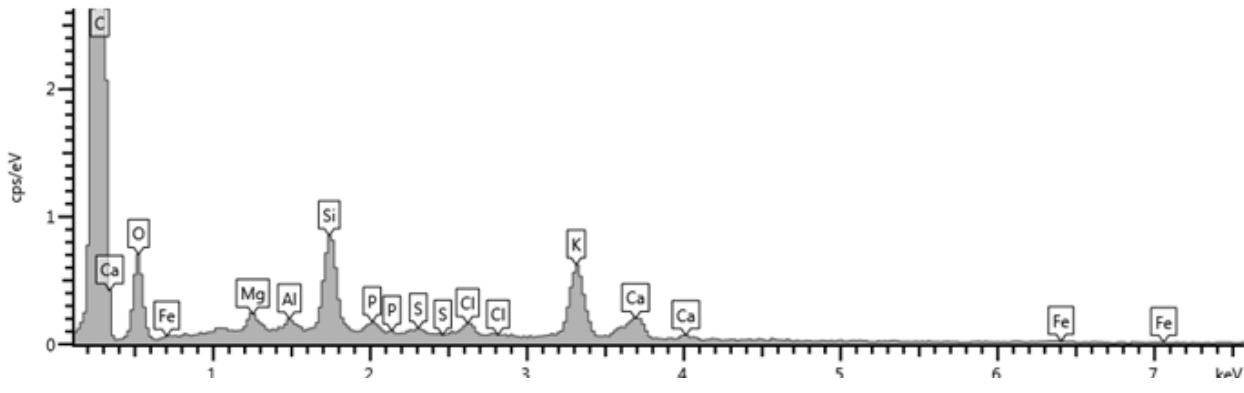


Figure 4.6 - Biochar powders EDS spectrum.

Table 4.1 - Weight percentages of element present in Biochar powders.

Element	wt%	wt% Standard deviation
C	82.74	0.39
O	10.80	0.36
Mg	0.31	0.04
Al	0.17	0.03
Si	1.67	0.06
P	0.23	0.04
S	0.12	0.04
Cl	0.31	0.04
K	2.57	0.08
Ca	0.93	0.06
Fe	0.16	0.10
Total	100.00	

4.1.5 Thermogravimetric analysis (TGA)

TGA on Biochar powders has been conducted to evaluate its thermal stability even at high temperatures. In Figure 4.7, the thermogram of the test carried out in Argon is shown both during the temperature ramp from 25 to 1500 °C and the isotherm at 1500 °C for 1 hour. Argon gas is used to provide inert atmosphere and prevent combustion of the samples.

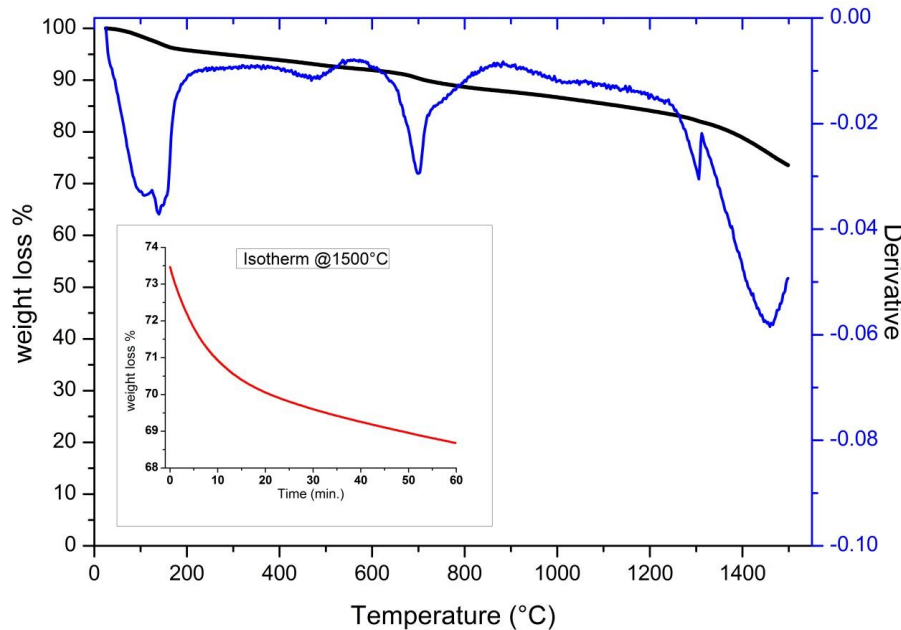


Figure 4.7 - TGA graph displaying the weight loss of Biochar powders during heating in argon with a temperature ramp from 25 to 1500 °C at heating rate of 10 °C/min, followed by an isotherm of 1 hour at 1500 °C.

As seen from the graph, the drop in weight at low temperatures is due to the loss of adsorbed humidity. Then, TGA has provided proof that the sample contains nearly 10 wt% of volatile content, which goes away during heating until 700 °C. The electrical conductivity of Biochar powders is affected by the volatile content. Volatiles are present in the pores of the Biochar and hinder its electrical conductivity properties. Finally, a residue of 73% is obtained at 1500 °C and, after one hour, it drops to 69%.

4.2 Preparation of polymer composites with Biochar

The experimental work began with the preparation of composite materials by injection moulding of the granules obtained through the measuring mixer or the twin screw extruder, both used to mix Biochar powders with the polymer pellets. Despite the high filler content, all types of dog-bone specimens have been moulded with ease. Even the extruded wire, before being granulated, did not show the expected fragility. That has demonstrated the possibility of loading this type of materials even in percentages of 40 wt% of Biochar.

4.3 Percolation threshold evaluation

Following the deposition of electrodes on non-lasered specimens, the linear surface electrical resistance measurement between the two was carried out to find the percolation threshold. Unfortunately, no test showed a linear surface resistance lower than the overflow limit of the equipment used. For this reason, it was not possible to evaluate the percolation threshold, and as a consequence, it was not feasible to choose the optimum percentage concentration of Biochar to be used in the laser specimens. Indeed, it is recalled that the specimens must be below the percolation to avoid electrical conduction between adjacent tracks, but the electrical signal should only pass along the laser track, where the percolation threshold is locally exceeded.

The results suggest a non-homogeneous distribution of Biochar within the specimen. In fact, the filler concentration would look greater in the bulk of the samples and less in their exterior parts. These trends can be explained by considering the skin effect on the surface of the composite due to the production process. On the surface of the composite, before the interaction with the laser beam, the Biochar concentration is nought because of the presence of polymeric skin formed during the moulding process due to the preventive cooling of the compound on the mould wall.

4.4 Evaluation of the influence of the variation of the laser parameters on conductivity

The aim is to obtain the minimal value of linear surface electrical resistance through a laser treatment that is reproducible and does not mechanically deform the sample at the macroscopic level. The presence of conduction between different non-continuous conductive tracks is also undesirable since such a signal could lead to the component short circuit during application. From what has just been shown, the action of the laser beam should be "limited" to the localised removal of matter to bring out a percolation network of the Biochar particles contained in the material on the surface. In fact, they are the main responsible of the electrical conduction of these composites. In reality, following the ablation phenomenon, there is the formation of a carbonaceous residue whose composition is not precisely known. While eliminating the residue by the technique described in paragraph 3.4, it is not excluded that part of this residue remains attached to the surface of the laser track and contributes in part to its electrical conductivity.

The CO₂ laser ablation mechanism in polymers, as clarified in paragraph 1.3.2, is essentially due to a photothermal process. The polymer undergoes thermal degradation and is removed from the surface by a depletion of macromolecular fragments and formation of volatile compounds. The Biochar particles present in the area affected by the ablation must, therefore, accumulate along the track, not being degraded by the temperatures achieved by the laser action. At the same time, the oxidative dehydrogenation reaction can lead to the creation of double bonds. When the number of these double bonds is sufficiently high to lead to their conjugation, the formation of π orbitals is capable of contributing to the electrical conduction of the laser track. These systems carry the electrical charge through a resonant mechanism of the double bonds, acting as a conductive connection between the network of particles contained in composites that do not reach the percolation threshold.

In next sections is shown how the different laser parameters work on the electrical resistance of the tracks.

4.4.1 Power

Initially, the influence of the variation of the power (P) parameter was tested. Figure 4.8 shows the trend of the linear surface electrical resistance per unit length as a function of the P% for the PP5BiocharMix, PP15BiocharMix and PP30BiocharMix specimens. For a simpler reading of graphs, the R per unit length values greater than the overflow limit of the used measuring equipment (120 M Ω or 80 M Ω /cm for 1.5 cm tracks) are considered to be 80 M Ω /cm.

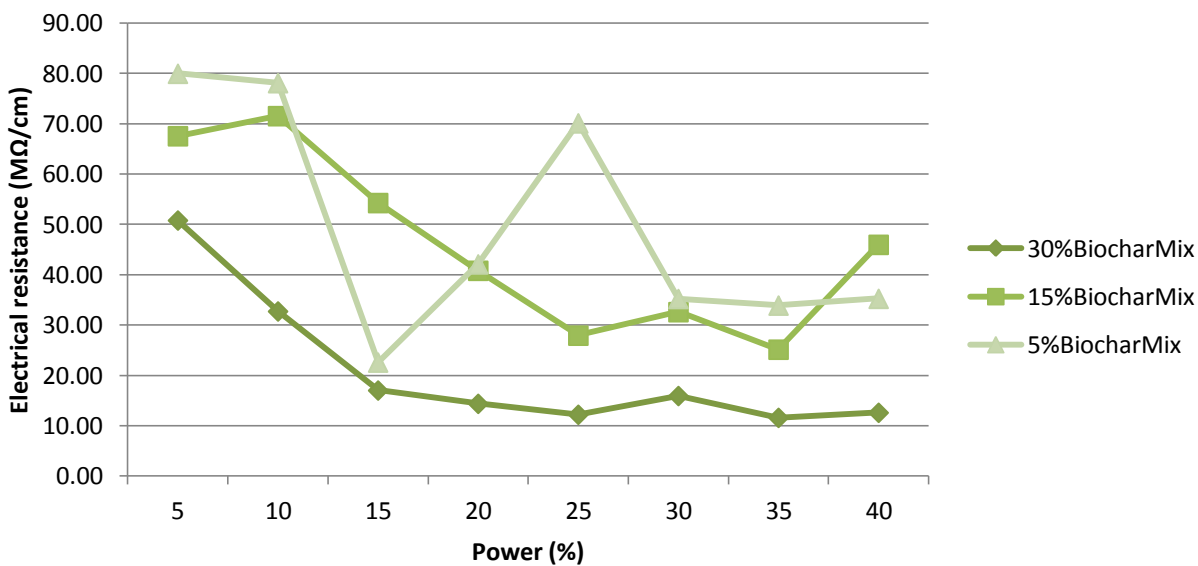


Figure 4.8 - Linear surface electrical resistance per unit length as a function of the power (%), for PP5BiocharMix, PP15BiocharMix and PP30BiocharMix specimens.

From the previous graph, it was first observed that the results obtained are very different depending on the power values set for the laser beam. For example, the resistances obtained vary from 50.84 MΩ/cm (SD = 1.20) for trial 2 (P = 5%) to 11.63 MΩ/cm (SD = 1.31) for trial 7 (P = 35%) for the same composite PP30BiocharMix. This trend highlights the importance of identifying the most appropriate laser treatment to reveal the conductive character of the material and how one cannot content itself with the simple ablation of the polymeric skin. Rather, it is necessary to optimize the interaction so that all parameters contribute synergistically and result in minimal surface electrical resistance. Also, from these first experiments, it seems that PP/Biochar composites respond well to laser treatment and are suitable for the optimisation of laser parameters. It is also necessary to report how all the samples are conductive only along the tracks and not between them.

The first linear surface electrical resistance per unit length measurements indicate that values of the order of MΩ/cm can be achieved by increasing the P for all the composites. That means that when the set power value increases, the average electrical resistance value (the response) decreases and this is broadly in line with what one would expect. In fact, for laser ablation, greater power indicates a more significant amount of insulating polymeric material removed increasing the local concentration of the conductive filler. There is, therefore, a lower electrical resistance. Increasing power values, though, the tracks are very deep, as the laser interacts most with the composite and this could be an applicative limit on low-thickness devices.

With the same laser treatment, there is a decrease in electrical resistance as the percentage of the filler contained in the polymer matrix is increased. In fact, at the same operating conditions, shallow R values are obtained with little "aggressive" treatments for composites with higher percentages of Biochar. That is largely in agreement with experimental predictions. In fact, an

increment in the content of Biochar particles makes them come into contact more easily, and that facilitates the formation of one or more percolative networks responsible for electrical conduction. It is clear that by decreasing the Biochar content in the composite, it's hard to obtain R values sufficiently small to achieve competitive materials with modern metal devices and printed circuits. In particular, to determine the set of parameters that lead to R values close to 1 MΩ/cm also with low Biochar percentages, it is necessary to impose P, v, N, f, and D values which produce very deep and wide tracks. That can cause, in many cases, even a deformation of the sample, which would be unsuitable for the application.

While PP30BiocharMix composites exhibit a regular decay of R with an increase in P, on the other hand, PP5BiocharMix and PP15BiocharMix composites have a more irregular trend and much higher resistance values. PP5BiocharMix and PP15BiocharMix composites have, for many laser treatments, electrical signals above the instrument's overflow limit. Also, their electrical resistance values are very variable depending on the pressure exerted with the cloth during the cleaning of the tracks following the treatment. That could mean a little adhesion between the Biochar particles and the polymer matrix. Following the considerations just described concerning composites with minor percentages, it has now been concluded that these materials are unsuitable for this thesis work.

The graph in Figure 4.9 shows the same set of experiments carried out on samples coming from the extrusion process to evaluate the effect that the method of mixing Biochar particles with the polymer matrix has on the electrical resistance. The PP30BiocharExtr tracks follow the same electrical resistance trend of the PP30BiocharMix as the laser parameters change. PP30BiocharMix, however, proved to be more conductive than PP30BiocharExtr, as discussed in section 1.2.3, where it was exposed how an anisotropic distribution of the CB particles could lead to higher conductivity and lower percolation concentration compared to isotropic samples. In fact, during mixing in the twin screw extruder, the aggregates start breaking down increasing the gap between the particles. However, PP30BiocharExtr specimens would appear less fragile than PP30BiocharMix due to a better dispersion of the filler reachable by the extrusion process.

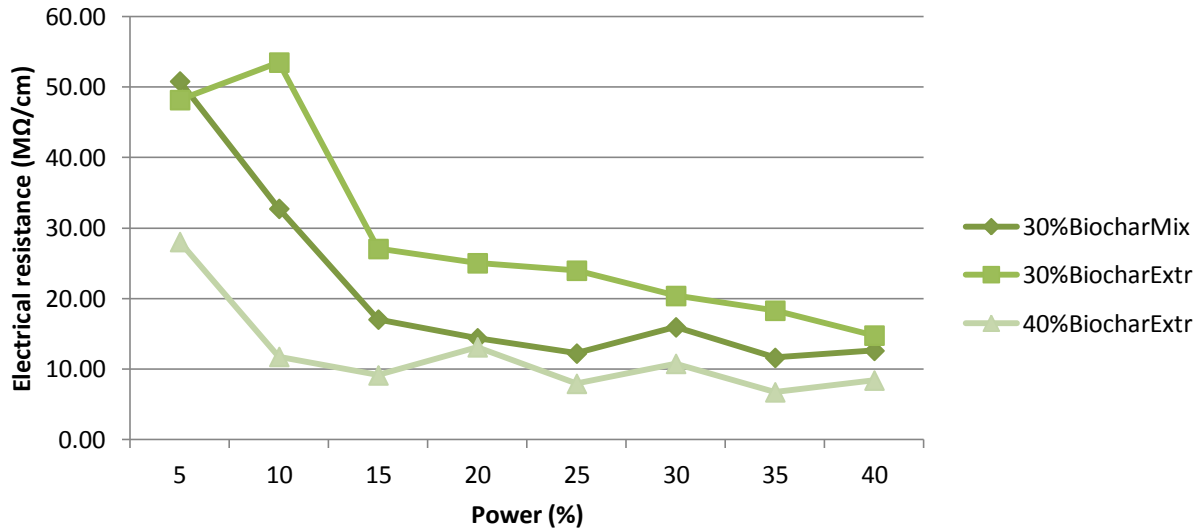


Figure 4.9 - Linear surface electrical resistance per unit length as a function of the power (%), for PP30BiocharMix, PP30BiocharExtr and PP40BiocharExtr.

The electrical resistance of the tracks on PP40BiocharExtr declines much faster than all the other types of specimens even after little invasive laser treatments. Although this may sound a good result, two major problems arose here.

Firstly, the electrical resistance reaches a plateau, just as it did with the PP30BiocharMix and PP30BiocharExtr specimens. That is presumably indicative of the fact that Biochar has a physical limit of electrical resistance and therefore it is difficult to further decrease the electrical resistance of these composites simply by increasing the filler content.

The second problem concerns inter-track conductivity. In effect, unfortunately, all the specimens showed lower electrical resistance values than the overflow limit of the multimeter. It is important to underline that if it is not possible to obtain an electrical signal between non-continuous tracks greater than the instrument's overflow limit, it is useless to optimise the parameters for the PP40BiocharExtr composites to increase the interaction of the laser beam. In fact, even if the resistance value found could be improved, the presence of transport of electrical current between non-continuous tracks does not make the material suitable for the use in electrical circuits.

For these reasons, the PP40BiocharExtr composites will automatically be excluded from the discussion, although the following graphics will also show the electrical resistances of these materials.

4.4.2 Scan rate

The scan rate (v) of the laser is another parameter that influences the conductivity and morphology of the laser track. The graphs in Figures 4.10 and 4.11, which are again representative of the trend of all the tests performed by varying the v , indicate that when decreasing the scan rate the electrical resistance decreases. The increase in electrical conductivity

at decreasing scan rate was predictable because the laser beam interacts longer on the surface of the sample, resulting in an ablation for major times and then of greater impact. Conversely, as the laser writing speed increases, the resistance increases as the laser beam lasts for less time on the surface, resulting in the removal of a smaller amount of polymer. The low-speed scanned tracks thus correspond to lower surface resistance values, but morphologically they are deeper and irregular than those at higher speeds. In some cases, the material has been deformed and perforated for low laser scan rates (15 mm/s for PP30BiocharMix, PP30BiocharExtr and PP40BiocharExtr, 20mm/s for PP15BiocharMix and 25mm/s for PP5BiocharMix).

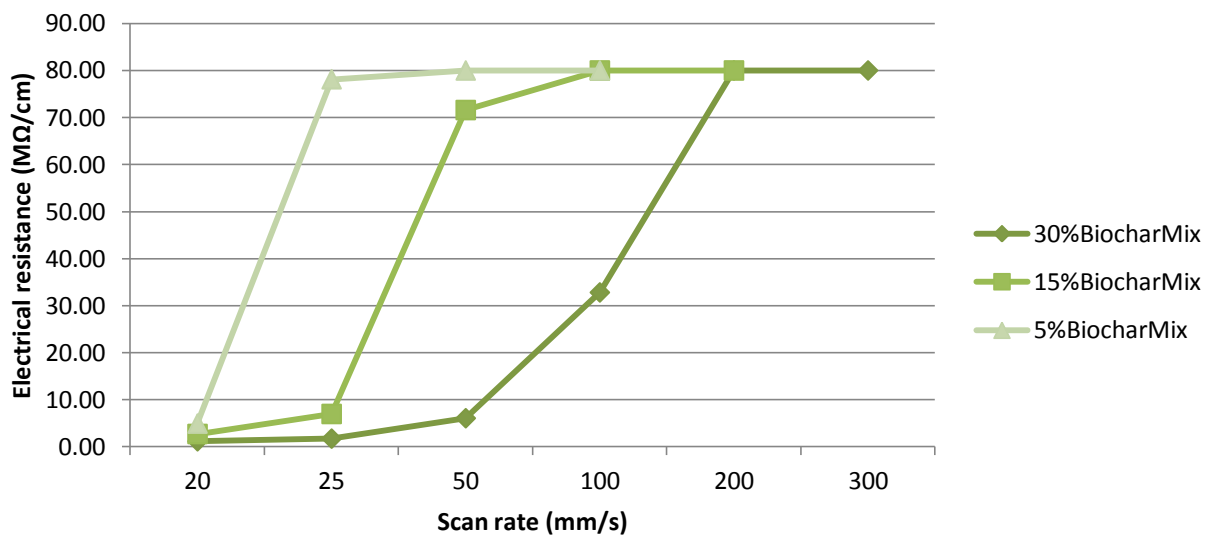


Figure 4.10 - Linear surface electrical resistance per unit length as a function of the scan rate, for PP5BiocharMix, PP15BiocharMix and PP30BiocharMix specimens. A scan rate equal to 25 mm/s brings to the perforation of the PP5BiocharMix specimens. A scan rate equal to 20 mm/s brings to the perforation of the PP15BiocharMix specimens.

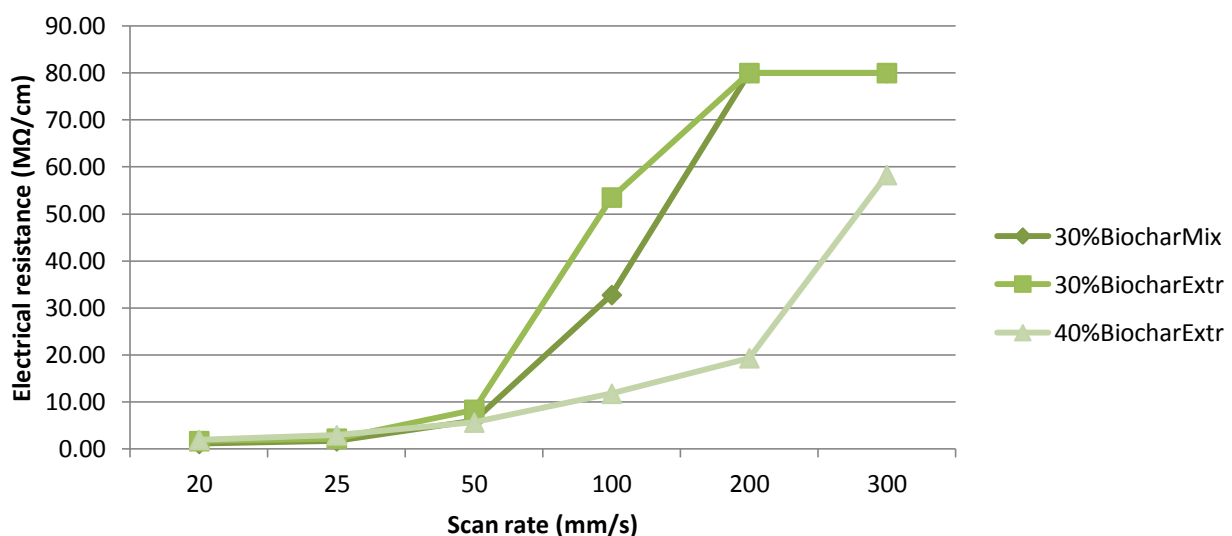


Figure 4.11 - Linear surface electrical resistance per unit length as a function of the scan rate, for PP30BiocharMix, PP30BiocharExtr and PP40BiocharExtr.

In general, the results are similar to the previous ones, i.e. the PP30BiocharMix specimens exhibit the lower electrical resistance values, without considering the PP40BiocharExtr which shows inter-track conductivity. The trial 11 has resulted in the lowest resistance value found in all laser tests performed in this work, precisely a value of $1.11 \text{ M}\Omega/\text{cm}$ ($\text{SD} = 0.31$) for PP30BiocharMix specimens. This trial is associated with very low write speeds (20 mm/s) and low power (10%). From these settings, it is understood that the scan rate has a greater weight than the power, in fact, electric resistance values of a lower order of magnitude than those in which the power was varied were achieved. Although the power was set to almost the minimum value established in this work, giving enough time to the laser beam to interact with the material is sufficient to obtain resistance values of a few $\text{M}\Omega/\text{cm}$. It is thus deduced that laser treatments with high scan rates are, albeit by a high power, certainly less invasive than those performed at low power but at a minimum speed that entails a significantly greater interaction.

4.4.3 Repetition number

It is possible to repeat the laser treatment several times by redirecting the beam on the same track. The repetition number (N) has been shown to be one of the parameters most influencing the conductivity values that can be reached following laser treatment on composites PP/Biochar, as evidenced by the trends shown in Figure 4.12 and Figure 4.13.

There is a marked reduction in resistance with increasing N . By modifying the number of repetitions of the treatment, shallow values of R were achieved, equal to $2.5 \text{ M}\Omega/\text{cm}$ ($\text{SD} = 0.55$) in the trial 22 (20 repetitions) for PP30BiocharMix. That confirms that N is the second most influential parameter for the conductivity of the tracks. In general, the importance of this variable is much greater for the first repetitions of writing; looking at the graph in Figure 4.12, for example, from 7 repetitions onwards, the R does not diminish much. Obviously, as the number of repetitions increases, the tracks become deeper, as a consequence of subsequent laser passages on the surface of the material.

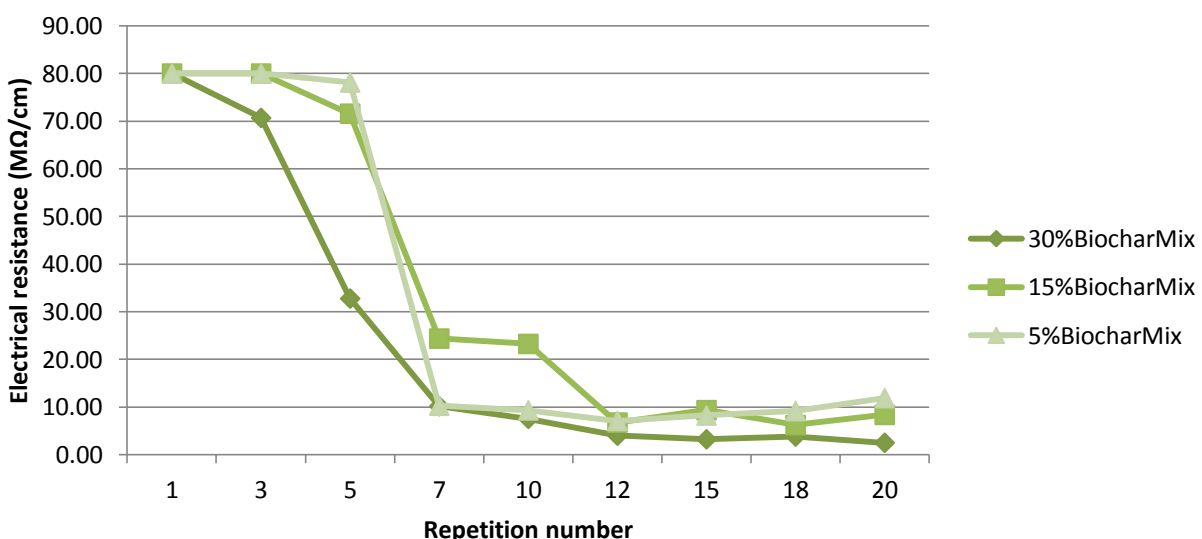


Figure 4.12 - Linear surface electrical resistance per unit length as a function of the repetition number, for PP5BiocharMix, PP15BiocharMix and PP30BiocharMix specimens.

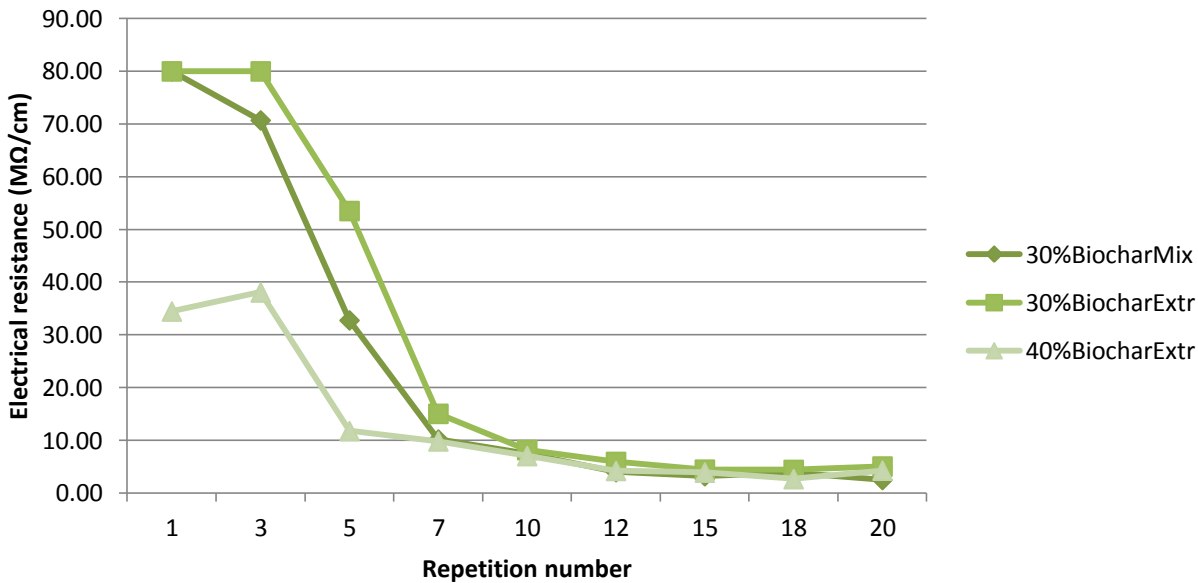


Figure 4.13 - Linear surface electrical resistance per unit length as a function of the repetition number, for PP30BiocharMix, PP30BiocharExtr and PP40BiocharExtr.

4.4.4 Frequency

The frequency (f), which represents the number of impulses per second, was the least influential variable concerning both surface electrical resistance values and the morphological quality of the track. The graphs in Figure 4.14 and Figure 4.15, again representative of the various tests performed on all PP/Biochar, confirm that at frequencies greater than 5 kHz, the resistance value remains almost constant. At the frequency of 0.1 Hz, the track was not homogeneously excavated but had grooves all along its length due to the low frequency with which the laser was digging the surface during its run. The lowest resistance value obtained was 22.7 MΩ/cm (SD = 1.53) achieved with trial 25 ($f = 50$ kHz) on PP30BiocharMix.

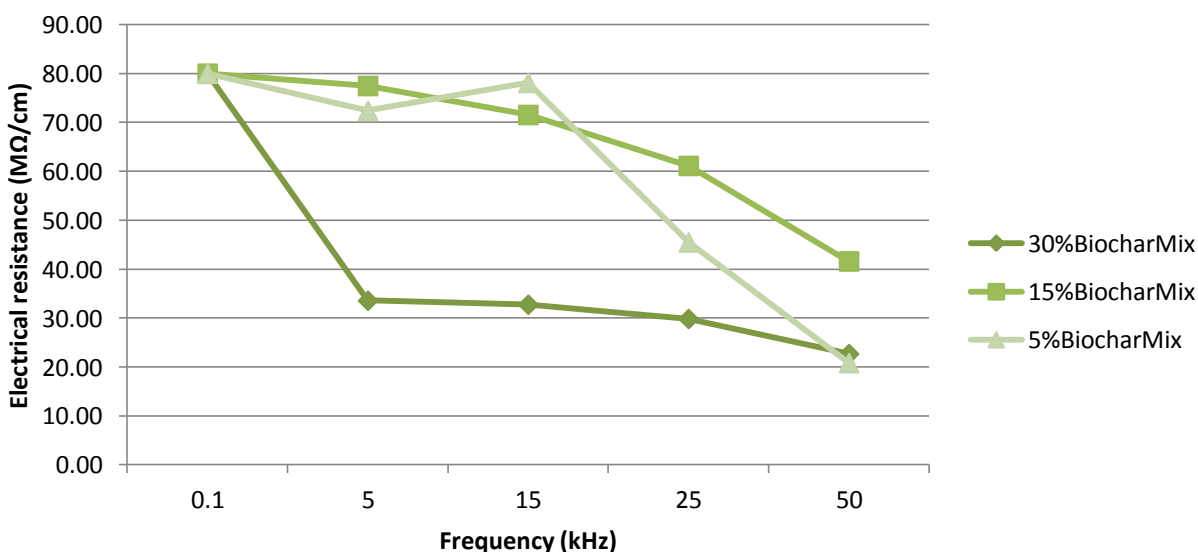


Figure 4.14 - Linear surface electrical resistance per unit length as a function of the frequency, for PP5BiocharMix, PP15BiocharMix and PP30BiocharMix specimens.

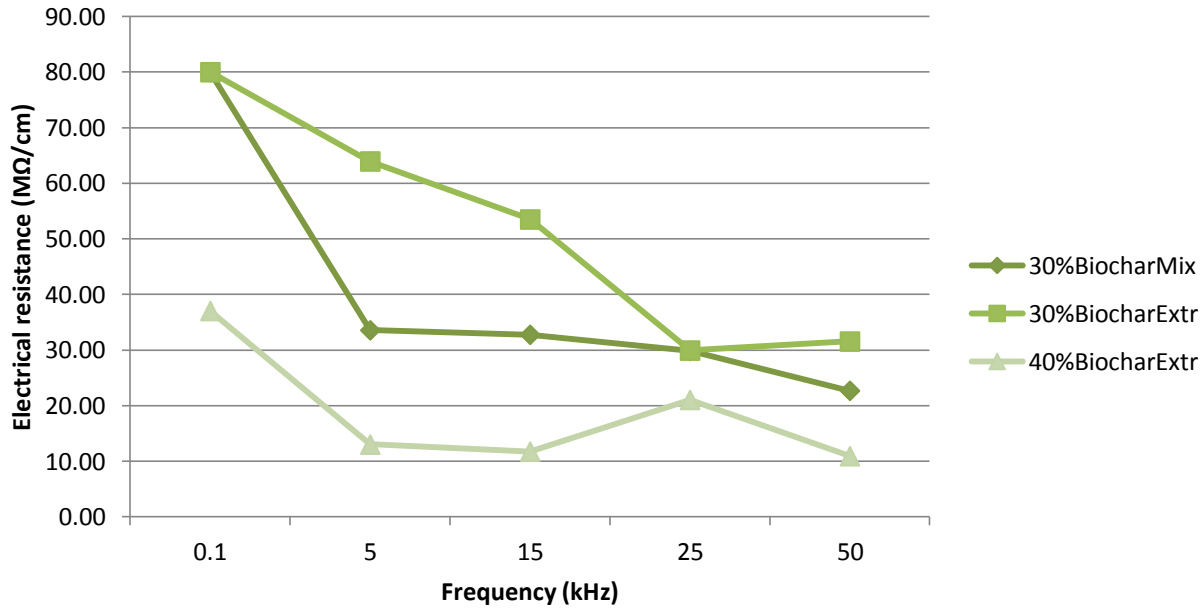


Figure 4.15 - Linear surface electrical resistance per unit length as a function of the frequency, for PP30BiocharMix, PP30BiocharExtr and PP40BiocharExtr.

4.4.5 Defocus

The defocus (D) of the beam on the surface of the specimen, which indicates the distance in the height, in mm, of the focus point from the sample, brought towards unpredictable results.

By keeping the other parameters fixed, the R trend as a function of the beam defocus appears irregular, with minus points and unexpected maximum (graphs in Figure 4.16 and Figure 4.17). The focal point represents the area where there is greater interaction between the laser and the surface of the specimen. From a qualitative point of view, laser tracks obtained with greater D values appear to be very different from those achieved with zero defocus. In fact, they are much wider and less profound, due to the more extensive projection of the beam on the surface of the samples, and the less interaction between radiation and matter. On the one hand, a wider track has less resistance, but on the other, its lower depth offsets this effect: that would explain the random resistance values. The lowest resistance value obtained was $7.78 \text{ M}\Omega/\text{cm}$ ($\text{SD} = 0.39$) achieved with trial 32 ($D = 60 \text{ mm}$) on PP30BiocharMix.

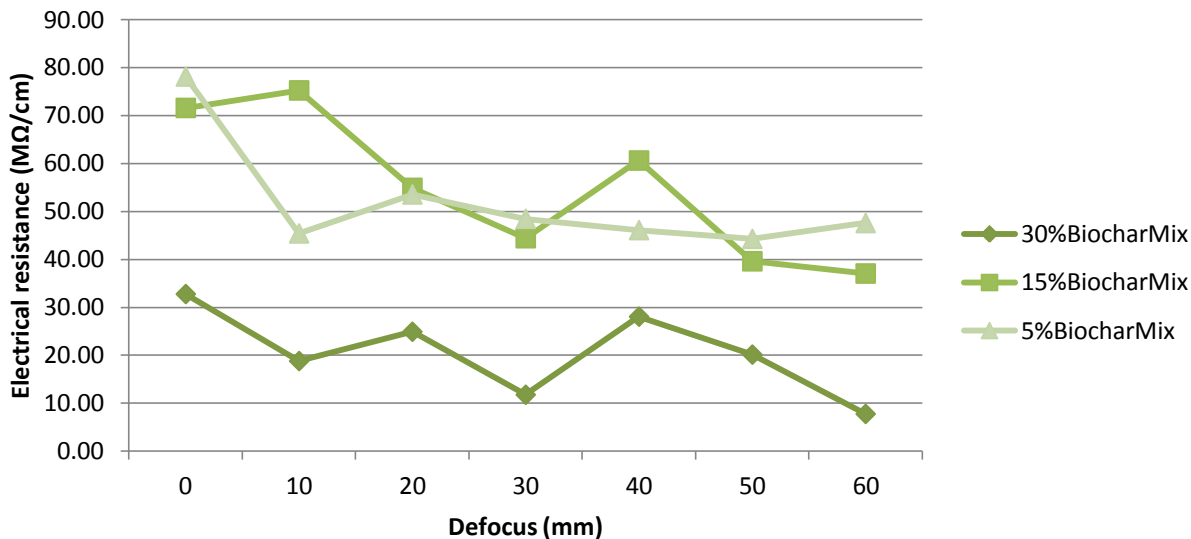


Figure 4.16 - Linear surface electrical resistance per unit length as a function of the defocus, for PP5BiocharMix, PP15BiocharMix and PP30BiocharMix specimens.

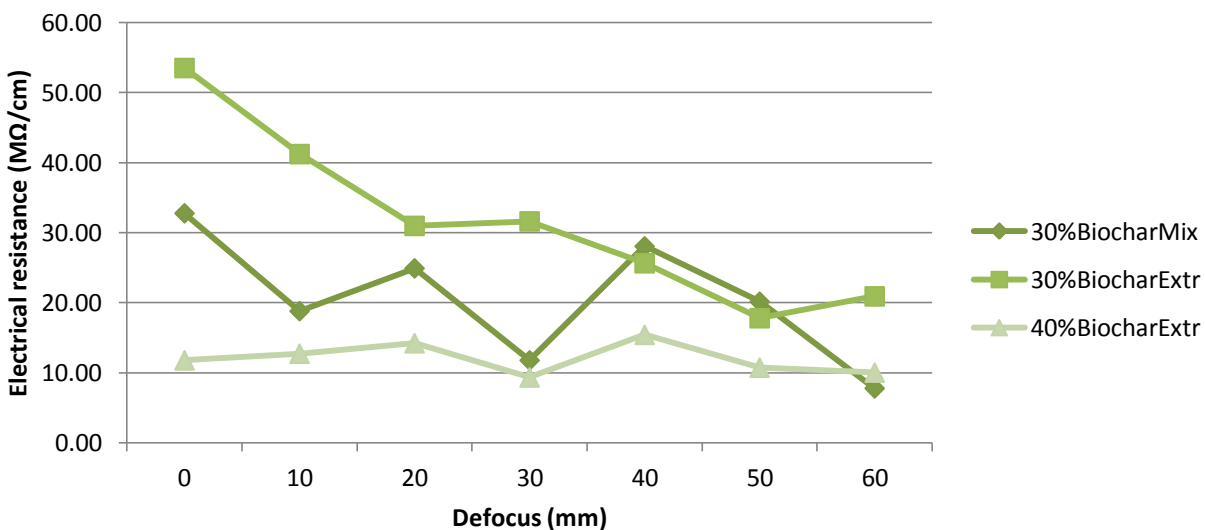


Figure 4.17 - Linear surface electrical resistance per unit length as a function of the defocus, for PP30BiocharMix, PP30BiocharExtr and PP40BiocharExtr.

4.4.6 Optimisation of the laser parameters

Once the right understanding of the way in which the individual parameters are responsible for the surface electrical resistance values found, it was decided to continue the experimental work by pointing to the purpose of this research: modulating the laser parameters to obtain electrically conductive tracks for the realisation of integrated circuits in a polymer. The optimisation of the laser parameters was carried out only on PP30BiocharMix specimens, which proved to be the most suitable materials for the objective mentioned above. The laser parameters that brought to an electrical resistance value beyond which the respective curve's trend stabilised (seemed to reach an asymptote) were chosen as "new standard parameters" for optimising the results for the

PP30BiocharMix material. To this end, the new standard parameters have been maintained constant while varying the remaining four (the laser operating conditions for this purpose are shown in Figure 4.18), similar to what was done for trials from 1 to 32.

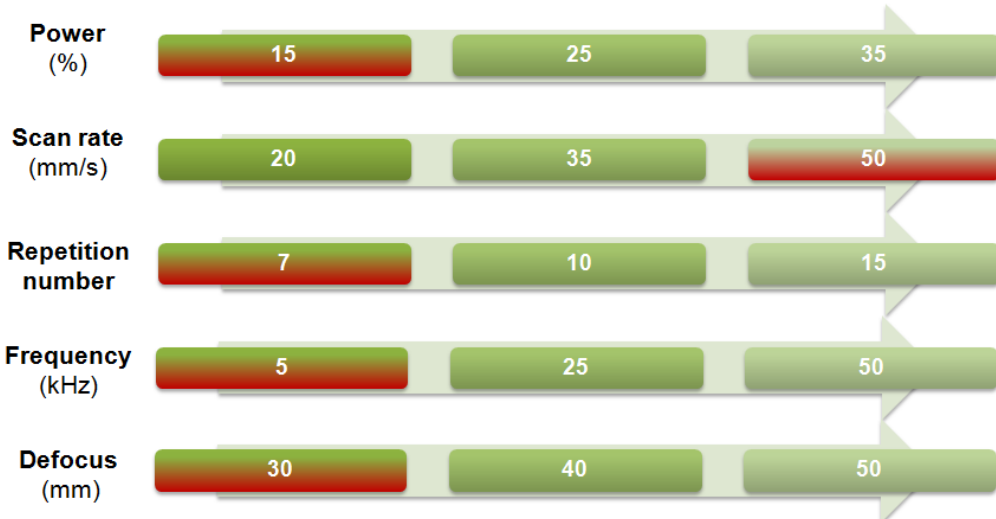


Figure 4.18 - New laser parameters range of variation. The values with a red background are the standard values chosen.

To facilitate the discussion, Table 4.2 shows the variation ranges of laser parameters that have allowed to get the tracks on the specimens.

Table 4.2 - List of values of the parameters chosen for each trial.

Trial	Power (%)	Scan rate (mm/s)	Repetition number	Frequency (kHz)	Defocus (mm)
33 (std.2)	15	50	7	5	30
34	25	50	7	5	30
35	35	50	7	5	30
36	15	35	7	5	30
37	15	20	7	5	30
38	15	50	10	5	30
39	15	50	15	5	30
40	15	50	7	25	30
41	15	50	7	50	30
42	15	50	7	5	40
43	15	50	7	5	50

Figures 4.19, 4.20, 4.21, 4.22 and 4.23 show linear surface electrical resistance per unit length as a function of new laser parameters for PP30BiocharMix samples.

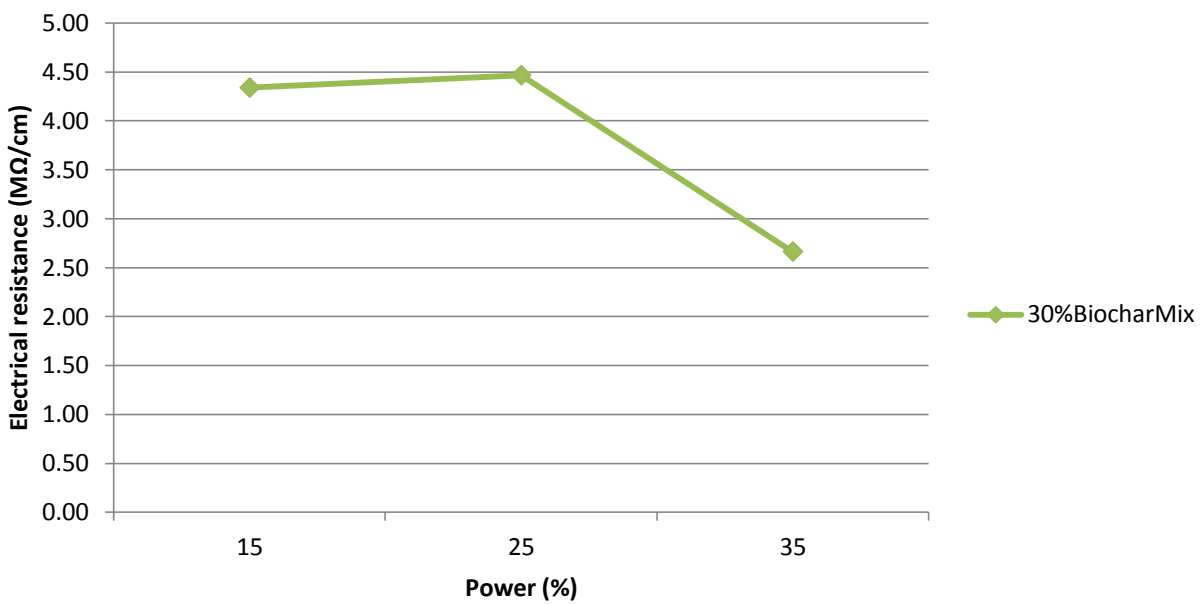


Figure 4.19 - Linear surface electrical resistance per unit length as a function of the power (%), for PP30BiocharMix specimens.

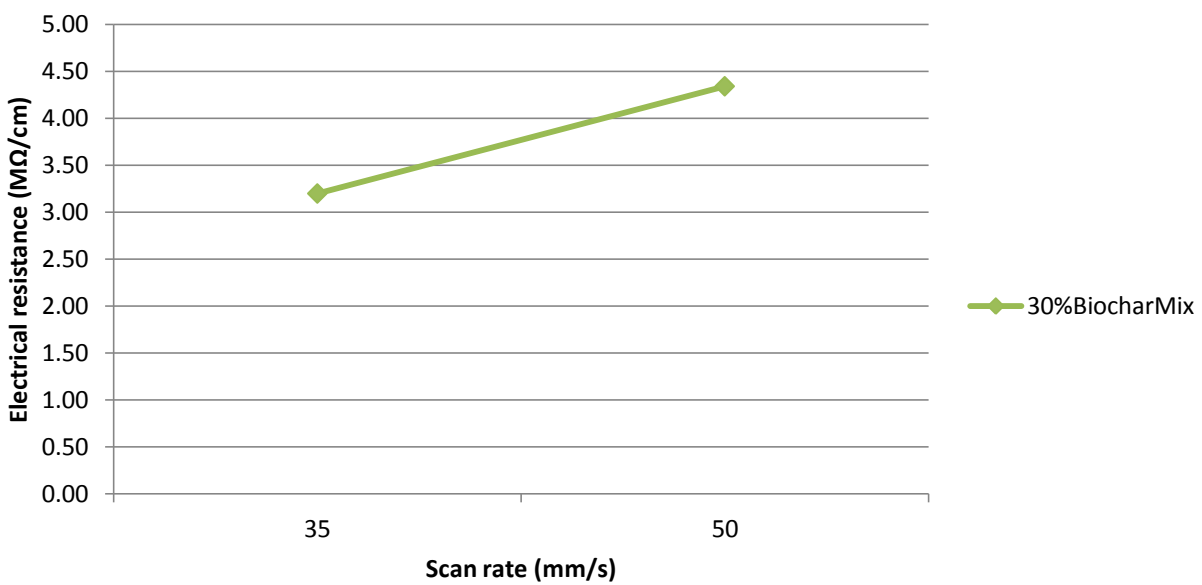


Figure 4.20 - Linear surface electrical resistance per unit length as a function of the scan rate, for PP30BiocharMix specimens. A scan rate equal to 20 mm/s brings to the perforation of the specimens.

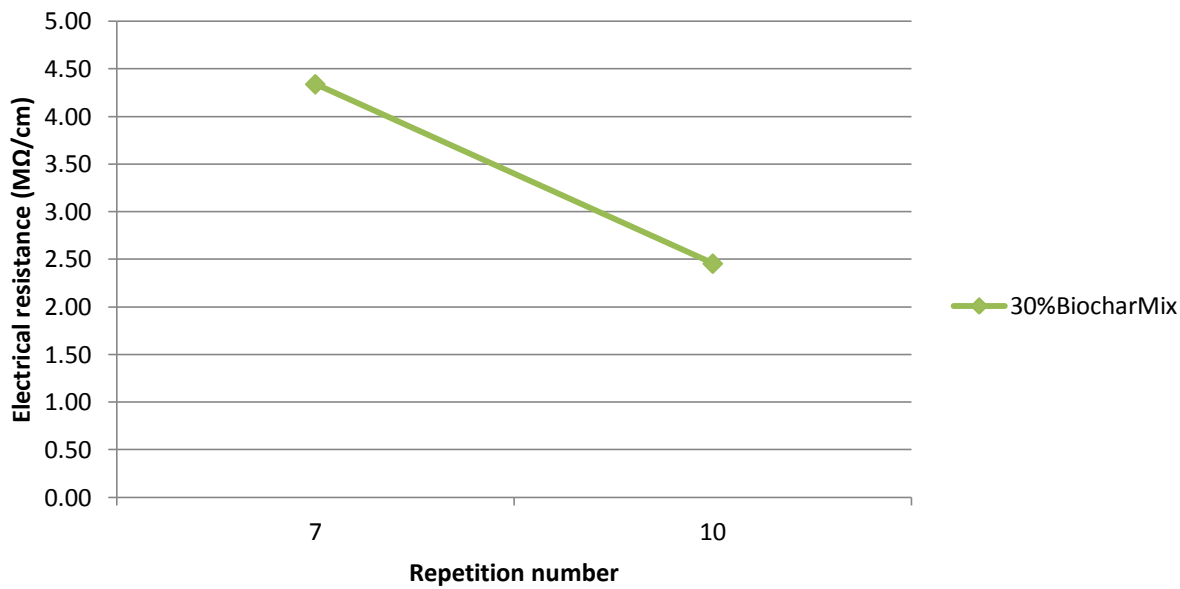


Figure 4.21 - Linear surface electrical resistance per unit length as a function of the repetition number, for PP30BiocharMix specimens. A repetition number equal to 15 brings to the perforation of the specimens.

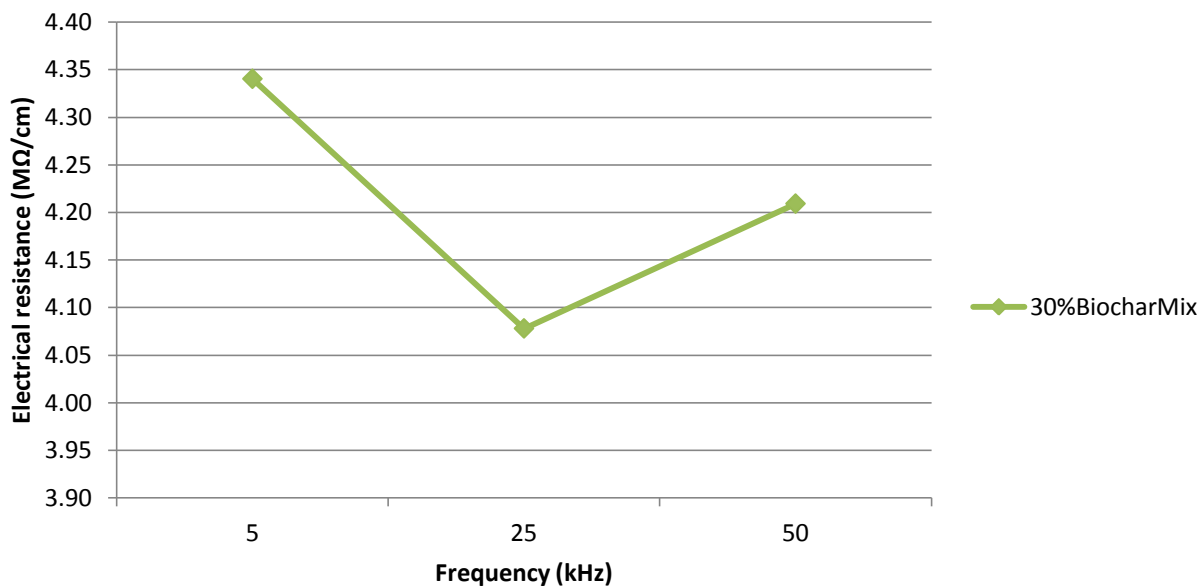


Figure 4.22 - Linear surface electrical resistance per unit length as a function of the frequency, for PP30BiocharMix specimens.

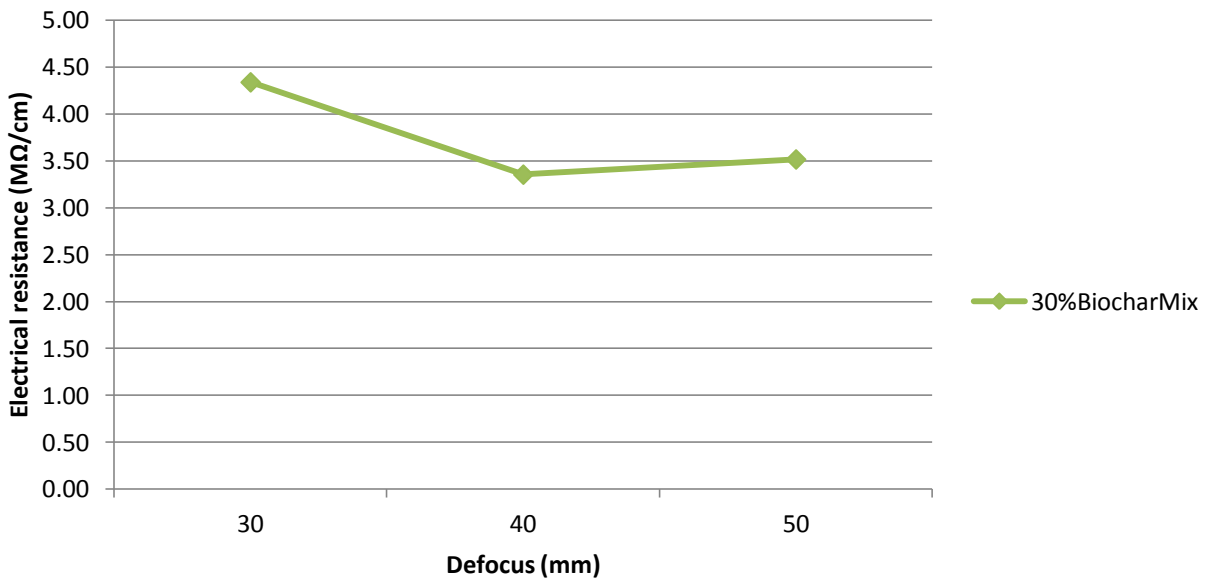


Figure 4.23 - Linear surface electrical resistance per unit length as a function of the defocus, for PP30BiocharMix specimens.

Focusing the attention on the values found in this experimental campaign, rather than on the trends, it is possible to notice that the values obtainable by all experiments range from few units of $M\Omega/cm$ but never goes below $1.11 M\Omega/cm$, achieved with trial 11. It would, therefore, appear that the PP30BiocharMix composite has reached an electrical resistance threshold under which it is prohibited to go. That may be due to an inherent electrical conductivity limit belonging to the Biochar, and not to a weak modulation of the laser parameters. In fact, the last laser treatments, following a visual inspection of the specimens, have proved to be very invasive and many times have led to the perforation of the sample. Therefore, there was no further push in choosing the laser parameters to reach better results.

At the end of this part of the experimental work, it was thus clear how the initial assumptions about replacing the metal wiring with an economical mono-material capable of carrying the signal were difficult to come true. The resistance value obtained is, however, largely sufficient to allow current passage for those applications where antistatic properties are required. Additionally, the resistance value beyond the instrument's overflow limit across adjacent tracks makes this technology easily manageable by simple and cheap electronics.

4.5 Mechanical characterisation of PP/Biochar composites

Table 4.3 shows the average values of the results of the various tensile tests conducted on samples moulded from granules obtained using the measuring mixer (PPUnfilledMix, PP5BiocharMix, PP15BiocharMix, PP30BiocharMix). In particular, the values of tensile strength, Young's modulus and deformation at break of these samples with different percentages of Biochar are compared with the help of histograms reported respectively in Figures 4.24, 4.25 and 4.26.

Table 4.3 - List of values of the parameters chosen for each trial.

	Tensile strength		Young's Modulus		Deformation at break	
	Average value (MPa)	Standard deviation	Average value (GPa)	Standard deviation	Average value (%)	Standard deviation
PPUnfilledMix	20.00	0.46	2.05	0.18	72.13	9.77
PP5BiocharMix	19.02	0.20	2.14	0.11	16.00	4.61
PP15BiocharMix	17.42	0.29	2.32	0.06	7.48	1.98
PP30BiocharMix	15.94	0.49	2.57	0.04	4.62	1.06

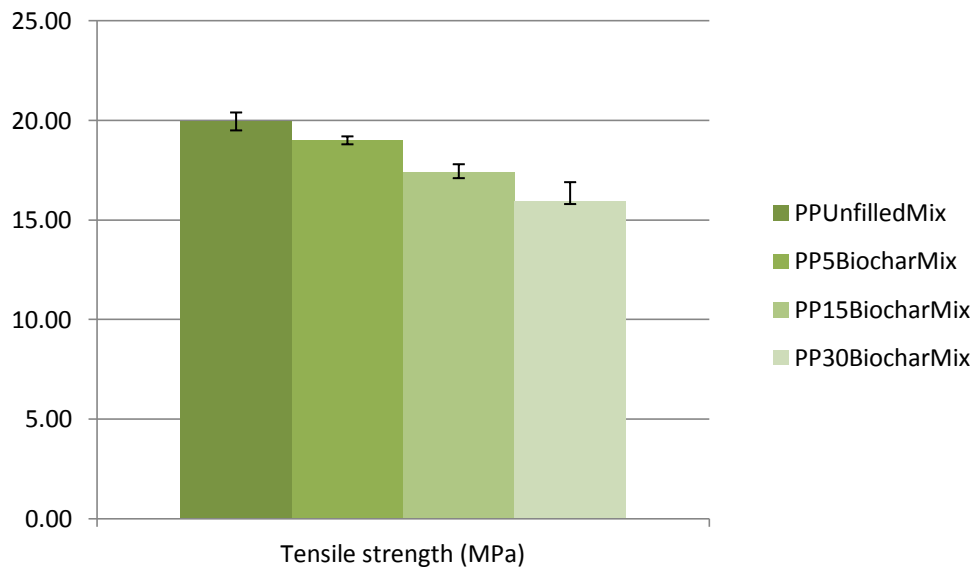


Figure 4.24 - Histogram comparing the tensile strength values for PPUnfilledMix, PP5BiocharMix, PP15BiocharMix, and PP30BiocharMix composites.

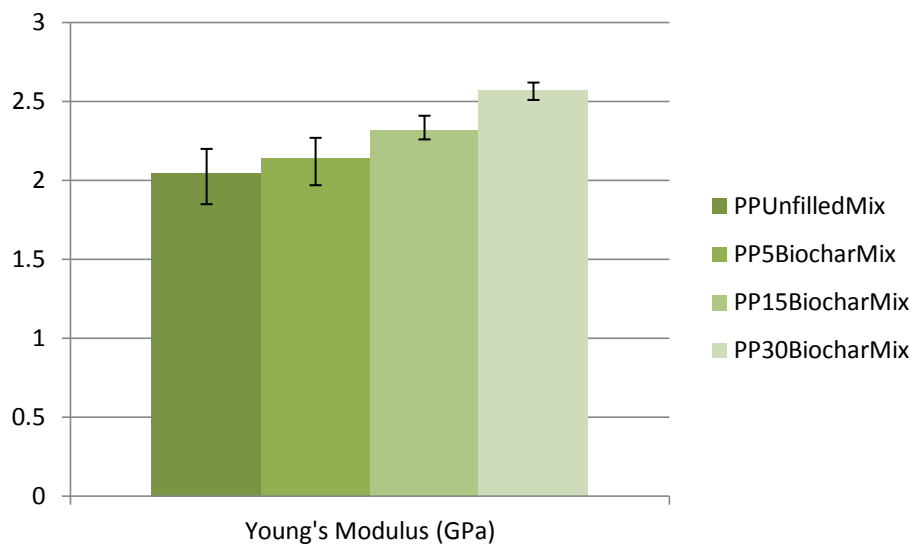


Figure 4.25 - Histogram comparing the Young's modulus values for PPUnfilledMix, PP5BiocharMix, PP15BiocharMix, and PP30BiocharMix composites.

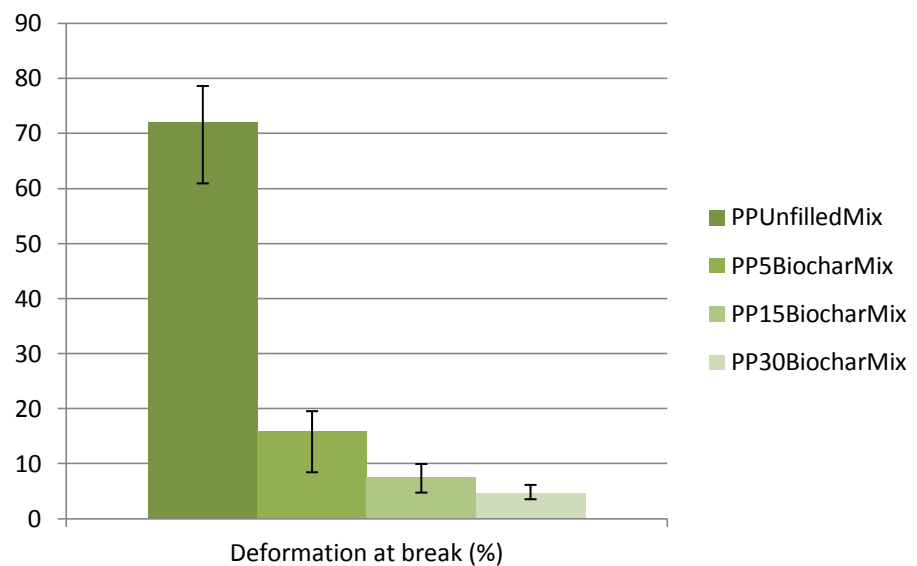


Figure 4.26 - Histogram comparing the deformation at break values for PPUnfilledMix, PP5BiocharMix, PP15BiocharMix, and PP30BiocharMix composites.

A decrease in ductility can be observed following filler addition: deformation at break collapses even with a small addition of 5% Biochar. There is also a declining trend for tensile strength, albeit less drastic. An addition of Biochar increases, on the contrary, the elastic modulus, due to the inherent particle rigidity.

Such results are probably also dependent on the poor dispersion degree of Biochar within the polymer matrix. In order to obtain a mechanical reinforcement, it is necessary to pay particular attention to the dispersion of the filler inside the matrix to provide a polymer/Biochar interface that can transfer the load from the matrix to the filler. However, mechanical reinforcement is not the purpose of this work, which instead aims to increase a functional performance for which very often excessive dispersion and distribution of the filler are not desirable. In fact, this would lead to electrical conduction phenomena also between non-continuous tracks, with the consequent impairment of the possibility of making integrated circuits.

4.6 Thermal characterisation of PP/Biochar composites

4.6.1 Thermogravimetric analysis (TGA)

Thermogravimetric analyses were conducted to assess the thermal stability of the composites made in the present thesis work. The analyses were carried out for all mixtures prepared by the measuring mixer (PPUnfilledMix, PP5BiocharMix, PP15BiocharMix, PP30BiocharMix).

In Figure 4.27, the results of the TGA conducted in an inert environment are presented. For all materials, degradation takes place in a single step starting at about 400 °C. This means that there was no improvement in thermal stability with the increase in the amount of added Biochar. PPUnfilledMix is associated with a residue of about 14 wt% due to inorganic filler content already present in it. All composites have a higher residue due to Biochar particles, which do not degrade at test temperatures (however, there is a loss in the volatile content). The composites residue percentage is in good agreement with theory since it increases with a higher amount of Biochar percentage which not burn in the neutral atmosphere. Consequently, TGA was able to confirm the percentages of added fillers.

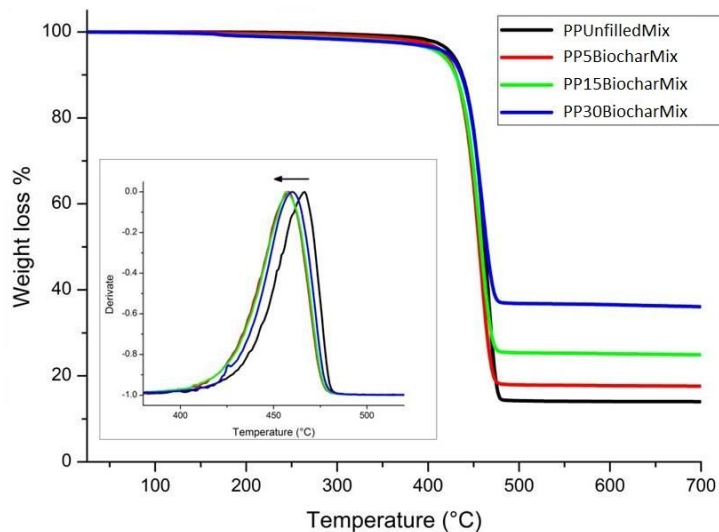


Figure 4.27 - Comparison between different TGA graphs for the following materials: PPUnfilledMix, PP5BiocharMix, PP15BiocharMix and PP30BiocharMix.

The TGA graphs in the air are not showed because they follow the same trend as those in the inert atmosphere. In fact, the degradation mechanism for all materials starts at about 350 °C and occurs in a single step. The only difference is that all organic (Biochar) residues are consumed at around 700° C by combustion with oxygen contained in the air and subsequent formation of volatile products. In all the composites there is a final 14 wt% residue consisting of inorganic filler which not burns (the same previously seen for the PPUnfilledMix in argon).

4.6.2 Differential scanning calorimetry (DSC)

Differential scanning calorimetry analyses were carried out on PP, on that after treatment in the Brabender mixer (PPUnfilledMix), and on PP5BiocharMix, PP15BiocharMix and PP30BiocharMix materials. In Figure 4.28, the DSC curve of PP30BiocharMix is shown as an example, while in Figure 4.29 the curves obtained for all materials are compared.

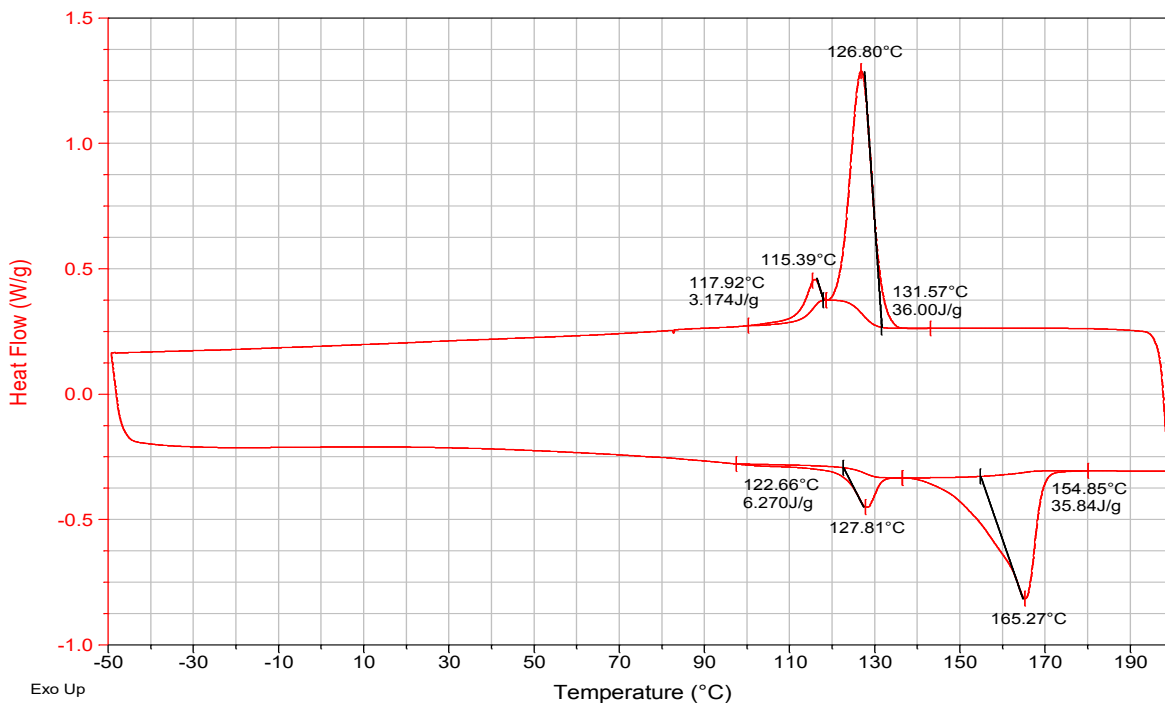


Figure 4.28 - DSC curve of the composite PP30BiocharMix.

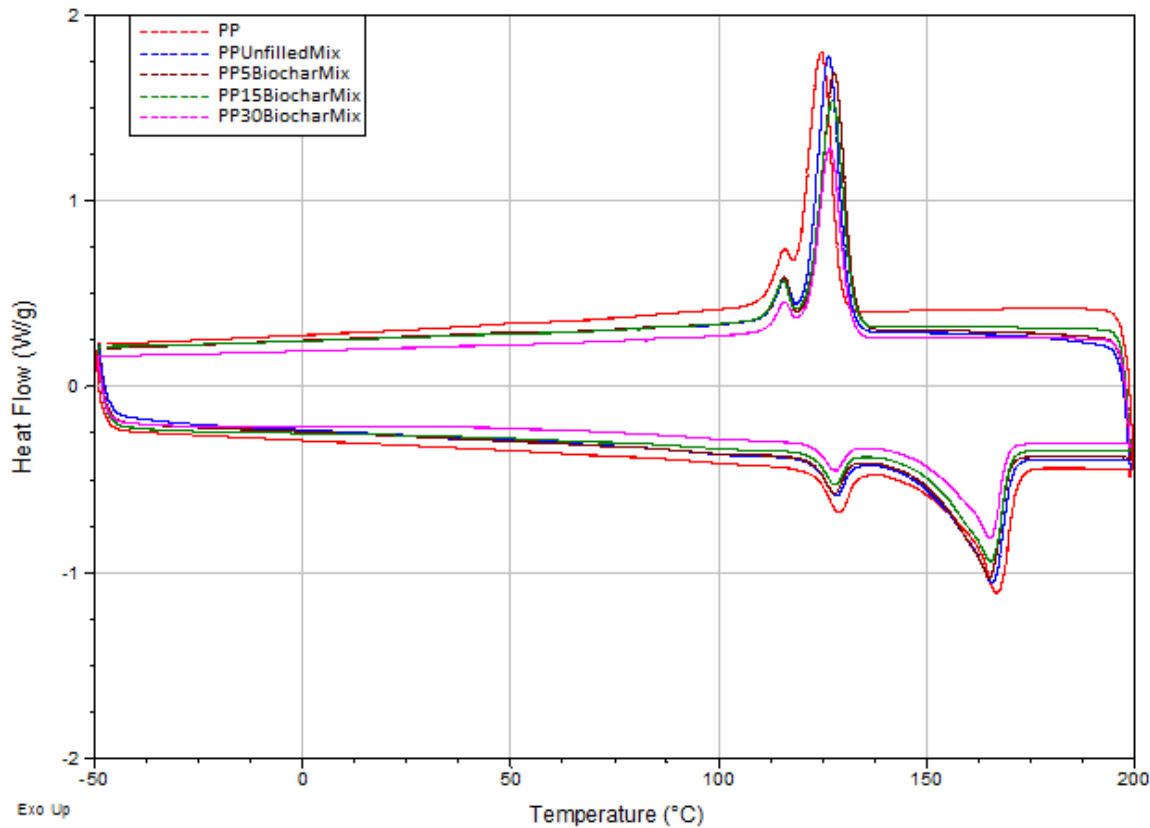


Figure 4.29 - Comparison between different DSC curves for the following materials: PP, PPUnfilledMix, PP5BiocharMix, PP15BiocharMix and PP30BiocharMix.

From the thermograms analysis, it is deduced that all the composites are semi-crystalline: the two peaks at the top are those of crystallisation, while the bottom ones are melting. Peaks of lesser intensity belong to the PE, while the highest to the PP, since the material in question is a copolymer. When changing Biochar's content, no change in the two transition temperatures of the polymer is observed, nor in its percentage of crystallinity, suggesting that there was no increase in thermal performance but, much more importantly, no property collapse.

4.7 Morphological characterisation of PP/Biochar composites

4.7.1 Optical microscopy

The PPUnfilledMix, PP5BiocharMix, PP15BiocharMix, and PP30BiocharMix specimens were subjected to optical microscopy analysis to study the dispersion degree of Biochar particles. Figure 4.30 shows the sections of these samples. Biochar particles appear opaque, while the polymeric matrix of a more brilliant black. It can be seen that, although the particles are well distributed within the matrix, these are not homogeneously dispersed within the same. In fact,

many agglomerates have not been crushed during the mixing process with the polymer matrix in the Brabender mixer. The presence of aggregates could explain the low deformation at break and tensile strength of these composites.

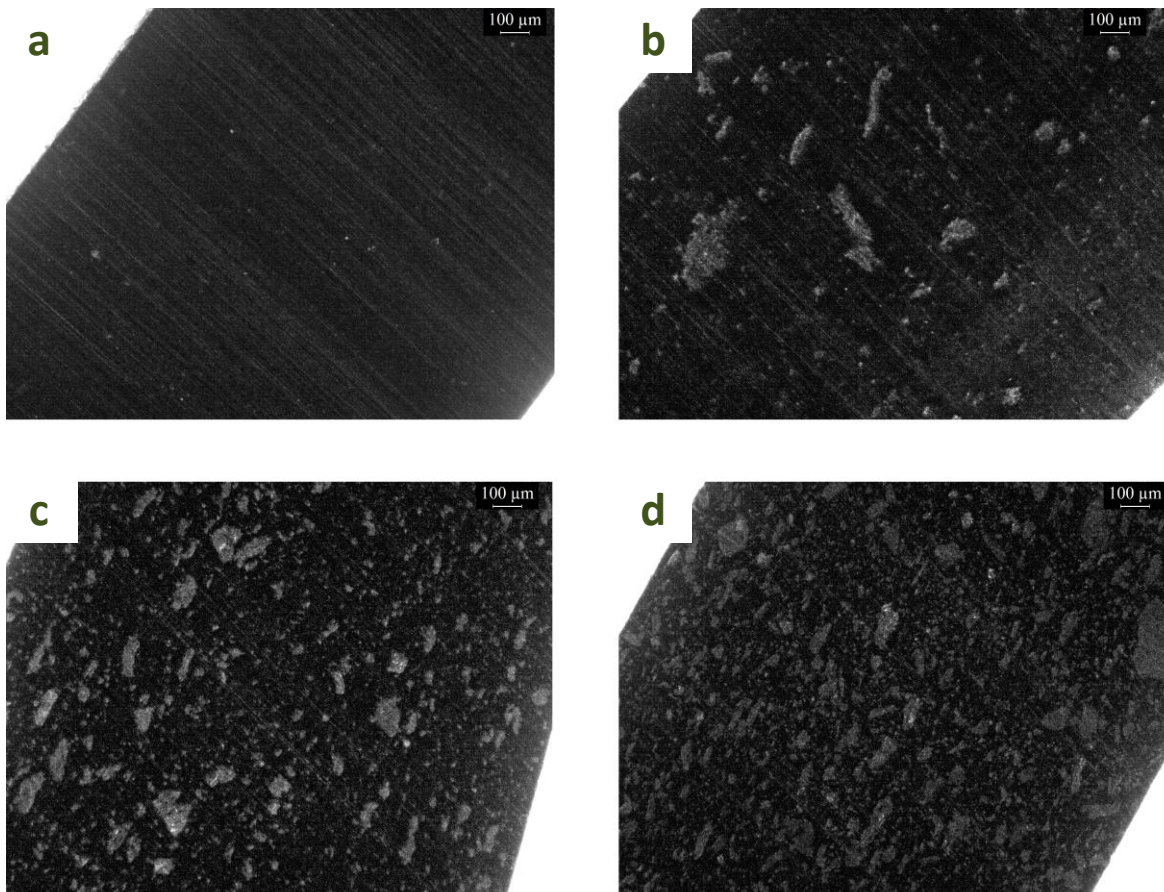


Figure 4.30 - Sections of PPUUnfilledMix (a), PP5BiocharMix (b), PP15BiocharMix (c), and PP30BiocharMix (d) specimens analyzed by optical microscope at 5X. The opaque parts represent the aggregates of Biochar particles immersed in the brilliant black polymer matrix.

4.7.2 Field Emission Scanning Electron Microscopy (FESEM) on laser tracks

The tracks were examined at FESEM to better determine their morphology with the variation of Biochar content. Microscopic analysis has been performed on four tracks. Specifically, the most efficient tracks regarding electrical conductivity for each composite material (PP5BiocharMix, PP15BiocharMix, PP30BiocharMix and PP40BiocharExtr) have been chosen.

Figure 4.31 shows the micrographs, from 100x to 5Kx magnification, of the track derived from trial 9 on PP5BiocharMix specimen. In Figure 4.31a, the irregular track structure, as well as its depth, is clear. In fact, at the edges of the track, there is evidence of accumulation of material likely due to the localised fusion and the trigger of a viscous flow of the polymer matrix. It is also possible to notice that the deeper zone of the track is located in the centre, which is the point of greater interaction between the laser and the material.

Larger magnifications (Figure 4.31b) show the almost total absence of Biochar particles, demonstrating how a percolating network could never be reached at these small filler percentages. Entering more in detail in the track (Figure 4.31c), confirms the absence of Biochar particles. In fact, the micrograph is very similar to that of a non-reinforced polymer.

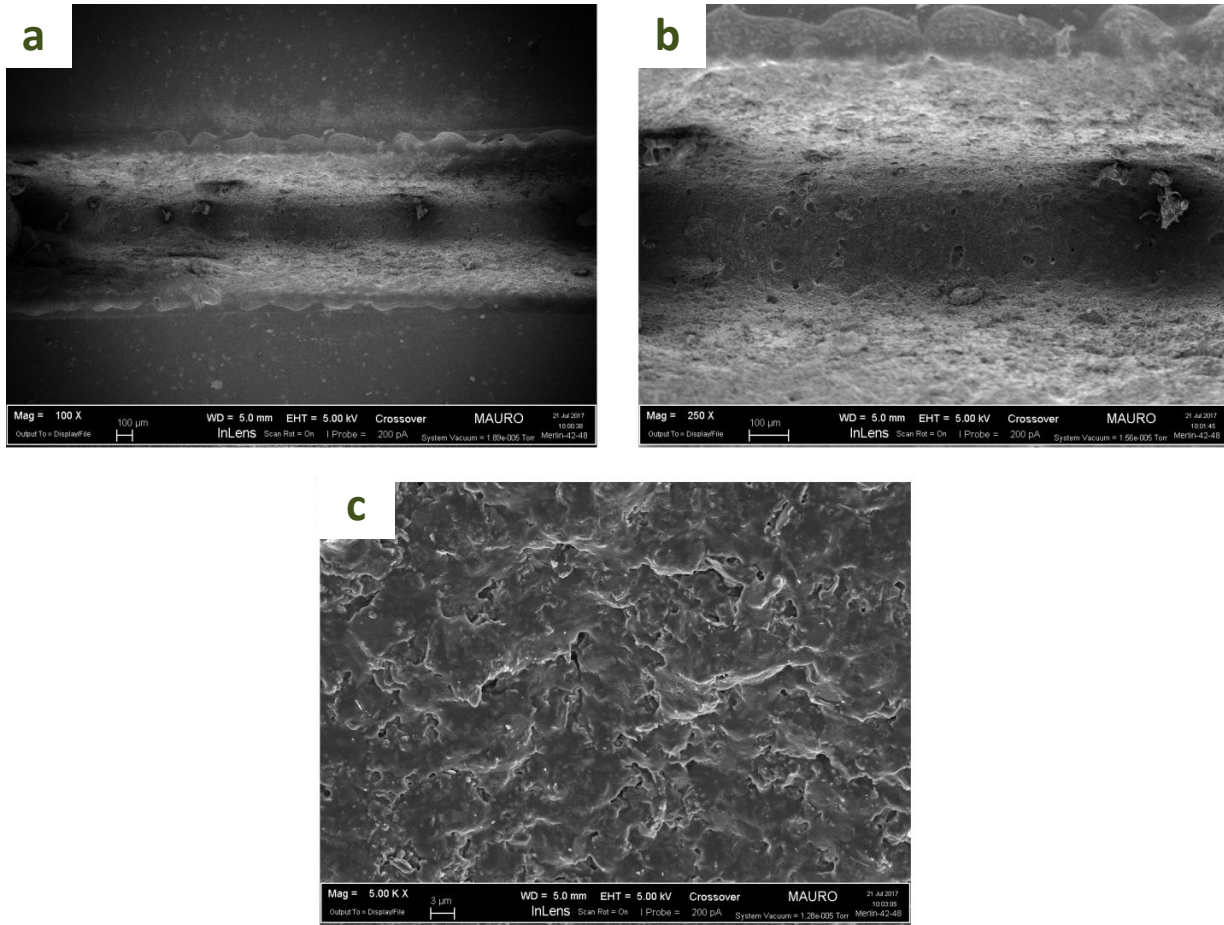


Figure 4.31 - FESEM micrographs of the surface of the laser track (trial 9) on the PP5BiocharMix composite at 100x (a), 250x (b), and 5Kx (c) magnification.

Figure 4.32 shows the micrographs of the track derived from trial 10 on PP15BiocharMix specimen. This time the track appears to be more rough, demonstrating the presence of a larger amount of filler in the carbonised material, which contains, in addition to Biochar, those conjugated structures responsible for the conductivity of the track.

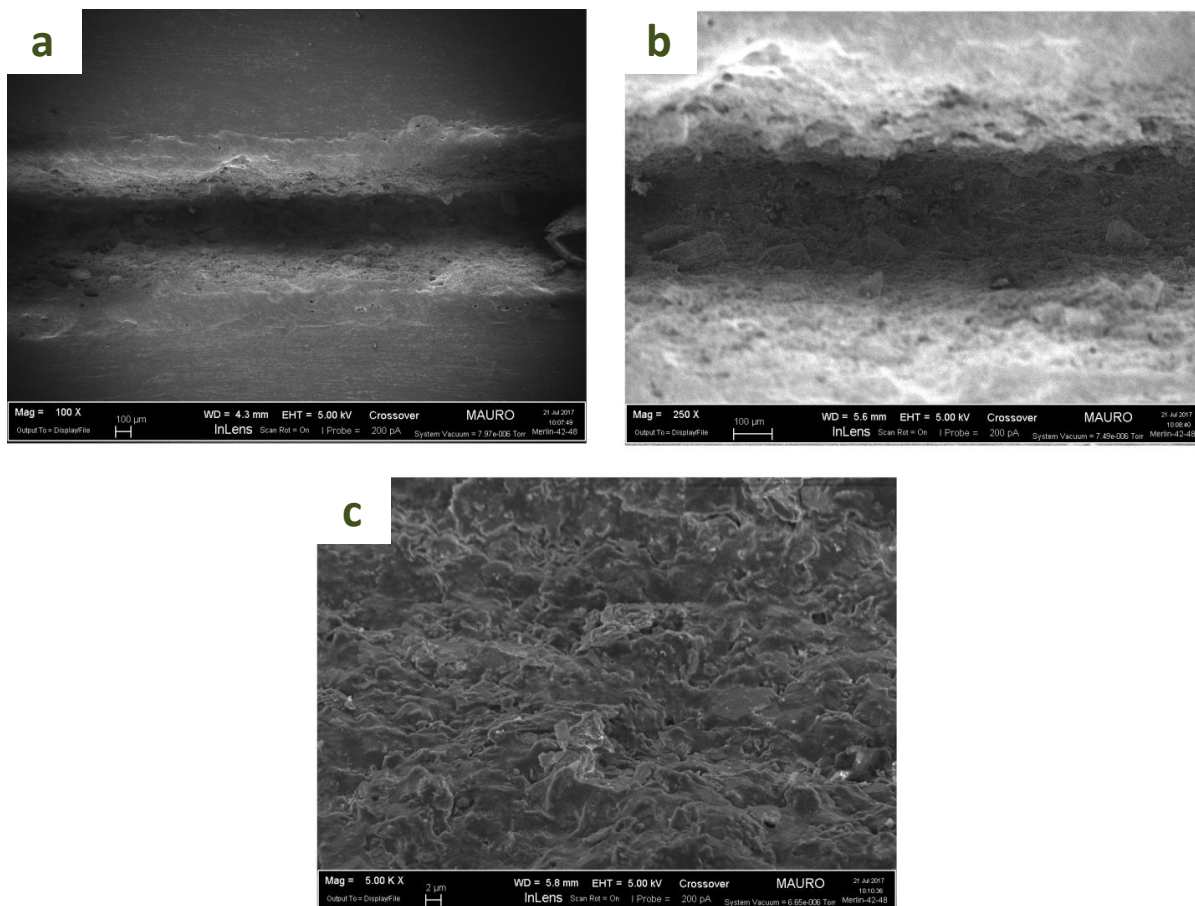


Figure 4.32 - FESEM micrographs of the surface of the laser track (trial 10) on the PP15BiocharMix composite at 100x (a), 250x (b), and 5Kx (c) magnification.

Figure 4.33 shows the micrographs of the track number 11 on PP30BiocharMix specimen. It is easy to notice the high opacity of the track given the huge amount of filler now available. At high magnifications Biochar aggregates also appear.

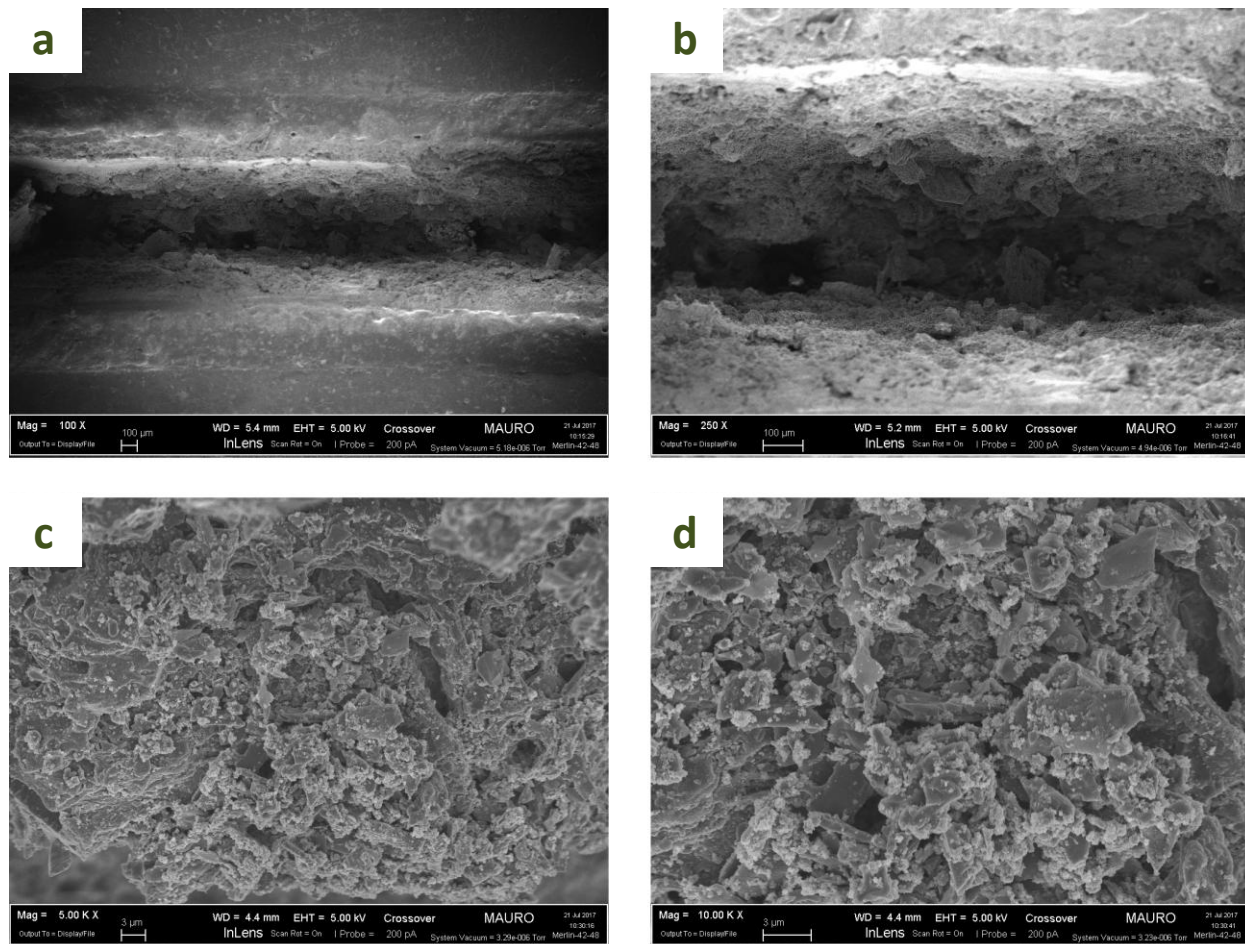


Figure 4.33 - FESEM micrographs of the surface of the laser track (trial 11) on the PP30BiocharMix composite at 100x (a), 250x (b), and 5Kx (c), and 10Kx (d) magnification.

The micrographs in Figure 4.34 and 4.35 always refer to the track 11 of the PP30BiocharMix, but this time recorded on the side walls of the track. At these magnifications, it is possible to notice the Biochar particles that emerge from the walls of the track.

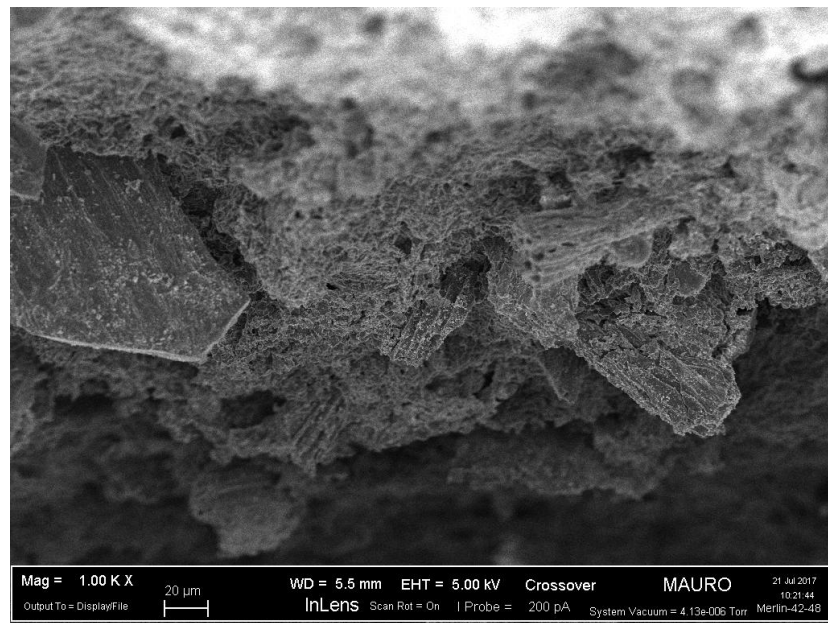


Figure 4.34 - FESEM micrograph of the surface of the laser track (trial 11) on the PP30BiocharMix composite at 1Kx magnification. The micrograph is centred on the side walls of the track, from which Biochar particles emerge.

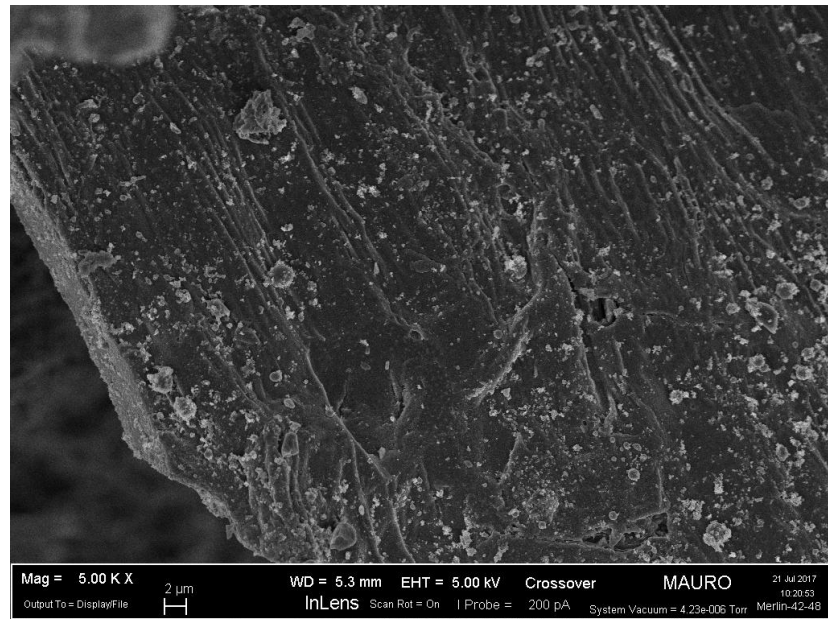


Figure 4.35 - FESEM micrograph of the surface of the laser track (trial 11) on the PP30BiocharMix composite at 5Kx magnification. The micrograph is centred on a Biochar particle surrounded by smaller satellites.

Figure 4.36 shows the micrographs of the track number 11 on PP40BiocharExtr specimen. The magnification again demonstrates the Biochar particle agglomerates, but in greater concentration than in the previous composite.

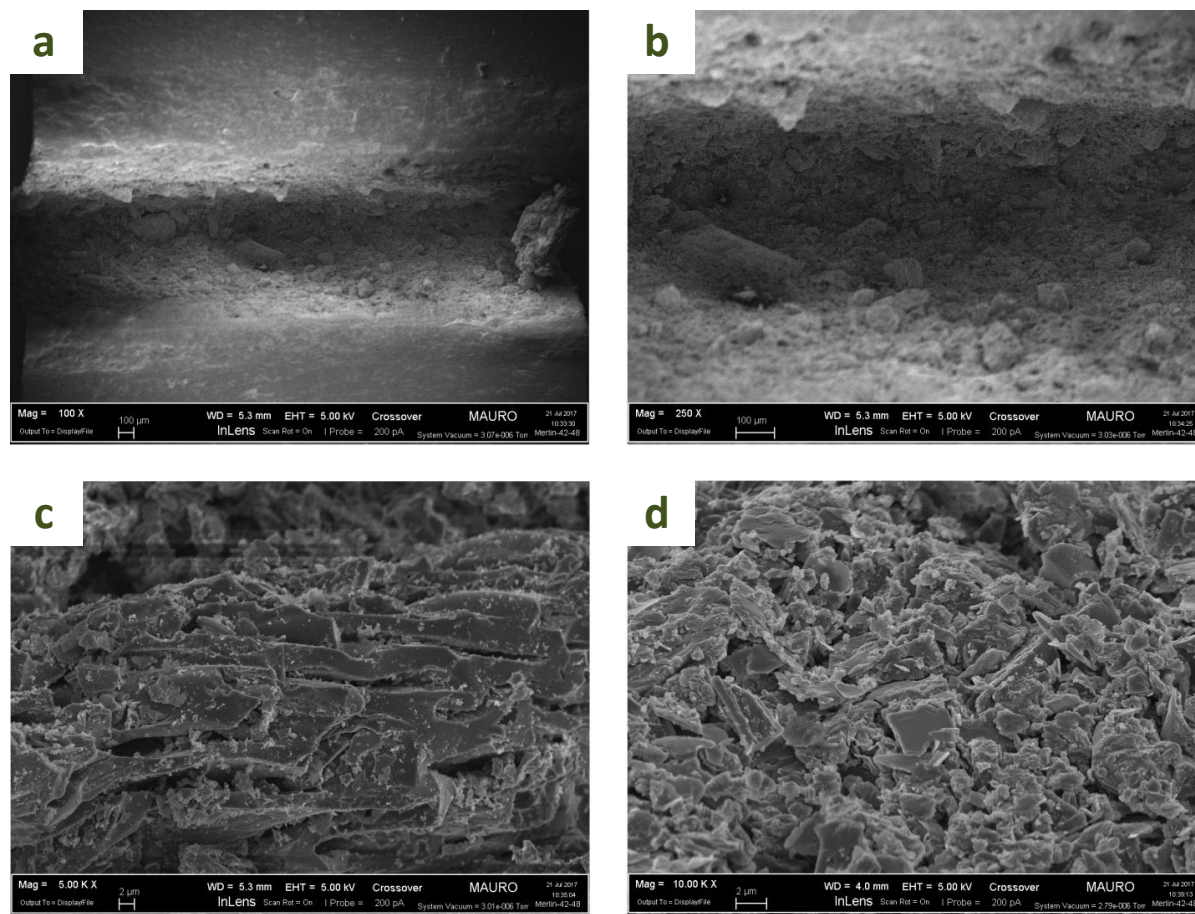


Figure 4.36 - FESEM micrographs of the surface of the laser track (trial 11) on the PP40BiocharExtr composite at 100x (a), 250x (b), and 5Kx (c), and 10Kx (d) magnification.

5. Conclusions

The work carried out in this experimental research has led to the realisation of electrical circuits integrated into an initially insulating polymeric material to be used for the building of a car dashboard or other car interiors. This functionalisation was possible by making a polypropylene composite filled with Biochar (from 5% to 40 wt%) and producing conductive tracks through the direct interaction between a CO₂ laser beam and the surface of the material.

The compositions of the different composites were obtained using a measuring mixer or a twin screw extruder. These two different technologies have been chosen to evaluate how a different degree of dispersion can affect the electrical properties of the final composite. The obtained granule materials were then subjected to injection moulding to produce the specimens used during the experiment. The experimental work was carried on to gain a greater understanding of the interaction phenomenon between the laser beam and the material to identify the parameters that mainly affect the performance of the material. The effects of the different parameters were evaluated based on the observed linear surface electrical resistance (R) value of the laser tracks. The work ended with a thermal, mechanical, and morphological characterisation of the obtained materials.

The industrial development of this technology would offer the possibility of making electrical circuits integrated into polymers by allowing to replace part of metallic wiring used today with a respective gain regarding lightness, corrosion resistance and certainly also costs. The use of a polymer matrix composite material also ensures easy component processing and the possibility of recycling it at the end of the life cycle.

Part of the experimental work has partly contributed to the confirmation of conclusions drawn from previous work carried out at CRF, thus deducing the uniqueness of the interaction between the laser beam and the material. It was concluded that the most influencing variable is the laser scan rate. In fact, since the effect to achieve is not only to eliminate the surface skin of the polymer, it is necessary to ensure sufficient time (low scan rate) for the laser beam to penetrate the material and interact with it. In particular, the action of the CO₂ laser on the surface of the composite results in a localised rise in temperature due to the absorption of infrared radiation by the material. Heating causes activation of a viscous flow that involves the accumulation of material at the edges of the trace, also contributing to the degradation of the polymer matrix by removal of macromolecular fragments and the formation of volatile products. The formation of new carbonaceous structures such as pyrolysis products induced by the photothermic ablation of the laser adds up to the conductive network of the Biochar particles.

Laser treatments that cause greater interaction of the laser beam with the surface of the material induce tracks with higher conductivity. But electrical conductivity is closely related to the Biochar's content as well as working conditions, in fact, at the same set of parameters, shallow R values were obtained for composites containing more Biochar. With excessively small

Biochar quantities (5% and 15% by weight), it's hard to obtain tracks with sufficient conductivity to guarantee their use in commercially attractive devices. Among these materials, only composites containing 30% fillers have shown to reach, by laser treatments that do not lead to deformation of the sample, R values of approximately $1 \text{ M}\Omega/\text{cm}$ (necessary for the transport of the electrical signal) and R values between adjacent tracks above the overflow limit of the multimeter used for the measurements. Materials loaded with 40% of Biochar not only resulted in the same resistance values as those at 30%, but exhibited conductivity between adjacent tracks: an undesirable effect as it would lead to the short circuit of the system. Therefore, research has continued in the 30% loaded materials.

The samples moulded from granules derived from the Brabender measuring mixer have been slightly more conductive than those derived from the twin-screw extruder. In fact, during the mixing in the twin screw extruder, the aggregates start breaking down increasing the gap between the particles. Thus, if with the extruder we can obtain a better distribution of the particles within the polymer matrix, it is also true that this process leads to an excessive dispersion (breakage of the aggregates). While these better dispersion and distribution result in less fragility for the composite, on the other, they hinder the formation of a percolating network and consequently worsens the electrical conductivity. However, after optimising the laser parameters, it seems that the electrical conductivity of the composites could not fall below $1 \text{ M}\Omega/\text{cm}$. These R values are still too high for the implementation of integrated circuits but may be suitable for all those applications that require antistatic properties (e.g. fuel system components). Sufficient is to think of those plastics that if they accumulate charges and if they come in contact with gasoline would lead to a triggering of the same.

In conclusion, the theoretical and practical results obtained are undeniably propitious: in fact, it was possible to make an electrically insulating material conductive only locally employing an extremely economical "green" filler. It has certainly been fundamental to demonstrate that the road to go for the production of polymeric wiring, albeit still long, extends under the best auspices. Before the industrialisation is made possible, it is certainly necessary to undertake a thorough study of the influence of working conditions and production processes on the conductivity of the sample. A weak point in this technology may be that some experiments are unrepeatable since little is known about the laser-matter interaction mechanisms and how the production process influences this interaction.

Future developments could, therefore, focus on a thorough study of the interaction, characterising the formation of the carbonaceous residue and species responsible for conductive behaviour. It can also be possible to study the process on a different material that has more affinity with Biochar particles, consequently facilitating their distribution within the matrix. But the most compelling option would be to evaluate the influence of adding other functional fillers, such as CNTs, to dilute them with Biochar, in order to reduce the costs of performing composites. That is due to the impossibility of going below $1 \text{ M}\Omega/\text{cm}$ of R even after optimising the laser parameters, just as if this kind of Biochar's particles intrinsic conductivity limit was reached. However, Randeep et al.³¹ in their work, explores the electrical conductivity of monolithic

Biochar and elucidates that the highest skeletal conductivity of heat-treated sugar maple Biochar was 343.2 S/m. That could be a great future solution for the CRF for the development of the Biochar-based composites, without involving other fillers such as CNTs.

Finally, it is possible to assess the utilisation of these composite materials also as pressure sensors by evaluating their piezoresistive properties. This research is being carried forward at CRF with polymeric composites containing CNTs. The combination of conductive behaviour associated with piezoresistivity would make possible to produce a complete metal free circuit directly on an insulating material also integrating the respective push-button.

The conductivity of "metal free" tracks on Biochar particle-filled polymeric composites functionalised by CO₂ laser treatments is an unexplored subject. The hope is that this work is only the eldest of a long list of future developments to optimise the process and would contribute to a better understanding in order to arrive at an industrial scale production.

List of acronyms

CNTs	Carbon nanotubes
CRF	Centro Ricerche Fiat
DSC	Differential Scanning Calorimetry
EDS	Energy-dispersive X-ray spectroscopy
FCA	Fiat Chrysler Automobiles
FESEM	Field Emission Scanning Electron Microscopy
HTC	Hydrothermal carbonisation
ISO	International Organization for Standardization
LASER	Light Amplification by Stimulated Emission of Radiation
MFI	Melt flow index
PE	Polyethylene
PP	Polypropylene
PP5BiocharMix	Compound between polypropylene and 5 wt% of Biochar processed in a measuring mixer
PP15BiocharMix	Compound between polypropylene and 15 wt% of Biochar processed in a measuring mixer
PP30BiocharExtr	Compound between polypropylene and 30 wt% of Biochar processed in a twin screw extruder
PP30BiocharMix	Compound between polypropylene and 30 wt% of Biochar processed in a measuring mixer
PP40BiocharExtr	Compound between polypropylene and 40 wt% of Biochar processed in a twin screw extruder
PPUnfilledExtr	Polypropylene pure processed in a twin screw extruder
PPUnfilledMix	Polypropylene pure processed in a measuring mixer
SD	Standard deviation
TGA	Thermogravimetric analysis
XRD	X-ray Powder Diffraction
UNI	Ente nazionale italiano di unificazione

List of symbols

Symbol	Meaning	Unit of measurement
C-C	Carbon-carbon chemical-bond in the Biochar	
C-H	Carbon-hydrogen chemical-bond in the Biochar	
C-O	Carbon-oxygen chemical-bond in the Biochar	
D	Defocus of the laser beam	mm
E ₁ , E ₂	Energies of electronic levels 1 and 2	eV
f	Frequency of the laser beam	Hz
n	Counting number	
N	Number of repetitions of the laser beam	
p	Conductivity exponent	
P	Power of the laser beam	%
R	Linear surface electrical resistance	Ω
T	Temperature	°C
v	Scan rate of the laser beam	mm/s
V	Volume fraction of filler	
V _C	Volume fraction of filler at percolation	
z	Filler coordination number	
ε	Specific pore volume of filler particles	g/cm ³
θ	Diffraction angle	°
ν	Frequency of a photon	Hz
ρ	Density of filler particles	g/cm ³
σ	Electrical conductivity of the composite	S/m
σ ₀	Electrical conductivity of the filler	S/m

Bibliography

1. Nan N., DeVallance D., Xie X., and Wang J., “The effect of bio-carbon addition on the electrical, mechanical, and thermal properties of polyvinyl alcohol/Biochar composites”. *Journal of Composite Materials*, **50**(9), pp.1161-1168, 2015. DOI: 10.1177/0021998315589770
2. Nanda S., Dalai A., Berruti F., and Kozinski J., “Biochar as an exceptional bioresource for energy, agronomy, carbon sequestration, activated carbon and specialty materials”. *Waste and Biomass Valorization*, **7**(2), pp.201-235, 2015. DOI: 10.1007/s12649-015-9459-z
3. Cha J., Park S., Jung S., Ryu C., Jeon J., Shin M., and Park Y., “Production and utilization of Biochar: A review”. *Journal of Industrial and Engineering Chemistry*, **40**, pp.1-15, 2016. DOI: 10.1016/j.jiec.2016.06.002
4. Abioye A. and Ani F., “Recent development in the production of activated carbon electrodes from agricultural waste biomass for supercapacitors: A review”. *Renewable and Sustainable Energy Reviews*, **52**, pp.1282-1293, 2015. DOI: 10.1016/j.rser.2015.07.129
5. Richard S., Selwin Rajadurai J., and Manikandan V., “Influence of particle size and particle loading on mechanical and dielectric properties of Biochar particulate-reinforced polymer composites”. *International Journal of Polymer Analysis and Characterisation*, **21**(6), pp.462-477, 2016. DOI: 10.1080/1023666X.2016.1168602
6. Azargohar R., Nanda S., Rao B., and Dalai A., “Slow Pyrolysis of Deoiled Canola Meal: Product Yields and Characterisation”. *Energy & Fuels* **27**, pp.5268–5279, 2013. DOI: 10.1021/ef400941a
7. Das O., Bhattacharyya D., and Sarmah A., “Sustainable eco-composites obtained from waste derived Biochar: a consideration in performance properties, production costs, and environmental impact”. *Journal of Cleaner Production*, **129**, pp.159-168, 2016. DOI: 10.1016/j.jclepro.2016.04.088
8. Das O., Sarmah A., and Bhattacharyya D., “Structure-mechanics property relationship of waste derived Biochars”. *Science of the Total Environment*, **538**, pp.611-620, 2015. DOI: 10.1016/j.scitotenv.2015.08.073
9. Huang J., “Carbon black filled conducting polymers and polymer blends”. *Advances in Polymer Technology*, **21**(4), pp.299-313, 2002. DOI: 10.1002/adv.10025
10. Ikram S., Das O., and Bhattacharyya D., “A parametric study of mechanical and flammability properties of Biochar reinforced polypropylene composites”. *Composites Part A: Applied Science and Manufacturing*, **91**, pp.177-188, 2016. DOI: 10.1016/j.compositesa.2016.10.010

11. Richard S., Selwin Rajadurai J., and Manikandan V., "Effects of particle loading and particle size on tribological properties of Biochar particulate reinforced polymer composites". *Journal of Tribology*, **139**(1), pp.462-477, 2017. DOI: 10.1115/1.4033131
12. Zhang W., Dehghani-Sanj A., and Blackburn R., "Carbon based conductive polymer composites". *Journal of Materials Science*, **42**(10), pp.3408-3418, 2007. DOI: 10.1007/s10853-007-1688-5
13. Ma P., Siddiqui N., Marom G., and Kim J., "Dispersion and functionalization of carbon nanotubes for polymer-based composites: A review". *Composites Part A: Applied Science and Manufacturing*, **41**(10), pp.1345-1367, 2010. DOI: 10.1016/j.compositesa.2010.07.003
14. Sumita M., Sakata K., Asai S., Miyasaka K., and Nakagawa H., "Dispersion of fillers and the electrical conductivity of polymer blends filled with carbon black". *Polymer Bulletin*, **25**, pp.265–271, 1991. DOI: 10.1007/bf00310802
15. Du J., Bai J., and Cheng H., "The present status and key problems of carbon nanotube based polymer composites". *Express Polymer Letters*, **1**(5), pp.253-273, 2007. DOI: 10.3144/expresspolymlett.2007.39
16. Balberg I., "A comprehensive picture of the electrical phenomena in carbon black-polymer composites". *Carbon*, **40**(2), pp.139-143, 2002. DOI: 10.1016/s0008-6223(01)00164-6
17. Bayer R., Ezquerra T., Zachmann H., Baltá Calleja F., Martinez Salazar J., Meins W., Diekow R., and Wiegel P., "Conductive PE-carbon composites by elongation flow injection moulding". *Journal of Materials Science*, **23**(2), pp.475-480, 1998. DOI: 10.1007/bf01174672
18. Maiman T. H., "Stimulated Optical Radiation in Ruby". *Nature*, **187**, pp.493-494, 1960. DOI: 10.1038/187493a0
19. Available online at: <http://hyperphysics.phy-astr.gsu.edu/hbase/mod5.html>
20. Ozdemir M. and Sadikoglu H., "A new and emerging technology: Laser-induced surface modification of polymers". *Trends in food science & technology*, **9**(4), pp.159-167, 1998. DOI: 2244(98)00035-1
21. Sohn I. B., Noh Y. C., Choi S. C., Ko D. K., Lee J., and Choi Y. J., "Femtosecond laser ablation of polypropylene for breathable film". *Applied Surface Science*, **254**(16), pp.4919-4924, 2008. DOI: 10.1016/j.apsusc.2008.01.166
22. Bachmann F. G., "Industrial laser applications". *Applied Surface Science*, **46**(1), pp.254-263, 1990. DOI: 10.1016/0169-4332(90)90153-q
23. Available online at:
<http://www.aml.engineering.columbia.edu/ntm/level1/ch05/html/11c05s02.html>
24. Lippert T. and Dickinson J. T., "Chemical and spectroscopic aspects of polymer ablation: special features and novel directions". *Chemical Review*, **103**(2), pp. 453-485, 2003. DOI: 10.1021/cr010460q

25. Uno K., Nakamura K., Goto T., and Jitsuno T., "Longitudinally Excited CO₂Laser with Short Laser Pulse like TEA CO₂Laser". *Journal of Infrared, Millimeter and Terahertz Wave*, **30**(11), pp.1123-1130, 2009. DOI: 10.1007/s10762-009-9542-2
26. Beyler C. L. and Hirschler M. M., "Thermal decomposition of polymers". *SFPE handbook of fire protection engineering*, **2**(1), 2002.
27. Bockhorn H., Hornung A., Hornung U., and Schawaller D., "Kinetic study on the thermal degradation of polypropylene and polyethylene". *Journal of Analytical and Applied Pyrolysis*, **48**(2), pp.93-109, 1999. DOI: 10.1016/s0165-2370(98)00131-4
28. Cesano F., Rattalino I., Demarchi D., Bardelli F., Sanginario A., Gianturco A., Veca A., and Viazzi C., "Structure and properties of metal-free conductive tracks on polyethylene/multiwalled carbon nanotube composites as obtained by laser stimulated percolation". *Carbon*, **61**, pp.63-71, 2013. DOI: 10.1016/j.carbon.2013.04.066
29. Colucci G., Beltrame C., Giorcelli M., Veca A., and Badini C., "A novel approach to obtain conductive tracks on PP/MWCNTs composites by laser printing". *Royal Society of chemistry*, **6**, pp.28522-28531, 2016. DOI: 10.1039/C6RA02726A
30. Liebscher M., Krause B., Potschke P., Barz A., Bliedtner J., Mohwald M., and Letzsch A., "Achieving Electrical Conductive Tracks by laser treatment of nonconductive polypropylene/polycarbonate blends filled with MWCNTs". *Macromolecular Materials and Engineering*, **299**, pp.869-877, 2014. DOI: 10.1002/mame.201300377
31. Gabhi R. S., Kirk D. W, and Jia C. Q., "Preliminary investigation of electrical conductivity of monolithic biochar". *Carbon*, **116**, pp.435-442, 2017. DOI: 10.1016/j.carbon.2017.01.069

Acknowledgements

I would first like to thank my thesis tutors prof. Claudio Francesco Badini and prof. Alberto Tagliaferro of the Politecnico di Torino, for helping me to get closer to the companies reality.

I would also like to acknowledge dr. Antonino Veca of the Centro Ricerche Fiat and dr. Andrea Caradonna of the Politecnico di Torino as the second readers of this thesis, and I am gratefully indebted to their very valuable comments on this thesis. Their door was always open whenever I ran into a trouble spot or had a question about my research or writing.

I would also like to thank the experts from the Politecnico di Torino, who were involved in this research project: prof. Alberto Frache, prof. Danilo Demarchi, dr. Mauro Giorcelli, dr. Elisa Padovano, and dr. Alessandro Sanginario. Without their passionate participation and input, the research work could not have been successfully conducted.

Finally, I must express my very profound gratitude to all my family for providing me with unfailing support and continuous encouragement throughout my years of study and through the process of researching and writing this thesis. This accomplishment would not have been possible without them. Thank you.

Author

Enrico Alfonzo